

**Ruthenium Half-Sandwich Zwitterions:
Coordination Behaviour of New Hemilabile
(Phosphino)benzimidazole Anions**

by

Jesse M. Walker

Department of Chemistry

A dissertation submitted in partial fulfillment of the
requirements for the Degree of Doctor of Philosophy

Supervisor: Dr. Gregory J. Spivak

Faculty of Graduate Studies,
Lakehead University
Thunder Bay, Ontario,
Canada

December 2016

To my wife Laura and our children Harrison and Hannah.

This is for you, in its entirety,
with all my love.

Abstract

A series of tetraphenylborate-functionalized anionic [P,N]-hybrid ligands based on a 2-(diaryl- or dialkylphosphino)benzimidazole scaffold were synthesized from conveniently accessible 1-(4-bromobenzyl)-2-(diaryl- or dialkylphosphino)benzimidazole precursors. The corresponding anionic 2-(diaryl- or dialkylphosphino)-1-(4-(triphenylborato(1-))benzyl)benzimidazole ligands were isolated as their lithium salts, and are abbreviated as $[\text{Li}(\text{THF})_x][\text{P}^{\text{R}}\text{NBPh}_4]$ (R = phenyl, $x = 2$ (**1a**); R = isopropyl, $x = 2$ (**1b**); R = cyclohexyl, $x = 4$ (**1c**)). The corresponding tetraphenylphosphonium salts (Ph_4P^+) of **1a-c** (**1a'**, **1b'**, and **1c'** respectively) are easily accessed via metathesis with Ph_4PX (X = Cl or Br). For comparative purposes, two charge-neutral variants of ligand **1a** were also prepared with methyl and benzyl substituents in the 1-position of the 2-(phosphino)benzimidazole scaffold. The corresponding selenides of all five [P,N]-ligands were prepared, and their electronic properties were assessed using $^{31}\text{P}\{^1\text{H}\}$ NMR spectroscopy.

The coordination behaviour of the anionic (phosphino)borate ligands with ruthenium was influenced by the identity of the ligand cation. In general, in all cases the lithium salts facilitated chloride abstraction from classic piano-stool ruthenium-chloro precursors resulting in the formation of chelated $\kappa^2\text{-P,N}$ complexes. No reactions were observed between **1a'-c'** with $(\text{C}_5\text{R}'_5)\text{RuCl}(\text{PPh}_3)_2$ (R' = H or Me); in contrast, the lithium salts promoted chloride and Ph_3P dissociation leading to the corresponding chelated $\kappa^2\text{-P,N}$ complexes

$[(C_5R'_5)RuCl(PPh_3)(\kappa^2P,N-P^RNBPh_4)]$. Interestingly, in reactions with $[(p\text{-cymene})RuCl_2]_2$, **1a'**-**c'** either produced the monodentate $\kappa^1\text{-P}$, complex exclusively (with **1a'**), or an equilibrium mixture containing $\kappa^1\text{-P}$ and $\kappa^2\text{-P,N}$ complexes (with either ligand **1b'** or **1c'**).

The propensity of the chelated ruthenium complexes to undergo ring-opening of the $\kappa^2\text{-P,N}$ ligands was examined in reactions with MeCN and CO. It was found that the extent of ring-opening was dependent upon the identity of the phosphine donor. Ruthenacycles formed by the anions of ligands **1b** and **1c** were observed to be more resilient towards ring-opening compared to the ruthenacycles formed with the anion of **1a**.

Ring-opening was also observed in reactions involving $[CpRuCl(PPh_3)(\kappa^2P,N-P^RNBPh_4)]$ or $[Cp^*RuCl(PPh_3)(\kappa^2P,N-P^RNBPh_4)]$ with 1-alkynes. Evidence suggests that these reactions proceed via ring-opened vinylidene intermediates that subsequently lead to products in which the vinylidene ligand has formally inserted into the ruthenium-nitrogen bond of the $\kappa^2\text{-P}^RNBPh_4$ ligand.

Ruthenium-vinylidene complexes of the form $[Cp^*Ru(CCHR)Cl(\kappa^2P,N-P^{Cy}NBPh_4)]$ (R= phenyl or *tert*-butyl) were formed by reacting ligand **1c** with $[Cp^*RuCl]_4$ followed by the addition of the corresponding 1-alkyne. Attempts to protonate the vinylidene ligands using HBF_4 at low temperatures to produce ruthenium carbynes resulted in the degradation of the tetraphenylborate functionality.

Acknowledgments

I must admit, I have been looking forward to writing this section for some time now and have been running over and over what to write in hopes to prevent leaving anyone out who deserves to be mentioned. So many people have made the pursuit of this degree possible as it transpired at a time in my life when many important events were occurring.

For instance, I became a father not once but twice during this project, which comes with its own sets of thrills and challenges. Our children immediately became the ultimate motivation to carry on and finish this degree so that it would hopefully better our lives one day. Harrison and Hannah, the unlimited joy that you bring to our lives is amazing! Your constant smiling and laughter are what true life is all about, and I have had the time of my life watching you grow and develop into the amazing kids that you are. I love you with all my heart and will be there for you, always.

Without a doubt, my wife Laura deserves a very special mention. The support that she has provided throughout this project has been immense in every way possible. It is astonishing that she has endured the challenges that this degree has imposed on our lives. The financial restraints, the extreme time commitments and overall uncertainty that have accompanied my graduate studies has certainly made for difficult times, and would have been impossible without her love and support throughout. Laura, thank you so much for your encouragement, patience, and overall support. I love you so much!

I truly have been blessed with the most unbelievably amazing parents in the entire world! Mom and Dad, thank you so much for all of the unconditional love, support and encouragement that you have given to me throughout my life. You have shown such positivity and kindness during this degree, and I certainly would not have come this far in my life if it were not for you both. Words cannot describe how much I love you. Thanks for everything!

My brother Casey has been a tremendous influence in my life. Not only is he one of my best friends, but he is also one of the most interesting people I know. His generosity and encouragement throughout my life has been amazing. He has always been there for me no matter what. Love ya Bruv!

My in-laws, Alex and Marilyn MacIver as well as Katherine MacIver, have been a huge help throughout this degree. Thanks so much for the endless generosity and hospitality that you have given me over the last 15 years.

Both Grandmas have been called in for emergency babysitting on many occasions. With the drop of a hat, they have travelled to take care of the kids during illnesses and other unforeseeable events. They have stayed with us for extended periods cooking, cleaning and doing everything in-between. The kids have loved the extra time they have spent with their Grandmas; Laura and I certainly could not have done it without them! Our other babysitter, Auntie Anne, has been a tremendous help in the last 4 years as well. Thanks so much, Annie!

Through the last stretch of this degree, part-time employment was necessary. I was very fortunate to find employment at the Cyclotron and

Radiopharmaceutical Facility here in Thunder Bay. Not only was this employment opportunity important financially but it was also important as a potential career to look forward to in post-PhD life since, by this time, it was decided not to pursue postdoctoral work. Of course, spreading my time even thinner posed a significant problem in making sure not all of the important aspects of my life suffered drastically. In this regard, I must thank Dr. Michael Campbell and Terry Föde for their kindness, understanding, and flexibility over the last year. I certainly would not have been able to make it through without their help. Being a part of the cyclotron team has absolutely been an amazing experience, not only because of the fascinating nature of the work but also because of staff.

The Department of Chemistry at Lakehead University deserve my acknowledgements for providing me with over eleven years of excellent undergraduate and graduate education. Early in my education at Lakehead, it became apparent that the Faculty and Staff of the Chemistry department at Lakehead are dedicated to the success of their students, and this notion has presented itself repeatedly. In particular, I would like to thank Dr. Christine Gottardo and Dr. Craig MacKinnon, not only for serving as committee members for this degree, but for my MSc and HBSc degrees as well. Their support throughout my time at Lakehead has been instrumental to my success.

Over the years, I have had a chance to work with at least ten other students in the lab. There is no doubt that some of these fine folks will remain lifelong friends. Most of the experimental work of this project was conducted on a lab

bench across from Joey 'T-bone' Tassone. I must say it has been a fantastic time getting to know Joe and his family, truly some of the most genuinely kind people that I know. Joe is always good for a laugh and his company throughout this project has been awesome! I wish Joe all the best at Dal, and wherever his career takes him.

The support and encouragement of my friend Dr. John Th'ng has also been a huge part of my success over the last nine years. The experience that I gained in his lab has certainly made me a more well-rounded and marketable chemist. I am so grateful that he had the courage to bring an inorganic chemist into his biochemistry lab! Thanks, John.

Thanks to Tyler Kellar, Jamie Varga, Todd Williamson and Kevin Harris. The friendship and comic relief is always greatly appreciated. Thanks fellas!

Thanks to Kol MacKay, the strongest person I know. His bravery and persistent fight has been such a big inspiration to everyone around him. Sadly, during the last stretch of writing this document, my dear friend Kol passed away from a brain tumor that he had been battling for more than 10 years. Through all of the surgeries, chemotherapies, radiation, and other hardships that he endured, he always remained positive and kept up his fight right to the end. After completing my MSc, Kol was a huge inspiration for me to remain in research and pursue doctoral studies. I knew Kol for most of my life and he has been such a positive influence; I've always been so proud to say that Kol was one of my closest friends. He was an incredible musician, a supreme entertainer, and a true jokester with an

amazing sense of humor. Kol made everyone feel welcome no matter what and he was such a kindhearted man. Thanks for everything Koly, you will be greatly missed for a lifetime my friend!

None of this would have been possible if I did not have Dr. Greg Spivak as a supervisor over the past eleven years. His encouragement and support throughout my entire education has been immense and I owe him everything for believing in me. Not only has he been an incredible mentor, but also an amazing friend as well. I have spent so much time in his lab over the years, at all hours of the day, that it has been a home away from home. I am so grateful to have ended up in Greg's lab and will forever look back at the time that I have spent there with warm regards and great appreciation. There were many life-changes that I experienced throughout this project, and I cannot imagine the stress I imposed on Greg with regard to me being able to finish. Greg, thanks so much for being there and guiding me through it!

Table of Contents

Acknowledgments	i
List of Key Abbreviations	xi
List of Figures	xiii
List of Schemes	xvii
List of Tables	xx
Chapter One: Introduction	1
1.1. Ruthenium Complexes and their Importance to Chemical Synthesis	1
1.2. The Success of Ruthenium-Mediated Olefin Metathesis and the Quest for an Alkyne Counterpart	6
1.3. Anionic Phosphine Ligands: An Underdeveloped, Yet Intriguing Collection of Ligands	12
1.4. Organometallic Zwitterions	21
1.5. [P,N] Hybrid Ligands: Implications of [P,N] Donor Systems, Hemilability and Ligand Cooperativity	27
1.6. Concluding Remarks	31
Chapter Two: Research Objectives and Rationale	32
2.1. Ligand Design	32
2.2. Coordination Chemistry	33

Chapter Three: Ligand Syntheses	35
3.1. Attempts to Synthesize Various [P,N] Ligands.....	35
3.2. The Synthesis of Anionic 2-(Diphenylphosphino)benzimidazoles	36
3.3. Synthesis of an Anionic 2-(Diphenylphosphino)benzimidazole Ligand	38
3.4. Ligand Derivatization: Chelate Expansion.....	43
3.5. Electron Donating Power: Assessment via ^{31}P - ^{77}Se Coupling Constants...	51
Chapter Four: Coordination Chemistry	54
4.1. Ligand Complexation Involving Ruthenium-Cp and Ruthenium-Cp* Precursors.....	54
4.2. Ligand Complexation Involving [(<i>p</i> -cymene)RuCl ₂] ₂	64
Chapter Five: Reactions of Ruthenium-(Phosphino)benzimidazole Complexes with Small Molecules	73
5.1. Reactions with MeCN: Evidence for Hemilability	73
5.2. Reactions with CO: Evidence for Hemilability	82
Chapter Six: Reactions of Ruthenium-(Phosphino)benzimidazole Complexes with Alkynes	85
6.1. Attempted Syntheses of Ruthenium Vinylidenes: Insertion of Alkynes into Ru-N bonds.....	85

6.2. Reaction of Ligand 1c with $[\text{Cp}^*\text{RuCl}]_4$ and 1-Phenylacetylene: The Formation of Ruthenium Vinylidenes	93
6.3. Attempted Synthesis of Ruthenium-Carbyne Complexes	99
Chapter Seven: Summary, Conclusions and Future Prospects	102
Chapter Eight: Experimental	109
8.1. General Experimental Details.....	109
8.2. Synthesis of 1-(4-bromobenzyl)benzimidazole	110
8.3. Synthesis of 1-(4-bromobenzyl)-2-(diphenylphosphino)benzimidazole.....	111
8.4. Synthesis of 1-(4-bromobenzyl)-2-(diisopropylphosphino)benzimidazole .	112
8.5. Synthesis of 1-(4-bromobenzyl)-2 (dicyclohexylphosphino)benzimidazole	113
8.6. Synthesis of 1-(4-bromobenzyl)-2-((diphenylphosphino)methoxy)- benzimidazole	114
8.7. Synthesis of $[\text{Li}(\text{THF})_2][\text{P}^{\text{Ph}}\text{NBPh}_4]$, (1a).....	115
8.8. Synthesis of $[\text{Li}(\text{THF})_2][\text{P}^{\text{iPr}}\text{NBPh}_4]$, (1b).....	116
8.9. Synthesis of $[\text{Li}(\text{THF})_4][\text{P}^{\text{Cy}}\text{NBPh}_4]$, (1c).....	117
8.10. Synthesis of 1-(benzyl)-2-(diphenylphosphino)benzimidazole, $[\text{PN}^{\text{Bz}}]$	118
8.11. Synthesis of 1-(methyl)benzimidazole.....	119
8.12. Synthesis of 1-(methyl)-2-(diphenylphosphino)benzimidazole, $[\text{PN}^{\text{Me}}]$	119

8.13. General procedure for the synthesis of phosphine selenides	120
8.14. Synthesis of $[\text{CpRu}(\text{PPh}_3)(\kappa^2P,N\text{-P}^{\text{Ph}}\text{NBPh}_4)]$, (2).....	121
8.15. Synthesis of $[\text{CpRu}(\text{MeCN})(\text{PPh}_3)(\kappa^1P\text{-P}^{\text{Ph}}\text{NBPh}_4)]$, (2a).....	122
8.16. Synthesis of $[\text{Cp}^*\text{Ru}(\text{PPh}_3)(\kappa^2P,N\text{-P}^{\text{Ph}}\text{NBPh}_4)]$, (3).....	122
8.17. Synthesis of $[\text{CpRu}(\text{PPh}_3)(\kappa^2\text{-P},\text{N}^{\text{Me}})][\text{BPh}_4]$	123
8.18. Synthesis of $[\text{CpRu}(\text{PPh}_3)(\kappa^2P,N\text{-P}^{\text{iPr}}\text{NBPh}_4)]$, (4).....	124
8.19. Synthesis of $[\text{CpRu}(\text{PPh}_3)(\kappa^2P,N\text{-P}^{\text{Cy}}\text{NBPh}_4)]$, (5).....	125
8.20. Synthesis of $[(p\text{-cymene})\text{RuCl}(\kappa^2P,N\text{-P}^{\text{Ph}}\text{NBPh}_4)]$, (6)	126
8.21. Synthesis of $[(p\text{-cymene})\text{RuCl}(\kappa^2P,N\text{-P}^{\text{iPr}}\text{NBPh}_4)]$, (7)	127
8.22. Synthesis of $[(p\text{-cymene})\text{RuCl}(\kappa^2P,N\text{-P}^{\text{Cy}}\text{NBPh}_4)]$, (8)	128
8.23. Synthesis of $[\text{Ph}_4\text{P}][(\text{p-cymene})\text{RuCl}_2(\kappa^1P\text{-P}^{\text{Ph}}\text{NBPh}_4)]$, (9).....	129
8.24. Synthesis of $[(p\text{-cymene})\text{RuCl}(\kappa^2P,N\text{-PN}^{\text{Bz}})][\text{BPh}_4]$, (10).....	130
8.25. Reaction of $[\text{PPh}_4][\text{P}^{\text{iPr}}\text{NBPh}_4]$ with $[(p\text{-cymene})\text{RuCl}_2]_2$	131
8.26. Reaction of $[\text{PPh}_4][\text{P}^{\text{Cy}}\text{NBPh}_4]$ with $[(p\text{-cymene})\text{RuCl}_2]_2$	131
8.27. Reaction of Complex 6 with MeCN	132
8.28. Reaction of Complex 10 with MeCN	132
8.31. Synthesis of $[\text{CpRu}(\text{PPh}_3)(\kappa^2C,P\text{-}(\text{CCHPh})\text{-P}^{\text{Ph}}\text{NBPh}_4)]$, (13).....	134
8.32. Synthesis of $[\text{CpRu}(\text{PPh}_3)(\kappa^2C,P\text{-}(\text{CCHBu})\text{-P}^{\text{Ph}}\text{NBPh}_4)]$, (14).....	136

8.33. Synthesis of $[\text{Cp}^*\text{Ru}(\text{PPh}_3)(\kappa^2\text{C},P\text{-}(\text{CCHPh})\text{-P}^{\text{Ph}}\text{NBPh}_4)]$, (15).....	137
8.34. Synthesis of $[\text{Cp}^*\text{Ru}(\text{PPh}_3)(\kappa^2\text{C},P\text{-}(\text{CCHBu})\text{-P}^{\text{Ph}}\text{NBPh}_4)]$, (16).....	138
8.35. General experimental procedure for the reaction of complex 6 and 1-phenylacetylene	139
8.36. General experimental procedure for the reaction of complex 6 and 1-hexyne	140
8.37. Synthesis of $\text{Cp}^*\text{RuCl}(\text{CCHPh})(\kappa^2P,N\text{-P}^{\text{Cy}}\text{NBPh}_4)$ (18)	140
8.38. Synthesis of $\text{Cp}^*\text{RuCl}(\text{CCH}^t\text{Bu})(\kappa^2P,N\text{-P}^{\text{Cy}}\text{NBPh}_4)$ (19)	141
8.39. General experimental procedure for the attempted protonation of 18 and 19 using HBF_4	142
8.40. X-ray Crystallography	143
References	162
Curriculum Vitae	177

List of Key Abbreviations

Å = angstroms, 10^{-10} m

Ar = Aryl group

COD = 1,5-cyclooctadiene

Cp = cyclopentadienyl

Cp* = 1,2,3,4,5-pentamethylcyclopentadiene

Cy = cyclohexyl group

d = doublet

DMSO = dimethylsulfoxide

dppb = 1,4-bis(diphenylphosphino)butane

dppe = 1,2-bis(diphenylphosphino)ethane

dppp = 1,3-bis(diphenylphosphino)propane

Et = ethyl group

{ ^1H } = proton decoupled

Hz = Hertz, cycles per second

iPr = isopropyl group

IR = infrared

J = coupling constant

m = multiplet

Me = methyl group

MeCN = acetonitrile

NMR = nuclear magnetic resonance

p-cymene = 1-methyl-4-isopropylbenzene

Ph = phenyl group

ppm = parts per million

PTA = 1,3,5-triaza-7-phosphaadamantane

R(') = generic organic group

s = singlet

THF = tetrahydrofuran

Tp = trispyrazolylborate

Triphos = 1,1,1-tris(diphenylphosphinomethyl)ethane

Wt = weight

List of Figures

Figure 1. Examples of olfactive compounds synthesized on an industrial scale using ruthenium catalysts	3
Figure 2. The structure of ciguatoxin CTX3C	6
Figure 3. Examples of early- and late-metal olefin metathesis catalyst developed by Schrock and Grubbs	8
Figure 4. Examples of the early-metal alkylidyne complexes developed by Furstner and Tamm	10
Figure 5. The structure of the anionic tridentate phosphino(borate) ligand $[\text{PhBP}_3^{\text{Ph}}]^-$	14
Figure 6. Molecular structure of $[(\text{PhBP}_3^{\text{Ph}})\text{Ru}(\text{MeCN})_3]\text{PF}_6$	15
Figure 7. The structure of the anionic bidentate phosphino(borate) ligand $[\text{Ph}_2\text{B}(\text{PPh}_2)_2]^-$	16
Figure 8. The structure of the anionic monodentate phosphino(borate) ligand $[\text{PR}_2(p\text{-Ph}_3\text{BC}_6\text{H}_4)]^-$	19
Figure 9. Examples of solvento-trapped ruthenium complexes containing the anionic $[\text{PR}_2(p\text{-Ph}_3\text{BC}_6\text{H}_4)]^-$ ligand	20
Figure 10. Molecular structure of $[\text{Rh}(\eta^6\text{-PhBPh}_3)(\text{COD})]$	22
Figure 11. Cationic and zwitterionic complexes developed by Stradiotto and coworkers	26

Figure 12. General molecular structure of the proposed anionic [P,N] ligand system	32
Figure 13. A neutral ligand analogue used for comparative purposes	33
Figure 14. Some Examples of target ligands explored during the first stage of the project.....	35
Figure 15. $^{31}\text{P}\{^1\text{H}\}$ NMR spectrum of the solution generated by the addition of BPh_3 to lithiated 1-(4-bromobenzyl)-2-(diphenylphosphino) benzimidazole	40
Figure 16. ^{11}B NMR spectrum of the mixture obtained by the addition of BPh_3 to lithiated 1-(4-bromobenzyl)-2-(diphenylphosphino)benzimidazole	41
Figure 17. ^{13}C NMR spectrum of ligand 1a	43
Figure 18: $^{31}\text{P}\{^1\text{H}\}$ spectrum of 1-(4-bromobenzyl)-2-(((diphenylphosphino)oxy)methyl)benzimidazole.	47
Figure 19. Molecular structures of $[\text{Li}(\text{THF})_2][\text{P}^{\text{iPr}}\text{NBPh}_4]$ (1b) and $[\text{Li}(\text{THF})_4][\text{P}^{\text{Cy}}\text{NBPh}_4]$ (1c).	48
Figure 20. $^{31}\text{P}\{^1\text{H}\}$ NMR spectra highlighting the effect of cation exchange for ligand 1c	50
Figure 21. ^1H NMR spectrum (CD_2Cl_2) of complex 2	56
Figure 22. Crystallographic representation of complex 2	58
Figure 23. Structure of complex 4 and 5	60

Figure 24. Molecular structure of complex 4	63
Figure 25. Proton NMR of complex 6	66
Figure 26. Proton NMR spectrum 30 minutes after reacting [PPh ₄][P ^{iPr} NBPh ₄] with [(<i>p</i> -cymene)RuCl ₂] ₂	71
Figure 27. Proton NMR Spectrum of complex 6 in CDCl ₃	76
Figure 28. ³¹ P{ ¹ H} NMR spectrum of complex 2a reverting back to the parent complex 2 after dissolving in CDCl ₃	80
Figure 29. ¹ H NMR of the benzyl -CH ₂ - signal generated by 2a	81
Figure 30. Products obtained by reacting complex 6 with 1-phenylacetylene...	91
Figure 31. Products generated from the reaction of complex 6 with 1-hexyne.	92
Figure 32. ³¹ P{ ¹ H} NMR spectrum of crude Cp*RuCl(CCHPh)(κ ² P, <i>N</i> - P ^{Cy} NBPh ₄)	96
Figure 33. ¹³ C{ ¹ H} NMR spectrum (C _α region only) of Cp*RuCl(CCHPh)(κ ² P, <i>N</i> - P ^{Cy} NBPh ₄)	97
Figure 34. ³¹ P{ ¹ H} NMR spectrum of Cp*RuCl(CCH ^t Bu)(κ ² P, <i>N</i> -P ^{Cy} NBPh ₄).	98
Figure 35. ¹³ C{ ¹ H} NMR spectrum (C _α region only) of Cp*RuCl(CCH ^t Bu)(κ ² P, <i>N</i> - P ^{Cy} NBPh ₄).	99
Figure 36. A potential ligand design for future study	106
Figure 37. Examples of dianionic (phosphino)borate ligand structures.....	107

Figure 38. Ligand numbering scheme for characterization	110
Figure 39. Fully labeled crystal structure of complex 2	145
Figure 40. Fully labeled crystal structure of complex 4	154

List of Schemes

Scheme 1. The general reaction scheme of olefin metathesis	7
Scheme 2. The general reaction scheme of alkyne metathesis	9
Scheme 3. Synthesis of diphenylphosphidoboratabenzene	13
Scheme 4. The protonation of $(\text{Ph}_2\text{B}(\text{PPh}_2)_2)\text{Pt}(\text{Me})_2$	17
Scheme 5. The different reactivity pattern displayed by zwitterionic $[\text{Rh}(\eta^6\text{-PhBPh}_3)(\text{COD})]$ and $[\text{Rh}(\text{dppb})(\text{COD})][\text{BPh}_4]$	24
Scheme 6. The hemilability of a [P,N] hybrid ligand	29
Scheme 7. Ruthenium-phosphinoimidazole complex displaying dynamic ring opening of the metallacycle	30
Scheme 8. Ring opening of a metallacycle containing the target anionic ligands.	34
Scheme 9. Proposed synthesis of a Ru carbyne target complex via protonation of a Ru vinylidene precursor.....	34
Scheme 10. Synthetic strategy for preparing 1-(4-bromobenzyl)-2-(diphenylphosphino)imidazole	37
Scheme 11. Synthesis of ligand 1a	39
Scheme 12. Proposed synthetic scheme to derivatize ligand 1a	45

Scheme 13. Attempted synthesis of 1-(4-bromobenzyl)-2- (((diphenylphosphino)oxy)methyl)benzimidazole	46
Scheme 14. Synthesis of neutral homologues of 1a	51
Scheme 15. Synthesis of complexes 2 and 3	54
Scheme 16. Synthesis of complexes 6 , 7 , and 8	64
Scheme 17. Synthesis of complex 9	67
Scheme 18. Synthesis of cationic complex 10	68
Scheme 19. Reaction ligands 1b' and 1c' with [(<i>p</i> -cymene)RuCl ₂] ₂	69
Scheme 20. Attempted derivatization of complex 6	74
Scheme 21. Some possible products formed by 6 in the presence of MeCN ...	75
Scheme 22. Synthesis of complex 2a via displacement of the coordinated benzimidazole N in complex 2	79
Scheme 23. Reversible displacement of the benzimidazole nitrogen by CO in the interconversion of complexes 11 and 12	84
Scheme 24. Reaction of complex 2 with phenylacetylene forming <i>E/Z</i> - 13	85
Scheme 25. Possible mechanism for the synthesis of complexes 13-16	88
Scheme 26. Alternate synthetic route to complex 15	89
Scheme 27: Proposed synthetic route to Cp* <i>Ru</i> vinylidenes beginning with [Cp* <i>RuCl</i>] ₄ and ligands 1a-c	94

Scheme 28. Proposed strategy for synthesizing ruthenium-carbyne complexes from ruthenium-vinylidene precursors	100
--	-----

List of Tables

Table 1. $^{31}\text{P}\{^1\text{H}\}$ NMR data for the phosphine selenides in CDCl_3	53
Table 2. Summary of key spectroscopic data for complexes 2-5	61
Table 3. Summary of key spectroscopic data for complexes 13-16	87
Table 4. Bond Lengths for complex 2	146
Table 5. Bond Angles for complex 2	148
Table 6. Bond Lengths for complex 4	155
Table 7. Bond Angles for complex 4	157

Chapter One: Introduction

1.1. Ruthenium Complexes and their Importance to Chemical Synthesis

There is no doubt that the field of organometallic chemistry has evolved into a mature and multifaceted subset of chemistry. In particular, ruthenium-based organometallic complexes have displayed astonishing diversity with respect to their functional roles in novel chemical applications. Modern applications of organometallic ruthenium compounds span from innovative biological functions, including anticancer^[1-5] and antiviral chemotherapies,^[6-8] to efficient catalytic hydrogen production via splitting water,^[9-15] a process crucial to the development of a dependable hydrogen-fuel economy. In fact, one area in which ruthenium compounds have attained a great deal of attention from the research community is in homogeneous catalytic applications, as illustrated by the fact that a share of two Nobel Prizes, to Grubbs (2005) and Noyori (2001), have been awarded recently for the development of novel ruthenium-catalyzed homogeneous chemical transformations.

Although organometallic chemistry has a historical prominence in homogeneous catalysis -- an application that has propelled its expansion since the field was in its infancy^[18] -- the development of catalytically active organometallic ruthenium complexes remains an intense and exceptionally productive area of research, having a profound impact on numerous areas of

chemical synthesis.^[19,20] Not only are ruthenium complexes valued from an industrial standpoint, but also with respect to more specialized processes such as fine-chemical^[21-23] and natural product synthesis,^[24-26] to name a few.

It is difficult to overstate the importance of catalysis to the chemical industry. The industry, undeniably, has become reliant on catalysis to operate in the most environmentally and economically viable fashion. Amazingly, it is estimated that 75% of industrial chemical processes utilize catalysts, and it is also projected that 90% of newly developed chemical transformations will employ a catalyst.^[27] These figures are incredible given the magnitude on which the present-day chemical industry operates. Often, when reviewing the importance of ruthenium as a transition metal for use in catalysis, many overlook the importance of cost a major contributing factor. Indeed, prices of this metal continue to remain low when compared to those of the other popular, catalytically significant metals such as Pd, Pt, Rh and Ir. This is an important factor that can have huge ramifications when dealing with chemistry on an industrial scale, large-scale research programs, or programs having a restricted budget.

Placing catalysis at the heart of the green-chemistry movement, the development of new catalysts that improve reaction efficiencies can have profound effects on the amount of chemical waste that is generated as well as the amount of energy and reagents required for the process.^[28-30] Also, the use of a catalyst may eliminate the requirement to use hazardous chemicals and specialized equipment.^[23] There have been a number of ruthenium complexes that

have found use as catalysts in industrial applications. Recent advancements involving the industrial-scale synthesis of some chemicals important to the flavor and fragrance trade (Figure 1) provide a perfect example of how the development of new, highly effective ruthenium catalysts can have incredible consequences pertaining to the aforementioned attributes of chemical transformations.^[23]

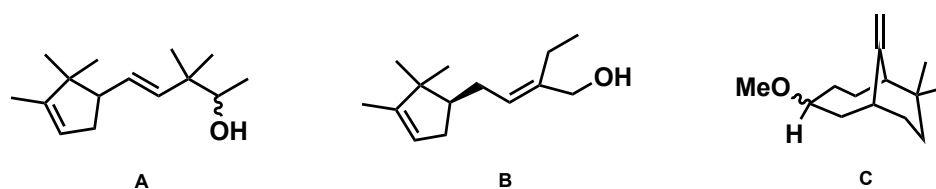


Figure 1. Examples of olfactory compounds synthesized on an industrial scale using ruthenium catalysts. A = Nirvanol®, B = Dartanol®, C = Pamplewood®.^[23]

The new methodologies reported, which produce various unsaturated alcohols on an industrial-scale, employ organometallic ruthenium complexes to perform catalytically key regio- and stereoselective hydrogenation reactions. These methods proved to be significantly advantageous when compared to traditional methods.^[23] The new synthetic approaches to these commercially relevant fine-chemicals allowed the company to avoid using wasteful stoichiometric reagents including Wittig reagents and traditional hydrides as well as evading the use of chemical feedstocks that are hazardous and difficult to employ.^[23]

Interestingly, these reactions were also used to produce naturally occurring chemicals or to provide easy access to suitable chemical substitutes for natural products.^[23] The design of synthetic chemical pathways that lead to the production of naturally occurring products is not only a fascinating area of synthetic chemistry, but is also extremely important from an ecological and environmental perspective.

Gaining access to a natural product by means of harvesting the organism that produces it poses great environmental complications. Typically, in order to obtain sufficient quantities of these naturally occurring compounds, a large number of a specific type of organism must be harvested.^[31] This can be due to low concentrations of the product in the organism or biological tissue as well as low yields from processing the biomaterial to obtain a pure compound. These aspects can cause difficulty in meeting the demand for the natural product while staying within the parameters of environmental and ecological sustainability. In addition, the environmental implications of natural product cultivation can be particularly problematic in areas that are less economically developed where the perceived economic benefits of harvesting the organism at a rapid and unsustainable pace may be greater than the environmental impact of such aggressive harvesting practices.^[32] Further complicating the situation, these geographical regions may lack enforced environmental regulations that would hinder such extreme exploitation of local flora and fauna.^[32]

From an environmental standpoint, it is of great importance that synthetic chemists are able to produce valuable natural products in the most efficient cost-effective manner possible to meet demand for the product while preventing the mismanagement of the organism that produces it. Indeed, complexes of ruthenium have not only played a vital role in the development of efficient natural product syntheses but have also expanded the scope of this branch of chemistry.^[24] There has emerged a number of natural products that are reliant on ruthenium catalysts for their efficient synthesis.^[24] Therefore, it is evident that the continued improvement of ruthenium catalysts and the study of their fundamental properties, will ensure that synthetic chemists are provided with the best tools possible to produce naturally occurring products in a cost-competitive manner and, thus, will contribute to the conservation and preservation of susceptible biological populations.

Undeniably, nature is a most formidable synthetic chemist, for the complexity of many naturally occurring biomolecules is simply amazing (Figure 2).^[24,33] As impressive as these molecules are, the architectural complexity of many biomolecules pose an ultimate challenge to synthetic chemists since naturally occurring chemicals are important to numerous aspects of human endeavors. Most notable are the applications of natural products in medicine. Interestingly, nature has evolved in such a way that has made it a master of stereochemistry and chemical selectivity.^[33] Many of these macromolecules have structures laden with stereocentres and functional groups making their synthesis

challenging in a laboratory setting without the intricate methodology inherent to biological systems. It is for these reasons that ruthenium has found much of its success in organic synthesis as a whole. Actually, ruthenium catalysts tend to display exceptional functional group tolerance and selectivity (Figure 2). It is on this basis that ruthenium-catalyzed olefin metathesis, for instance, has become one of the most important and successful chemical transformations to emerge from organometallic chemistry.

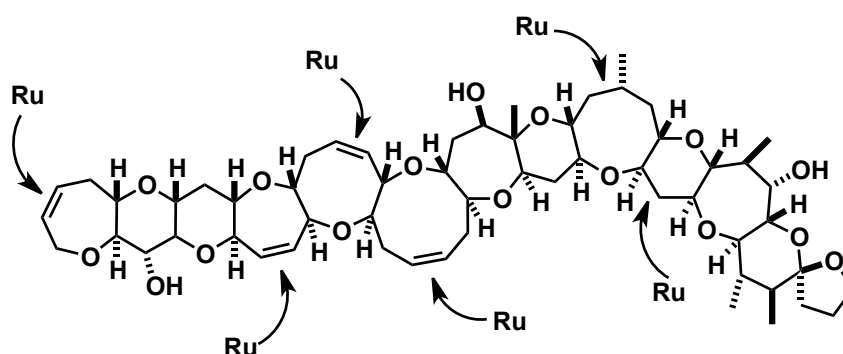
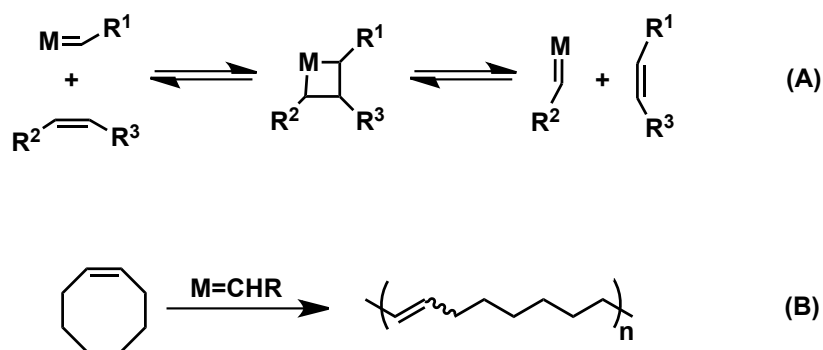


Figure 2. The structure of ciguatoxin CTX3C, an example of the chemical complexity present in many natural products. The arrows indicate the bonds that are formed by ruthenium catalysis during the synthesis of this compound.^[24]

1.2. The Success of Ruthenium-Mediated Olefin Metathesis and the Quest for an Alkyne Counterpart

Olefin metathesis is certainly one of the most successful and renowned developed chemical reactions in catalysis. It has been hailed as one of the most

prominent triumphs in advanced organic synthesis.^[24] The reaction, in essence, is the scrambling of groups across carbon-carbon double bonds as illustrated in Scheme 1. Olefin metathesis is applicable to a wide range of syntheses including polymerization^[34] (Scheme 1), natural products^[24] and pharmaceuticals.^[35] One feature that stands out with regard to olefin metathesis, is that it affords chemists a facile route to construct macrocyclic-ring structures that are frequently encountered in natural product and pharmaceutical molecular scaffolds.^[24,36]



Scheme 1. Olefin metathesis: A) The general reaction scheme illustrating the exchange of functional groups.^[37] B) an example of ring-opening metathesis polymerization.^[34]

There remain two broad classes of organometallic catalysts that are used for olefin metathesis, those that are based on early metals such as the Schrock-type carbenes, and those based on late-metals such as the Grubbs-type carbenes (Figure 3). In particular, the Grubbs-type ruthenium catalysts have been immensely successful.

Enhancing functional group tolerance, the utilization of ruthenium as the core of these catalysts is beneficial for olefin metathesis in that it takes advantage of the preferential soft-Lewis acid/soft-Lewis base interaction between the ruthenium metal-centre and the olefinic substrate. In fact, the expansion of olefin metathesis catalysts to include ruthenium complexes was accompanied by other important

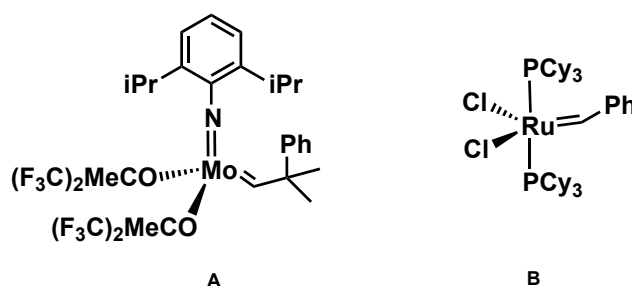
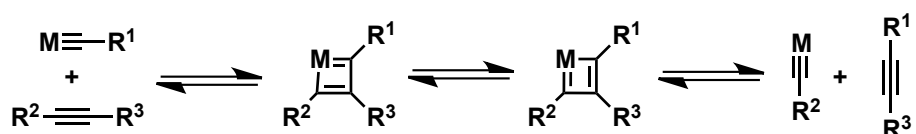


Figure 3. Examples of early- and late-metal olefin metathesis catalyst developed by Schrock (A) and Grubbs (B).^[36]

benefits in addition to the enhanced functional group tolerance, when compared to metathesis initiators based on early metals. The ruthenium complexes afforded practitioners the ability to store the catalysts in an air atmosphere for weeks without considerable degradation, making them easier to employ.^[36] Not only were these complexes tolerant to small amounts of reagent impurities, but they were also cheaper to synthesize and, therefore, more readily available.^[36] Indeed, they were truly olefin metathesis catalysts for the masses.

Based on the metallacyclobutane-containing reaction mechanism inherent to metal-catalyzed olefin metathesis, it would seem logical that this general

transition would be amenable to alkyne substrates as well, if the metal-carbon double bond of the catalyst was substituted for a triple bond. In fact, metal-catalyzed alkyne metathesis (Scheme 2) has been lurking in the shadow of its more renowned counterpart, olefin metathesis, for some time now.



Scheme 2. The general reaction scheme of alkyne metathesis illustrating the exchange of functional groups.^[38]

Interestingly, its initial developmental progression has mimicked that of olefin metathesis to some degree, since catalysts based on early-metal carbyne scaffolds hold prominence in the field (Figure 4). Research in this area has gained momentum recently with a series of molybdenum and tungsten alkylidyne complexes developed by the groups of Furstner and Tamm (Figure 4), some of which have shown remarkable stability and functional group tolerance.^[39,40]

Intriguingly, these molybdenum carbyne catalysts have been used to synthesize some macrocyclic alkyne-containing rings of natural products in the presence of numerous functional groups.^[41] Furthermore, some of the novel molybdenum carbyne complexes were shown to catalyze alkyne metathesis of some challenging substrates including a few examples of the unprecedented

alkyne metathesis involving terminal alkynes.^[40] This reaction has typically been complicated by alkyne cyclotrimerization as well as catalyst degradation when using traditional alkyne metathesis catalysts, and has posed a significant hurdle

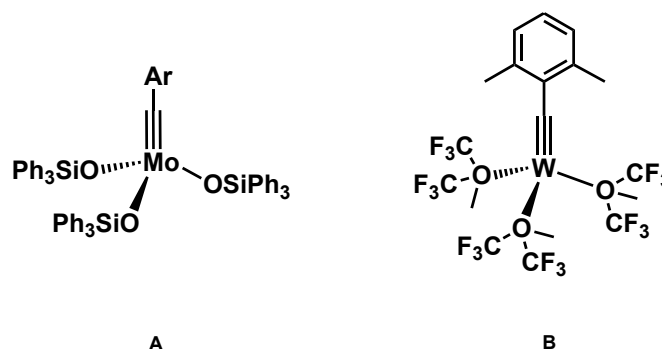


Figure 4. Examples of the early-metal alkylidyne complexes developed by Furstner (A) and Tamm (B). These alkyne metathesis catalysts are stable and functional group tolerant.^[39,40]

in widening the substrate-base of alkyne metathesis.^[38,40,42,43] The recent development of these complexes has certainly expanded the scope of alkyne metathesis, and it will prove interesting to observe future advancement of this innovative class of catalyst.

Indeed, the synthetic utility of alkyne metathesis does not stop at offering chemists the ability to construct new alkynyl functionalities. This transformation can also afford a convenient method of synthesizing stereospecific alkenes, by using established, methods to partially reduce the newly formed alkyne,^[44,45] a limitation of olefin metathesis that has only recently been addressed with headway by Hoveyda and Grubbs though the development of olefin metathesis catalysts

capable of selective Z-isomer formation.^[45,46] Furthermore, groups can be added across the alkyne providing a wealth of synthetic possibilities.^[24,45,47]

In light of the success and advantages that ruthenium-based catalysts have contributed to olefin metathesis, the expansion of metal catalysts capable of initiating alkyne metathesis to include ruthenium complexes may benefit from the same advantages, and would propel alkyne metathesis to the main stage of organic synthesis. Therefore, it is surprising that the development of ruthenium alkyne metathesis chemistry has received considerably less attention from the organometallic research community,^[48-51] as compared to ruthenium-catalyzed alkene metathesis. Not only are ruthenium carbyne complexes rare in the literature, but ruthenium complexes that display the ability to catalyze alkyne metathesis also remain elusive. Only a single example of a ruthenium carbyne complex that can dimerize terminal alkynes exists in the literature.^[52] In light of the scarcity of ruthenium carbyne complexes capable of catalyzing this reaction, more insight with regards to structure/activity relationships is required to push the development of ruthenium-mediated alkyne metathesis forward.

Tuning the reactivity patterns of organometallic complexes through variation of ligand structure remains a vital component to their development and is a fundamental process in the art of organometallic chemistry. Subtle structural differences in ligand configuration may lead to surprising differences in chemical reactivity and, perhaps, superior catalysts. Since ligands can provide both a supportive role as well as being active participants in organometallic processes,

innovative ligand structures can have profound effects on all aspects of the catalytic performance of metal complexes.

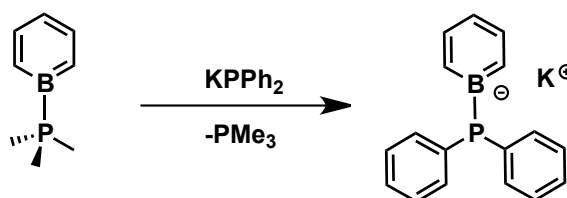
1.3. Anionic Phosphine Ligands: An Underdeveloped, Yet Intriguing Collection of Ligands

Undoubtedly, tertiary phosphine ligands are amongst the most diverse and well-developed ligand systems used in the design of coordination compounds. Variation in the groups attached to the phosphorus donor atom allows for a versatile means of manipulating both the electronic and steric effects, providing an easily accessible method to fine-tune the reactivity of the metal complexes that incorporate these structural variants. The search for phosphine ligands that have enhanced electron-donating abilities remains an important focus in the development of transition metal catalysts since electron-rich phosphine ligands are able to provide stabilizing effects during key stages in catalytic processes including coordinatively-unsaturated intermediates as well as transient species that contain metal centres in elevated oxidation states. Furthermore, electron-rich phosphine ligands can provide a level of activation in pre-catalyst complexes by exerting a labilizing effect on other ligands within the coordination sphere (high *trans* influence), thereby facilitating the generation of the active catalyst.

One design strategy that could potentially improve the activity of metal-based catalysts is to incorporate an anionic charge into the phosphine ligand structure. However, most of the methods used to generate anionic phosphine ligands employ electron withdrawing groups such as sulfonates, which often

decrease the electron-donor power of this class of ligand.^[53] In an attempt to circumvent these electronic effects, the use of a less electronegative group, such as an alkyl- or aryl-borate, to generate the anion allows for the negative charge to be less polarized and the donating power of the phosphine may be improved.^[54-58] Interestingly, only a few examples of these types of ligands appear in the literature.

The first reported anionic phosphinoborate emerged from Fu's synthesis of the PMe_3 adduct of boratabenzene.^[57] Reaction of this precursor with KPh_2 (pK_a of $\text{PMe}_3 = 8.70$ vs pK_a of $\text{Ph}_2\text{PH} = 22.9$)^[58] resulted in the formation of diphenylphosphidoboratabenzene (Scheme 3), an elegant anionic and isosteric homologue of the ubiquitous PPh_3 ligand.^[57]



Scheme 3. Synthesis of diphenylphosphidoboratabenzene.^[57]

Initial studies with regard to the coordination chemistry of this unique ligand provided evidence that it was considerably more electron donating than PPh_3 as indicated by the carbonyl stretching frequencies in analogous Fe-CO complexes.^[57] Surprisingly, although it has now been twenty years since its

inception, very little has been published regarding this innovative ligand. However, the simple synthetic utility of the (formally negative) BC_5H_5 unit as a means to render traditional and well-established phosphine ligands anionic is a seemingly untapped resource to establish innovative ligand structures that have enhanced electron-donating power.

One of the earliest reported anionic phosphinoborate ligands was a phenylborate-derivative of the classic 1,1,1-tris(diphenylphosphinomethyl)ethane (*triphos*) tridentate ligand, introduced by the Tilley group.^[59] The novel design of this ligand adopted the basic framework of a tetra-coordinate boron moiety, commonly utilized as weakly coordinating counterions in cationic transition metal salts, and incorporated this molecular unit into the ligand backbone (Figure 5) thereby replacing the apical ethyl bridgehead of *triphos* with an anionic PhB-group. By far, this ligand, and its derivatives of the form $[\text{RB}(\text{CH}_2\text{PR}'_2)_3]^-$ (hereafter abbreviated as $[\text{RBP}_3^{\text{R}'}]^-$ accordingly), represent the most studied class of anionic (phosphino)alkylborates with almost fifty publications reporting their use.^[60]

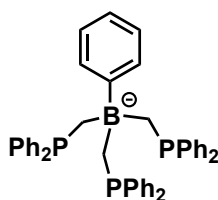


Figure 5. The structure of the anionic tridentate phosphino(borate) ligand $[\text{PhBP}_3^{\text{Ph}}]^-$.^[59]

Interestingly, these alkylborate-derivatives of triphos are isoelectronic with cyclopentadiene (Cp) and tris(pyrazolyl)borate (Tp) and their derivatives are arguably two of the most popular and well-studied ligand systems in coordination chemistry. However, evidence from CO stretching frequencies in corresponding Ir complexes suggests that $^{\text{Ph}}\text{BP}_3^{\text{Ph}}$ is a better electron-donor than both pentamethylcyclopentadiene (Cp*) and hydridotris(3,5-dimethylpyrazolyl)borate. There are numerous accounts of $[\text{R}^{\text{BP}_3\text{R}^{\text{I}}}]^-$ being employed as supporting ligands in transition metal complexes,^[60] and many of these complexes have displayed interesting reactivity, including the activation of silanes,^[61-63] CO,^[64] H₂,^[65,66] and CO₂.^[67]

Our experience with $[\text{Ph}^{\text{BP}_3\text{Ph}}]^-$ in ruthenium chemistry resulted in the study of a highly active transfer hydrogenation catalyst (Figure 6).^[68] Even though the steric demand of the face-capping $[\text{Ph}^{\text{BP}_3\text{Ph}}]^-$ ligand was rather large (as evidenced

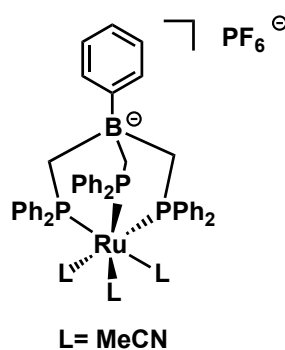


Figure 6. Molecular structure of $[(^{\text{Ph}}\text{BP}_3^{\text{Ph}})\text{Ru}(\text{MeCN})_3]\text{PF}_6$, a highly active catalyst for the transfer hydrogenation of acetophenone and other ketones.^[68]

by the MeCN displaying limited substitution chemistry, and being displaced only by ligands which have modest steric profiles) this complex catalyzed the transfer hydrogenation of ketones at very high turnover frequencies.^[68]

Another notable catalytic reaction of a ruthenium complex containing $[\text{P}^{\text{h}}\text{BP}_3^{\text{Ph}}]^-$ was the selective hydrogenation of cinnamaldehyde to cinnamyl alcohol by the ruthenium dimer $[\text{Ru}(\text{P}^{\text{h}}\text{BP}_3^{\text{Ph}})(\mu\text{-Cl})]_2$.^[69] Amazingly, this dimer represents one of the most powerful catalysts for this transformation in terms of both activity and selectivity.^[60] The novel reactivity patterns displayed by complexes containing $[\text{R}^{\text{B}}\text{BP}_3^{\text{R}^{\text{1}}}]^-$ fueled research focused on the study of other anionic (phosphino)borate ligands.

Soon after the initial reports of the novel $[\text{P}^{\text{h}}\text{BP}_3^{\text{Ph}}]^-$ ligand, other anionic phosphines featuring an alkyl/aryl-borate backbone appeared in the literature. A bidentate version of the $[\text{R}^{\text{B}}\text{BP}_3^{\text{R}^{\text{1}}}]^-$ system was synthesized by the Peters group.^[70] Essentially, these ligands are homologues to the classic bidentate bis(dialkylphosphino)propane ligands (Figure 7).^[71] Initial efforts to explore these ligands in Pt chemistry resulted in a complex

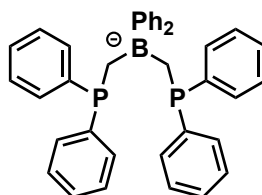
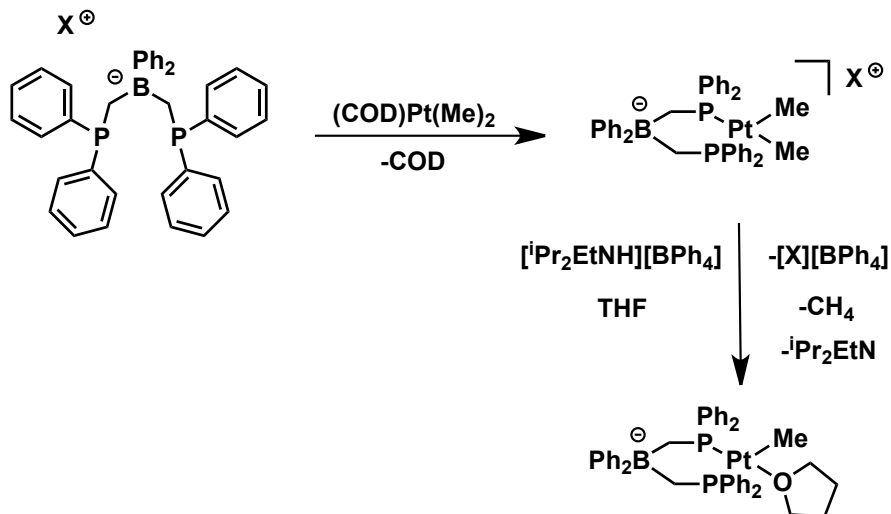


Figure 7. The structure of the anionic bidentate phosphino(borate) ligand $[\text{Ph}_2\text{B}(\text{PPh}_2)_2]^-$.^[71]

capable of benzene C-H activation. Interestingly, access to the active Pt-THF species was only possible using the anionic (phosphino)borate ligand whereas the analogous precursor containing 1,3-bis(diphenylphosphino)propane was not susceptible to protonation to generate the active species (Scheme 4). This illustrates the differing reactivity patterns that anionic phosphinoborates complexes can impart compared to their neutral analogues.^[71]



Scheme 4. The protonation of $(\text{Ph}_2\text{B}(\text{PPh}_2)_2)\text{Pt}(\text{Me})_2$ to afford an active Pt-THF complex, a reaction not observed for the analogous complex containing a neutral dppp ligand.^[71]

The bulky $[\text{R}'_2\text{B}(\text{P}^t\text{Bu}_2)_2]^-$ anion was explored as a supporting ligand in Cu chemistry and was shown to stabilize low-coordinate complexes,^[72] including the first examples of fully characterized Cu(I)-diazoalkane complexes.^[73] Although some very interesting and unique features have emerged concerning the use of

tridentate $[\text{RBP}_3\text{R}^1]^-$ and bidentate $[\text{R}'_2\text{B}(\text{PR}_2)_2]^-$ monoanionic (phosphino)borate ligands in coordination chemistry, there were a few problems with regard to the stability of these ligands towards air oxidation and hydrolysis as well as rapid decomposition in chlorinated hydrocarbons such as chloroform and methylene chloride.^[55,74,75]

It was suspected that the instability aspects of the alkyl-bridged bis- and tris(phosphino)borate ligands were a result of the $-\text{B}-\text{CH}_2-$ tether. This notion was supported by the detection of MePPh_2 as a hydrolysis decomposition product^[75] of $[\text{Li}(\text{TMEDA})][\text{Ph}_3\text{B}(\text{CH}_2)\text{PPh}_2]$ (TMEDA = $\text{N,N,N}',\text{N}'$ -tetramethylethylenediamine). Since it had been established that arylborate groups are generally more stable than alkylborates,^[54] a logical progression of these ligands would be to generate an anionic (phosphino)borate containing only aryl linkages to the boron atom. Indeed, a series of $[\text{PR}_2(p\text{-Ph}_3\text{BC}_6\text{H}_4)]^-$ ligands were synthesized by the Peters group containing, at least conceptually, R_2P -donor moieties bound to a $[\text{BPh}_4]^-$ anion (Figure 8). The initial series of this type of ligand was varied with respect to the substituents at the phosphorus (Ph and ^iPr) as well as the substitution geometry about the aryl bridging unit (*meta*- and *para*-substitution). It was found that these ligands were more robust with regard to stability towards solvents, hydrolysis and air oxidation, more so than the aforementioned ligands containing the $-\text{B}-\text{CH}_2-$ linker.^[75]

The seminal communication describing this ligand series briefly described preliminary coordination chemistry regarding Rh and Pt. In the case of Pt, a

complex that incorporated the meta-substituted (diisopropylphosphino)borate was shown to promote the Suzuki cross-coupling of aryl halides in significantly greater yields than analogous complexes containing neutral isosteric phosphines.^[54]

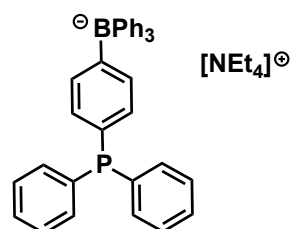


Figure 8. The structure of the anionic monodentate phosphino(borate) ligand $[\text{NEt}_4][\text{PR}_2(p\text{-Ph}_3\text{BC}_6\text{H}_4)]$.^[54]

These observed differences in reactivity were attributed to the greater electron-donating power of the anionic phosphine ligand.^[54]

As novel as these ligands are, they have not received considerable attention from the research community. Our group expanded the series to include the para-substituted -PCy_2 analogue and explored the use of these ligands in Ru-arene chemistry.^[76] From this work emerged interesting observations of unique solution dynamics involving these types of complexes, including pronounced chloride dissociation taking place which seemed to be dictated by increased donor-power of the phosphines.^[76] It was proposed that we were witnessing the formation of a three-component equilibrium between monomeric dichloride species and both mono and di- μ -chlorido complexes.^[76] In addition, facile chloride abstraction from

RuCl₂-arene complexes containing the monodentate (phosphino)borates resulted in the isolation of numerous solvento-trapped, zwitterionic complexes incorporating either acetonitrile or pyridine into the coordination sphere (Figure 9).^[76]

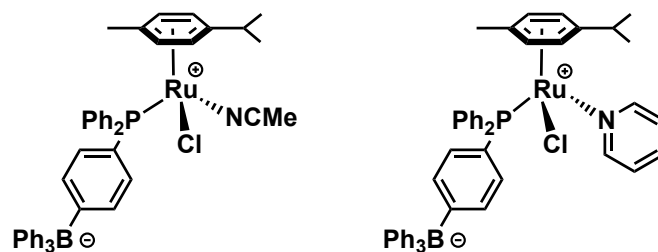


Figure 9. Examples of solvento-trapped ruthenium complexes containing the anionic $[\text{PR}_2(p\text{-Ph}_3\text{BC}_6\text{H}_4)]^-$ ligand.^[76]

Another study from our laboratory using these anionic (phosphino)borate ligands probed the electron-releasing power as a function of borate proximity to the phosphorus donor atom. By converting analogous sets of anionic and neutral phosphine ligands to the corresponding selenides, these experiments employed the use of ^{31}P - ^{77}Se coupling constant data, obtained by ^{31}P NMR spectroscopy, to compare the effects of inserting aryl and alkyl groups between the phosphorus donor centre and the $[\text{BPh}_4]^-$ unit.^[77] It was found that, in all instances, the σ -donating ability of the anionic ligands were enhanced, albeit to varying degrees, compared to their neutral counterparts.^[77] Certainly, the proximity of the borate group to the phosphine donor has a pronounced impact on the electronic properties of these anionic ligands. It was found that attaching the $[\text{BPh}_4]^-$ unit

directly to the phosphine had the greatest effect on σ -donation, whereas introducing an aryl group between the borate and the phosphine moieties resulted in diminished electronic effects.^[77]

In retrospect, this year marks the 20th anniversary of the first anionic phosphino(borate) ligand, diphenylphosphidoboratabenzene, introduced by the pioneering work of Fu and coworkers.^[57] Given that, for some time now, the search for new ligands with enhanced electron-donating abilities has been a continuous theme in organometallic research, it remains puzzling that anionic (phosphino)borate ligands have not received more interest from the research community. Despite the fact that most studies on this class suggest that they have unique properties as compared to their neutral counterparts, anionic (phosphino)borate ligands continue to be an underdeveloped, yet extremely promising, class of ligand.

1.4. Organometallic Zwitterions

Since the majority of transition metal compounds used in homogeneous catalysis are cationic, incorporation of an anionic ligand could afford charge-neutral zwitterionic catalysts having several advantages over their cationic analogues. For example, charge-neutral zwitterionic catalysts would eliminate the need for a counterion, thereby alleviating any inhibitory ion-pairing interactions between the active catalyst and the counterion.^[78-81] Furthermore, cationic catalysts usually display poor solubility in low-polarity solvents whereas

zwitterionic alternatives may be soluble in these types of media.^[79,82] This can be beneficial from a catalytic standpoint in alleviating solvent/substrate incompatibilities as well as gaining mechanistic insight through solution phase studies.^[79]

Amongst the first zwitterionic complexes in the literature are those reported by Schrock and Osborn. It was found that, when studying hydrogenation reactions involving complexes of the general form $[\text{Rh}(\text{PPh}_3)_2\text{H}_2(\text{sol})_2][\text{X}]$ (where sol = solvent, X = OCl_4^- , PF_6^- or BPh_4^-), a mechanism was present that selectively hindered the activity of the BPh_4^- salt. Further investigation revealed that the $[\text{BPh}_4]^-$ counterion was coordinating to the metal via one of the Ph groups through a facial η^6 -type coordination mode. This discovery led the researchers to synthesize systematically a series of Rh and Ir complexes featuring this new zwitterionic motif. However, it wasn't until much later that Alper and co-workers realized the true potential of these systems when they discovered that $[\text{Rh}(\eta^6\text{-PhBPh}_3)(\text{COD})]$ (COD= 1,5-cyclooctadiene) (Figure 10) was capable of catalyzing a plethora of chemical transformations^[79,83], a true catalytic 'workhorse'. Indeed, a

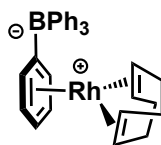
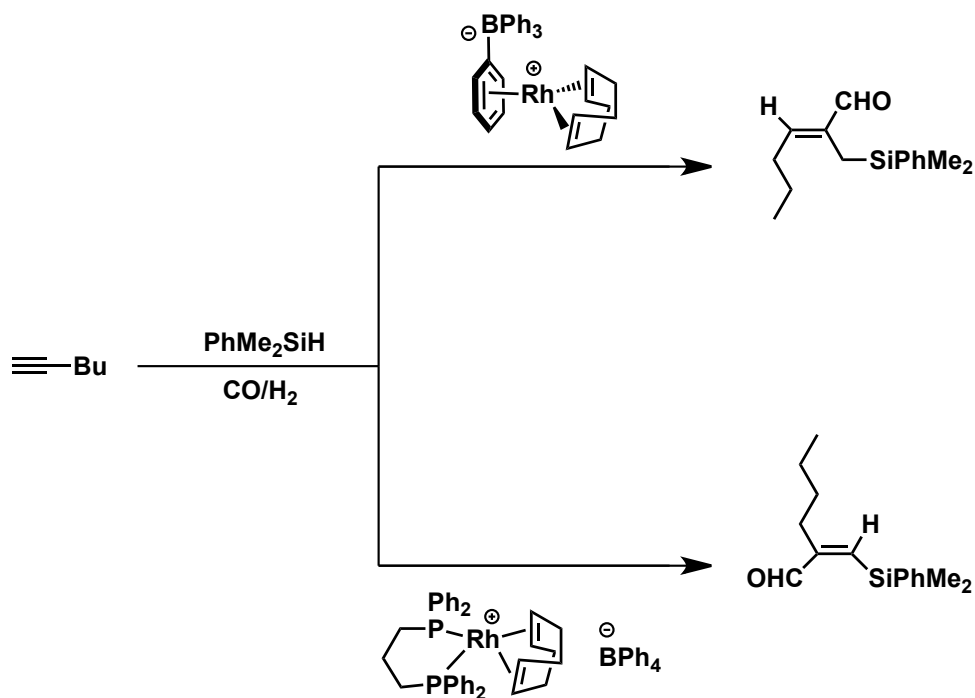


Figure 10. Molecular structure of $[\text{Rh}(\eta^6\text{-PhBPh}_3)(\text{COD})]$. This zwitterionic complex features a coordinated BPh_4^- group.^[82]

number of zwitterionic complexes have appeared in the literature since these Rh systems were reported, yet the rational design of this class of complex with respect to late transition metals is a fairly recent phenomenon,^[79] aided by the development of novel ligand structures that sequester anionicity from the ligated metal cation.

Although a few comparative studies involving zwitterionic organometallic complexes and suitable cationic analogues have emerged in the literature, clear insight concerning the structure/activity relationships of these complexes is rather limited. However, in many of these comparative studies, the contrast between the zwitterionic and cationic analogues can be very pronounced exposing differences in chemoselectivity and/or activity.^[70,82,84,85]

When Alper and co-workers were studying the catalytic performance of $[\text{Rh}(\eta^6\text{-PhBPh}_3)(\text{COD})]$, they noticed, in a number of reactions, that this complex behaved differently, with respect to stereochemical outcomes, than analogous cationic or charge-neutral counterparts.^[79,86,87] For instance, when comparing $[\text{Rh}(\eta^6\text{-PhBPh}_3)(\text{COD})]$ with cationic $[\text{Rh}(\text{dppb})(\text{COD})][\text{BPh}_4]$ (where dppb= 1,4-bis(diphenylphosphino)butane) for use in the silylformylation of terminal alkynes, it was found that the zwitterionic and cationic complexes afforded different isomeric alkenes as illustrated in Scheme 5.^[86]



Scheme 5. The different reactivity pattern displayed by zwitterionic $[\text{Rh}(\eta^6\text{-PhBPh}_3)(\text{COD})]$ and $[\text{Rh}(\text{dppb})(\text{COD})][\text{BPh}_4]$.^[79]

Keeping with the theme of (phosphino)borate zwitterion chemistry, an exemplary study highlighting the reactivity difference between complexes differing by the presence of a negative charge residing on the backbone of the ancillary ligand was published by Betley and Peters. The authors describe the difference between complexes of the form $(\text{P}^+\text{P})\text{Rh}(\text{MeCN})_2$ (where $\text{P}^+\text{P} = [\text{Ph}_2\text{B}(\text{CH}_2\text{PPh}_2)_2]^+$, $\text{Ph}_2\text{Si}(\text{CH}_2\text{PPh}_2)_2$, $\text{Ph}_2\text{P}(\text{CH}_2)_2\text{PPh}_2$ or $\text{Ph}_2\text{P}(\text{CH}_2)_3\text{PPh}_2$) to catalyze the hydroacylation of 4-methyl-4-pentenal.^[88] The results of this comparative study revealed that the hydroacylation activity of the zwitterionic

complex containing the (phosphino)borate was around forty times greater than the activity observed for its cationic relatives.^[88]

Interestingly, changing the solvent identity (for example, C₆H₆, THF, MeCN) decreased the hydroacylation activity significantly for the reactions involving the cationic catalyst, whereas the zwitterionic catalyst was not affected by this parameter.^[88] The authors suggested that the solvent effects were likely due to the cationic complexes being only marginally soluble in C₆H₆, whereas neither THF nor substrate were able to break up Rh-Rh dimer intermediate species, and strong ligation of MeCN may occur thereby inactivating the cationic complexes.^[88] Surprisingly, in switching to the zwitterionic catalyst, these issues were avoided.^[88]

A remarkable set of zwitterionic complexes reported by Stradiotto and coworkers employ an alternate approach to ligand anionicity than the aforementioned borate ligands. This approach utilizes a *P,N* donor set with an anionic indenide backbone to sequester the charge on the ligand.^[89] Interesting comparative studies were reported with regards to the catalytic activity of a zwitterionic ruthenium half-sandwich complex containing the indenide-*P,N* ligand compared to the analogous cationic complex containing the protonated version of the ligand (Figure 11). It was observed that the cationic complex was only marginally active for the transfer hydrogenation of acetophenone, providing final conversion to 1-phenylethanol of less than 25%. However, the zwitterionic complex was extremely active under the same conditions, yielding 99% conversion to 1-phenylethanol after five minutes. Amazingly, this complex is

amongst the most active catalysts for transfer hydrogenation that have been reported.^[90]

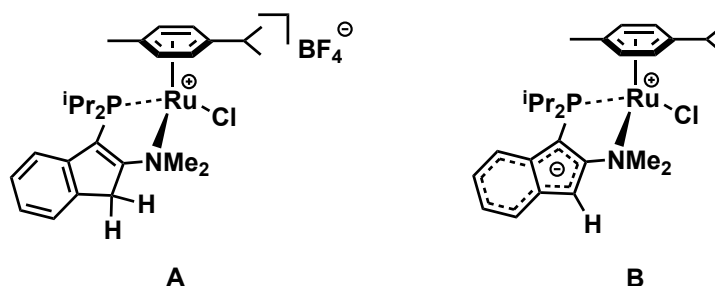


Figure 11. Cationic (A) and zwitterionic (B) complexes developed by Stradiotto and coworkers. Where the cationic complex is only marginally active for transfer hydrogenation, the zwitterionic complex is amongst the most active transfer hydrogenation catalysts reported.

When structural alterations of metal complexes give rise to pronounced distinctions in catalytic activity, there exists unique opportunities for the organometallic chemist to provide additional tools to widen the scope of chemical synthesis. The development of organometallic zwitterions represents such an opportunity, for it is clear from comparative studies involving these complexes and their corresponding cationic analogues that organometallic zwitterions can provide complementary stereochemical outcomes as well as increased catalytic activity compared to traditional cationic complexes.

1.5. [P,N] Hybrid Ligands: Implications of [P,N] Donor Systems, Hemilability and Ligand Cooperativity

Another ligand design strategy that has gained popularity is the incorporation of two or more distinctive donor functionalities into the ligand framework. These multidentate structures, termed hybrid ligands, can have remarkable ligative properties. Indeed, this is an expansive class of ligand, as one can imagine, due to the virtually endless possible combination of donor groups that are capable of binding to metal centers. Arguably, the most well-studied and abundant hybrid ligands reported in the literature are those based on a combination of phosphorous and nitrogen (that is, [P,N] donors).^[91] This is not surprising since, independently, P and N donor ligands are both ubiquitous in organometallics. Interestingly, when embedded within the same ligand architecture, [P,N] ligands display noteworthy properties not only as supporting ligands but also with regard to more functional roles by displaying hemilability and/or ligand cooperativity.

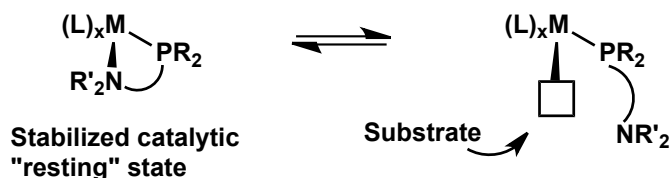
Having both P and N donor groups arranged to facilitate chelation can amalgamate their complimentary donor properties into a single ligand structure. In late metal chemistry, the P donor can provide a strong σ -donating anchor to the metal as well as the stabilization of electron-rich metal centres through its propensity to act as a π -acceptor.^[91-94] Furthermore, the N donor can help stabilize higher oxidation states and facilitate oxidative addition through added σ -

donation.^[95] Metal complexes containing [P,N] hybrid ligands have shown outstanding catalytic activity for a multitude of transformations.^[91,96]

In addition to the mixed donor characteristics, [P,N] hybrid ligands can display other interesting phenomena as a consequence of their heterodentacity. Not only can [P,N] ligands provide stabilizing effects through hemilability they can also play more of an active role in catalytic transformations, a process termed ligand cooperativity.^[97] These functional roles of [P,N] hybrid ligands can serve to stabilize catalysts throughout the catalytic cycle as well as dramatically increase catalytic activity.

Hemilability is a process that arises through the ability of one of the donor groups of a multidentate ligand system to exhibit reversible displacement. The labile nature of a donor group serves to preserve the integrity of the catalyst by reversibly occupying vacant site(s) on the metal during catalysis,^[96-99] prohibiting potential degradation pathways that would otherwise inactivate the catalytic species. In essence, these ligands act as organometallic protecting groups thereby generating a more robust catalyst (Scheme 6).

With respect to [P,N] ligands and late transition metals, the favourable soft/soft P-metal interaction provides a strong anchor of the ligand to the metal, whereas the generally hard/soft incongruity of the N-metal interaction usually serves as the site of hemilability. Indeed, substitution of the N donor group can provide a means by which to fine-tune the extent of hemilability.^[100,101] However, there exists a balance where the N-donor must be sufficiently labile to allow for



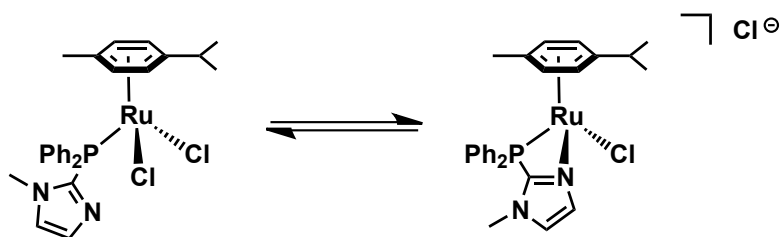
Scheme 6. The hemilability of a [P,N] hybrid ligand. Chelation stabilizes the complex whereas displacement of the N provides a vacant site on the metal for substrate interaction.

displacement, either by substrate or other species involved in the catalytic transformation, but still able to bind to the metal when stabilization is necessary. The chelation effect certainly promotes N-metal interaction since the ligand remains bound to the metal through the P donor moiety holding the N donor close to the coordination sphere. Therefore, the proximity of the two donor groups can also be utilized as a hemilability tuning mechanism since hybrid [P,N] ligands that chelate to form strained metallacycles contributes to the degree of hemilability.^[102-104]

Remarkably, in addition to the stabilization effects inherent to hemilability, hybrid [P,N] ligand systems can exhibit cooperative effects that can influence catalytic performance dramatically. Ligand cooperation refers to a ligand partaking directly in the catalytic transformation through secondary interactions which promote the catalytic activity of the complex.^[97] This chemical interaction has also been referred to as ligand non-innocence since ligands acting in a cooperative fashion are more than just innocent spectators serving exclusively as electron-

donor functionalities. Certainly, a testament to the advantageous nature of this concerted metal-ligand partnership is the fact that the metalloenzyme galactose oxidase has evolved to include a cooperative tyrosinyl ligand which aids in the conversion of primary alcohols to aldehydes with extraordinary activity.^[97]

Interestingly, in most reports of metal complexes containing hybrid ligands, hemilability and cooperativity are implied and not often observed directly.^[91,99] Computational, crystallographic, and spectroscopic evidence have been employed to support the formation of transient species that result from hemilabile and/or cooperative processes.^[96,105-110] One method to provide experimental evidence for hemilability is to document the reversible ring-opening of metallacycles containing [P,N] chelates. For example, phosphino(imidazole) ligands have been established as useful [P,N] hybrid ligands in a variety of catalytic transformations, including Suzuki C-C bond couplings,^[111-113] Buchwald-Hartwig aminations,^[111,114] and hydrogenation reactions.^[103,115] These ligands have displayed reversible metallacyclic ring-opening in both Ru^[103] and Pd^[116] systems. The Ru complexes containing (phosphino)imidazoles (Scheme 7)



Scheme 7. Ruthenium-phosphinoimidazole complex displaying dynamic ring opening of the 4-membered metallacycle.^[103]

studied by Caballero and co-workers displayed dynamic solution behavior where equilibrium was established through reversible displacement of the coordinated imidazolyl N donor by a chlorido ligand. Similar observations have been reported by Lee and co-workers involving Ru-PTA-amine (PTA= 1,3,5- triaza-7-phosphaadamantane) complexes.^[96]

1.6. Concluding Remarks

Organometallic ruthenium complexes have proven to be among the most remarkable classes of homogeneous catalysts. Through novel ligand design, the integration of such concepts as zwitterionicity, hemilability, and ligand cooperativity continue to push the boundaries of organometallic chemistry providing synthetic chemists with state of the art methodologies to perform a plethora of catalytic transformations in various areas of chemistry. Advancement with regard to the understanding of these complexes is crucial in order to continue the design of innovative complexes in a coherent and rational manner.

Chapter Two: Research Objectives and Rationale

2.1. Ligand Design

The focus of the research presented within this work centres on the development of novel [P,N] hybrid ligands based on the benzimidazole scaffold (Figure 12). It was reasoned that this general scaffold would provide a highly tunable ligand system, providing control over the electronics of the P-donor group as well as the hemilability of the N-donor. Altering the identity of the groups on the phosphorus centre would allow for the regulation of the electronic and steric nature of this group, whereas variation of the chelate ring size by variation of the proximity between the phosphine group and the benzimidazole backbone, may provide a means to manipulate the hemilability of these ligands. In addition, we aimed to sequester sufficiently a negative charge within the framework, through a BPh_4^- group tethered to N-1 of the heterocycle by a $-\text{CH}_2-$ spacer (Figure 12), providing

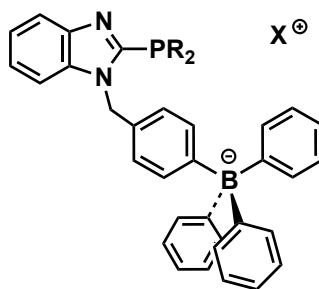


Figure 12. General molecular structure of the proposed anionic [P,N] ligand system.

access to zwitterionic ruthenium complexes. Initial focus would be on the development of a reliable synthetic method to provide access to these ligands followed by investigations concerning their electron-donating power. Derivatization by substitution of the groups at the phosphorus donor or by distancing the phosphorus group from the benzimidazole ring would ensue. Analogous neutral ligands having a similar steric profile, as the example illustrated in Figure 13, would be synthesized and serve for comparative purposes.

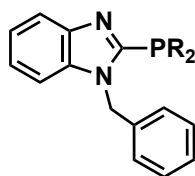
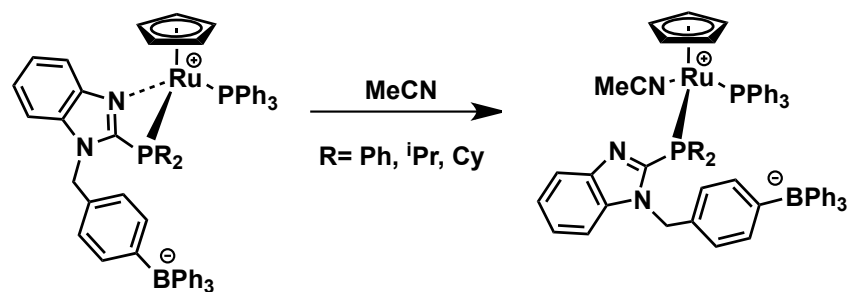


Figure 13. A neutral ligand analogue used for comparative purposes.

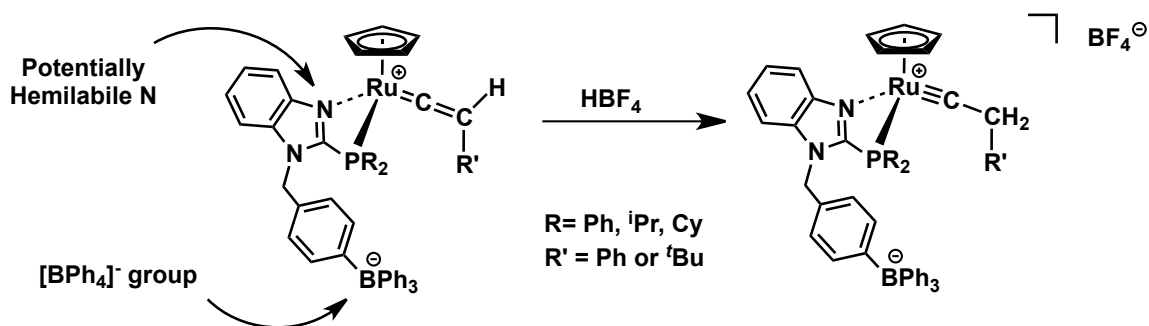
2.2. Coordination Chemistry

Our intent was to explore the use of these new ligands in ruthenium half-sandwich complexes containing facially coordinated Cp, Cp* and *p*-cymene supporting ligands. Reactions with small, potentially coordinating, molecules were chosen to investigate the ability of the anionic phosphino(benzimidazole) ligands to display hemilability (Scheme 8). In addition, due to our long-standing interest in the synthesis of ruthenium-carbyne complexes as potential initiators of alkyne metathesis, we planned attempts to synthesize these types of complexes



Scheme 8. Ring opening of a metallacycle containing the target anionic ligands.

incorporating our new [P,N] hybrid ligand systems. Previous success with synthesizing ruthenium-carbynes via the protonation of ruthenium-vinylidene precursors prompted us to explore this technique to synthesize our target carbyne complexes (Scheme 9).^[117-119]



Scheme 9. Proposed synthesis of a Ru carbyne target complex via protonation of a Ru vinylidene precursor. Specific features of the new [PN] ligands are highlighted.

Chapter Three: Ligand Syntheses

3.1. Attempts to Synthesize Various [P,N] Ligands

At the onset of this project, the intent was to synthesize a library of heterobidentate [P,N] chelating ligands with the common feature of a pendant $[\text{RBPPh}_3]^-$ anion incorporated into the ligand architecture. Much time and effort during this venture was spent exploring the synthesis of different [P,N] scaffolds, largely trying to install the borate unit (Figure 14). However, introducing the boron-containing functionality strategically into the general ligand

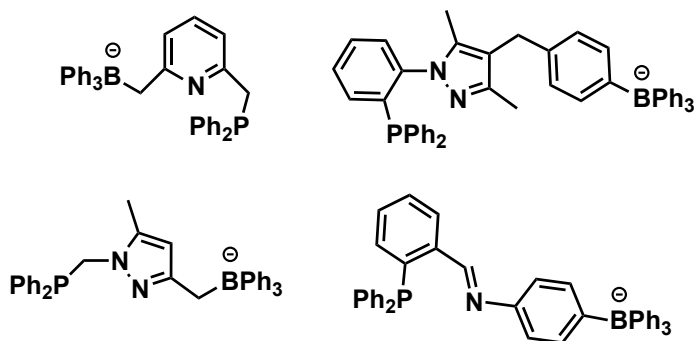


Figure 14. Some Examples of target ligands explored during the first stage of the project.

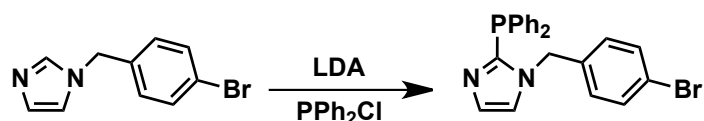
framework proved to be a very synthetically challenging task, and during the early stages of exploration, ^{11}B NMR spectroscopy was not being utilized to its full extent to monitor the fate of the boron.

As research progressed, it became clear that ^{11}B NMR spectroscopy was perhaps the best tool to monitor the synthesis stages involving the introduction of boron to the general ligand scaffold. Ultimately, this assisted with the successful development of the ligand systems reported herein, and which formed the basis of the majority of the research. Nonetheless, it is important that a general statement be made regarding attempts to design and synthesize a number of different libraries of anionic phosphine-based ligands, as it would represent a disservice to the amount of time and work that was devoted to the early stages of this research project. However, discussing the details regarding the composition and structure of these other ligand targets would largely be speculative. Thus, in order to provide congruence with respect to the progression of this research project, any discussion on the synthesis of these other targets has been omitted.

3.2. The Synthesis of Anionic 2-(Diphenylphosphino)benzimidazoles

Tertiary phosphine ligands containing imidazole groups have been used in transition metal chemistry for decades ^[120-122] and these hybrid ligands have attracted much interest over recent years.^[112-114,116,123-126] When we originally set out to synthesize a library of [P,N] hybrid ligands containing N-heterocycles, we first considered utilizing imidazole as a building block in order to access (ultimately) heterobidentate [P,N]-ligands. Installing the necessary 4-bromobenzyl group at the N-1 position of imidazole to produce the required 1-(4-bromobenzyl)imidazole precursor was straightforward.^[127] The subsequent

phosphination step also proceeded smoothly using LDA as base, and yielded 1-(4-bromobenzyl)-2-(diphenylphosphino)imidazole in reasonable yields (Scheme 10). However, during the final step in the synthesis of the desired target – the installation of the BPh₃ group at the C-Br bond of the pendant 4-bromobenzyl substituent – difficulties were encountered with regioselectivity. In



Scheme 10. Synthetic strategy for preparing 1-(4-bromobenzyl)-2-(diphenylphosphino)imidazole.

particular, the use of ⁿBuLi as a metallating agent not only lithiated the C-Br bond of the 1-(4-bromobenzyl)-2-(diphenylphosphino)imidazole precursor but also at C-4 and C-5 positions of the imidazole core.^[128] The resulting mixture of phosphine-containing products proved difficult to purify, and modifying the reaction parameters (*e.g.*, temperature, time and solvents) and metallating agents (*e.g.*, ^tBuLi) did not improve the product distribution. It was therefore decided that a slightly different approach would be pursued.

In an effort to circumvent the reactivity issue of the imidazole backbone, benzimidazole was chosen as an alternative heterocyclic scaffold. We reasoned that, if deprotonation was occurring at the 4- and 5-positions of the imidazole ring,

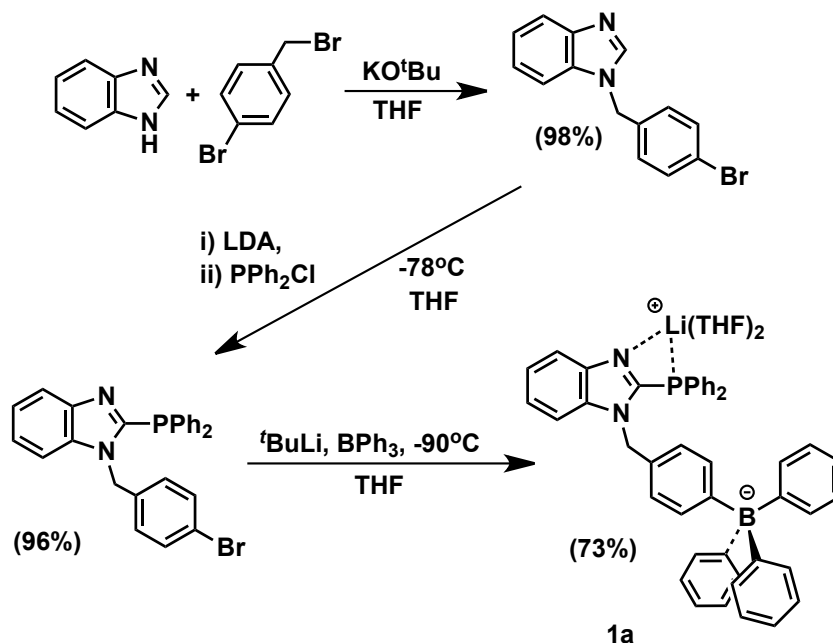
then employing benzimidazole would eliminate these sites, and preference for lithiation would be at the desired C-Br bond of the 4-bromobenzyl substituent. Indeed, switching to the benzimidazole group would also preserve the desired ligand characteristics of the imidazole design.

3.3. Synthesis of an Anionic 2-(Diphenylphosphino)benzimidazole Ligand

A major convenience of including benzimidazole into the ligand design was that benzimidazole is readily available and inexpensive. In addition, coupling of a benzyl group to the 1-position of benzimidazole can be achieved in a fairly straightforward manner using KO^tBu and 4-bromobenzyl bromide (Scheme 11).^[127] With this precursor in hand, the plan was first to introduce a -PPh₂ group at the 2-position of the benzimidazole ring using LDA and PPh₂Cl. It was expected that the use of LDA would selectively lithiate at the 2-position leaving the Br-phenyl group intact for subsequent functionalization with BPh₃. After lithium-halogen exchange at the 4-bromophenyl group via ^tBuLi, the final step of this synthetic approach would be to displace the lithium using BPh₃. This last step in the synthesis would be congruent with the installation of the borate group on (phosphino)borate ligands of the form [PR₂(*p*-Ph₃BC₆H₄)].^[54,76] The complete synthesis of the target anionic [P,N] ligand (*i.e.*, ligand **1a**) is outlined in Scheme 11.

The penultimate step in the synthesis of **1a** involved the introduction of the -PPh₂ group to the 1-(4-bromobenzyl)benzimidazole scaffold. LDA proved

effective at regioselectively deprotonating the C-1 position of the 1-(4-bromobenzyl)benzimidazole precursor, and subsequent quenching with the



Scheme 11. Synthesis of ligand **1a**.

electrophile PPh_2Cl led to the synthesis of 1-(4-bromobenzyl)-2-(diphenylphosphino)benzimidazole in very high yields (96%). Strict attention to reaction temperature, base and time was required for the synthesis of the precursor 1-(4-bromobenzyl)-2-(diphenylphosphino)benzimidazole otherwise tetraphenyldiphosphine monoxide was observed to form as a by-product after work-up.^[129]

Similarly, the final step in the synthesis of **1a** from 1-(4-bromobenzyl)-2-(diphenylphosphino)benzimidazole also required special consideration. Through experimentation, it was determined that $^t\text{BuLi}$ worked well at regioselectively

lithiating the C-Br bond of the 1-(4-bromobenzyl)-2-(diphenylphosphino)benzimidazole precursor. The metalating agents $^n\text{BuLi}$, $^i\text{PrMgCl}$ and $^i\text{PrMgCl}\cdot\text{LiCl}^{[130]}$ were less effective than $^t\text{BuLi}$. However, the addition of the BPh_3 electrophile to the metalated intermediate proved to be more challenging. For example, rapid addition (<1 minute) of the BPh_3 produced a solution whose $^{31}\text{P}\{^1\text{H}\}$ NMR spectrum revealed two signals at δ -30.2 ppm and δ -30.6 ppm (Figure 15). Through the use of ^{11}B NMR spectroscopy, it was

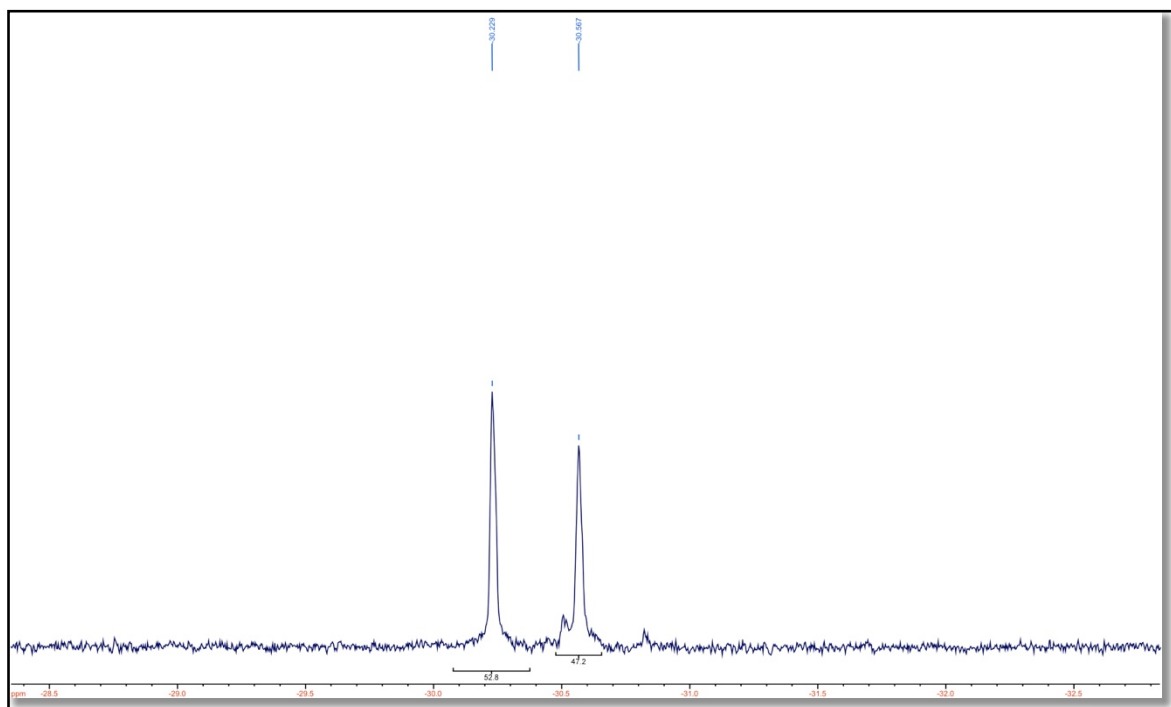


Figure 15. $^{31}\text{P}\{^1\text{H}\}$ NMR spectrum of the solution generated by the addition of BPh_3 to lithiated 1-(4-bromobenzyl)-2-(diphenylphosphino)benzimidazole. The peak upfield is a result of the compound formed by BPh_3 attaching to the N-3 of the benzimidazole ring. A sealed capillary tube containing D_2O was used along with a sample of the reaction mixture to obtain *in situ* NMR data.

speculated that, in addition to the production of **1a**, a second product, arising from the BPh_3 adding to the N-3 position of the benzimidazole unit, was also forming (Figure 16), appearing as a broad signal at δ 0.26 ppm.^[131-133] Independent

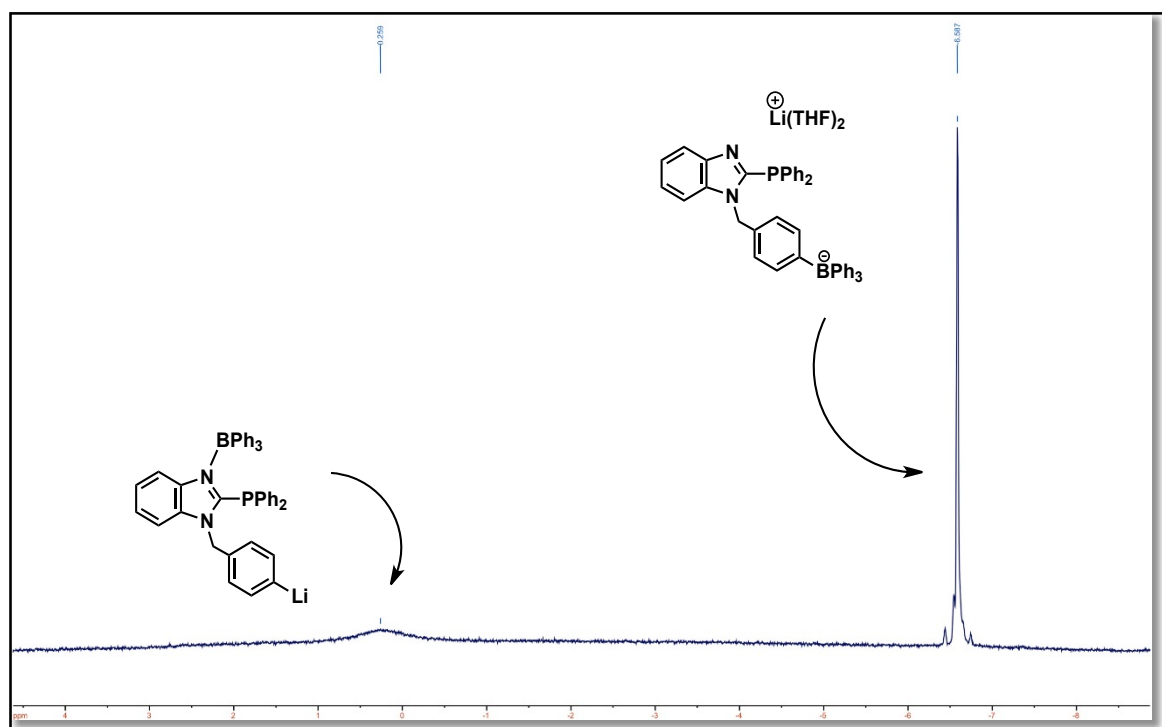


Figure 16. ^{11}B NMR spectrum of the mixture obtained by the addition of BPh_3 to lithiated 1-(4-bromobenzyl)-2-(diphenylphosphino)benzimidazole. The broad signal at δ 0.26 ppm is from the B-N adduct as illustrated whereas the signal at -6.6 pertains to the desired product.

experiments between 1-(4-bromobenzyl)-2-(diphenylphosphino)benzimidazole alone with BPh_3 also produced ^{11}B NMR spectra with a broad signal around δ 0.26 ppm. Eventually, it was determined that the rate of BPh_3 addition, as well as the

temperature, had a significant effect on the formation of the N-addition product. Very slow addition of this reagent, as a dilute THF solution, at $-90\text{ }^{\circ}\text{C}$ produced maximum yield of ligand **1a** (73%).

Ligand **1a** produces a singlet at δ -24.1 ppm in the ^{31}P NMR spectrum, while the ^1H NMR spectrum reveals that two equivalents of THF are retained in the product. The ^{11}B NMR chemical shift for ligand **1a** appears at δ -6.7 ppm, which is similar to that observed for NaBPh_4 (δ -6.2 ppm).^[134] The Ph_4P^+ salt of ligand **1a** (**1a'**) can easily be prepared via cation metathesis using Ph_4PX (X = Cl or Br) in CH_2Cl_2 . Interestingly, the ^{31}P chemical shift of the anion of **1a'** appears further upfield (δ -28.1 ppm) of that observed for **1a**, suggesting that in the latter case the anion $[\text{P}^{\text{Ph}}\text{NBPh}_4]^-$ chelates to the $[\text{Li}(\text{THF})_2]^+$ cation in solution. Indeed, the ^7Li NMR spectrum of **1a** in CDCl_3 shows a sharp singlet at δ -0.35 ppm, and appears in a region observed for other similar systems,^[135-137] at lower temperatures, however, this signal only broadens, and unfortunately no distinct coupling to phosphorus is observed. A set of 1:1:1:1 quartets with different intensities were observed in the ^{13}C NMR spectrum of **1a**, appearing downfield around 164 ppm pertaining to the *ipso* carbons of the two different B-Ph linkages (Figure 17). The multiplicity of these signals arises from ^{11}B - ^{13}C coupling (^{11}B has a nuclear spin of 3/2).

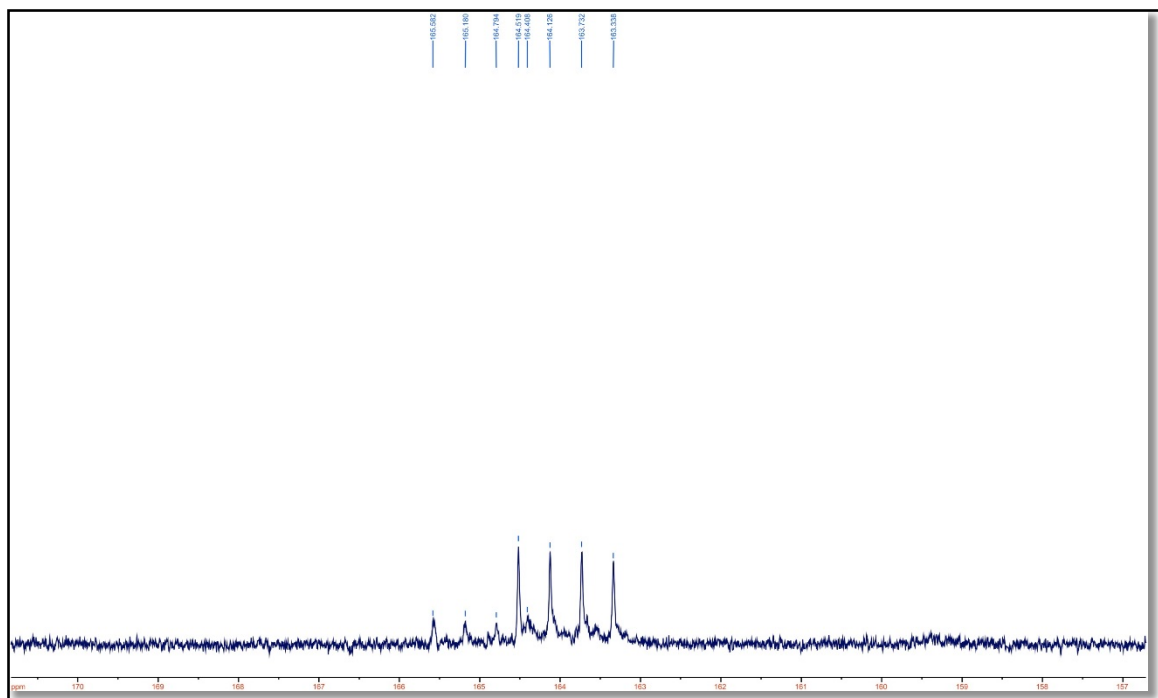


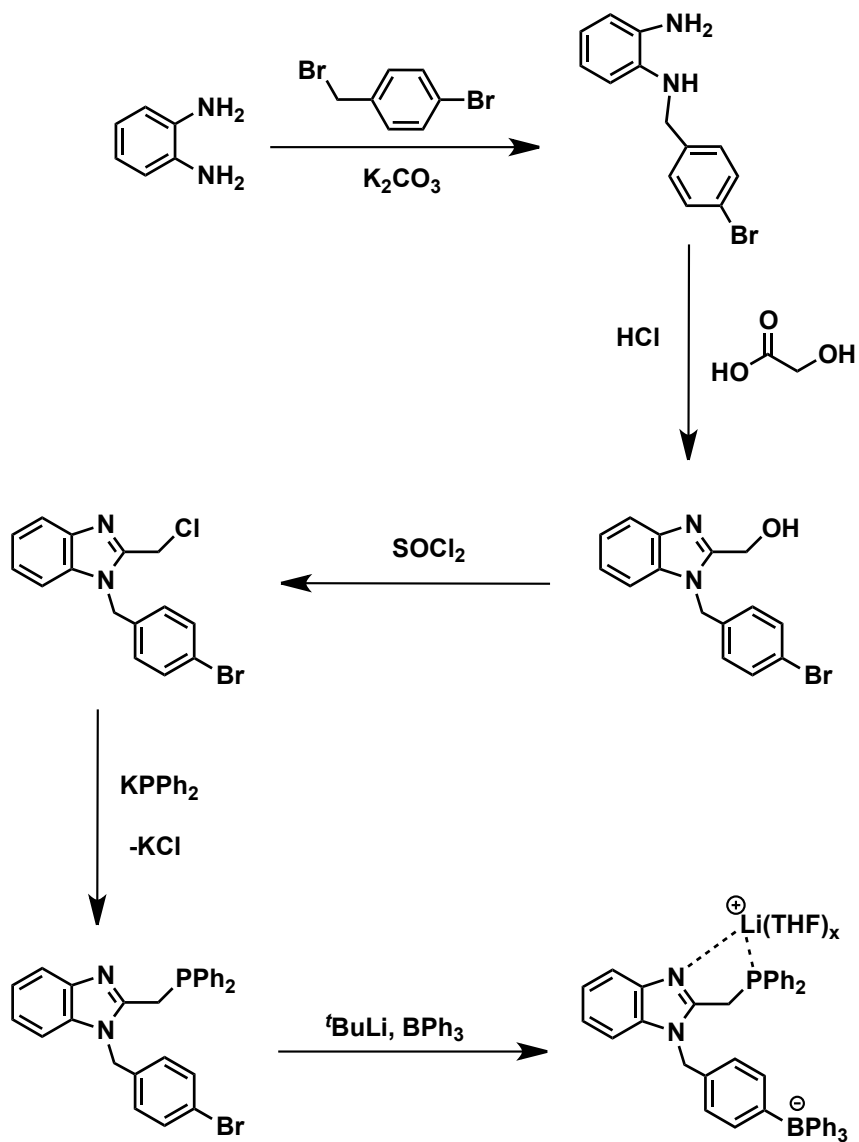
Figure 17. ¹³C NMR spectrum of ligand **1a** revealing the two quartets generated by the set of chemically inequivalent B-Ph carbon atoms.

3.4. Ligand Derivatization: Chelate Expansion

In an effort to explore the impact of the distance between the donor atoms of the anionic (phosphino)benzimidazole ligands on their hemilability, a number of different strategies geared towards increasing the distance between the -PR_2 group and N-3 of the benzimidazole core were explored. Unfortunately, these strategies eventually revealed several synthetic challenges. One method which provides access to the general benzimidazole ring structure is through condensation of 1,2-diaminobenzene, or its derivatives^[138], with carboxylic

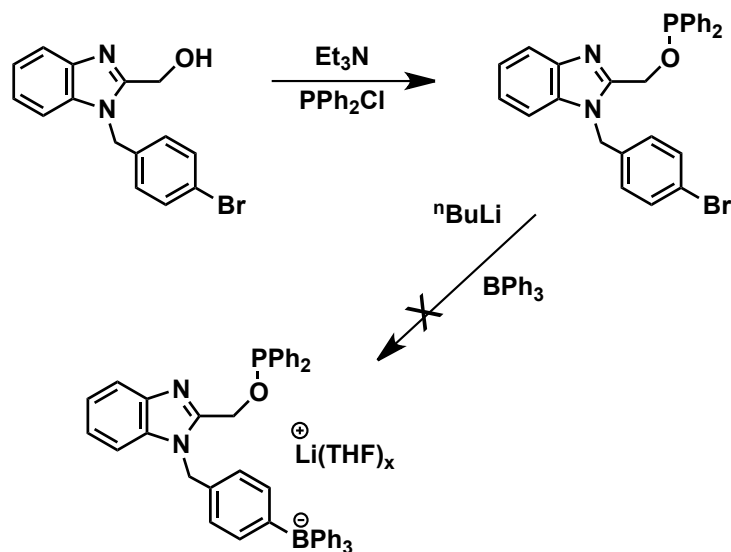
acids.^[139] We chose to explore this method in order to generate ligands which would allow an expanded chelate ring size compared to **1a**. However, these efforts were met with difficulties, either during the phosphine or boron addition steps. For example, we envisioned a synthetic path to insert a methyl spacer between the phosphorus and the benzimidazole groups as illustrated in Scheme 12. Although laborious, the steps towards generating 1-(4-bromobenzyl)-2-(chloromethyl)benzimidazole proceeded smoothly. However, addition of the $-PR_2$ group to this precursor using $KPPh_2$ proved to be problematic, and produced significant amounts of $HPPH_2$ as the major product. It was suspected that perhaps the proton source for the $HPPH_2$ might be the chloromethyl group of the 1-(4-bromobenzyl)-2-(chloromethyl)benzimidazole precursor since this group would be experiencing electronic effects from both the chloride as well as the benzimidazole ring. To try and impart selective phosphine addition at the desired position, the same reaction was tried, but instead with 1-(4-bromobenzyl)-2-(bromomethyl)benzimidazole, reasoning that Br, a better leaving group, would help in this regard. Unfortunately, a number of species were generated from this reaction, as evidenced by multiple peaks in the $^{31}P\{^1H\}$ NMR spectrum. Variation of the reaction parameters (time, temperature, solvent) also did not provide a viable pathway to the target ligand precursor.

An alternative strategy which would allow distancing the phosphine donor from the benzimidazole core was to install a phosphite group using a



Scheme 12. Proposed synthetic scheme to derivatize ligand **1a**.

2-(hydroxymethyl)benzimidazole precursor (Scheme 13). Addition of PPh_2Cl to the benzimidazole precursor in the presence of trimethylamine as a chloride



Scheme 13. Attempted synthesis of 1-(4-bromobenzyl)-2-(((diphenylphosphino)oxy)methyl)benzimidazole.

scavenger afforded the phosphite in good yield (Figure 18). It was necessary to be very vigilant and ensure that the reaction vessel, reagents, and syringes were devoid of residual moisture to ensure clean conversion to the product. Unfortunately, lithiation of the phosphite precursor, *en route* to the installation of the borane moiety in the final step of the synthesis of the target, resulted in cleavage of the P-O bond. Evidence for this degradation pathway was provided by an upfield shift in the ${}^{31}\text{P}\{^1\text{H}\}$ NMR spectrum from δ 119 ppm (parent phosphite) to δ -15 ppm when ${}^n\text{BuLi}$ was used as the lithiating agent.

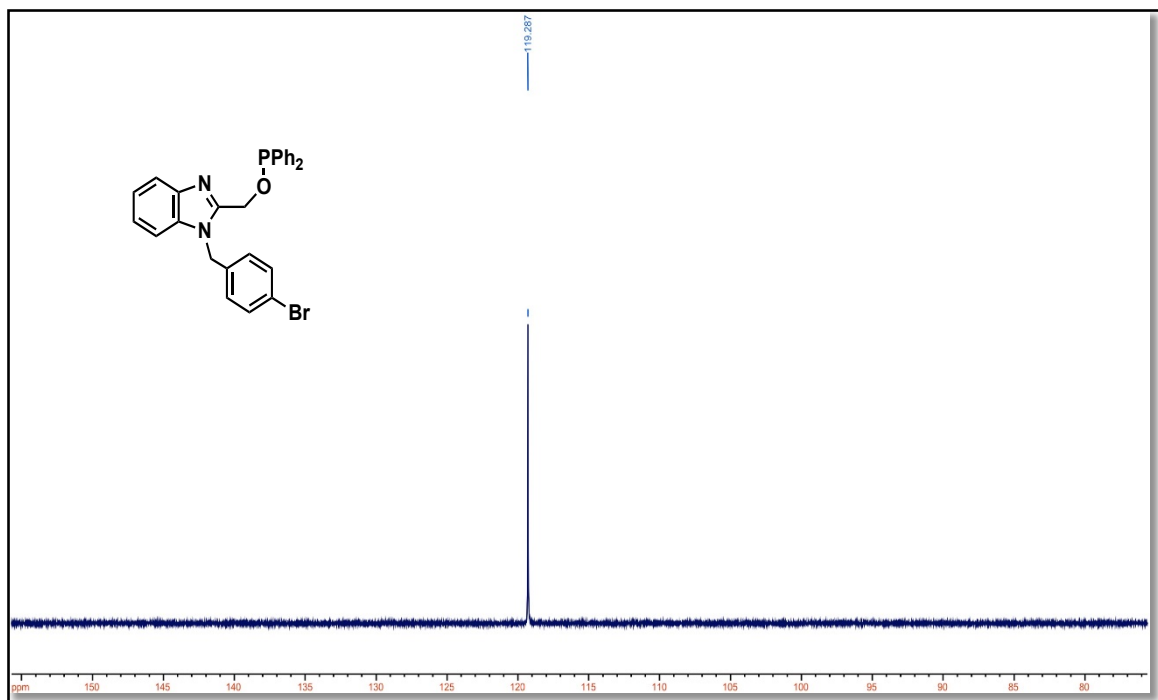


Figure 18: $^{31}\text{P}\{^1\text{H}\}$ spectrum of 1-(4-bromobenzyl)-2-(((diphenylphosphino)oxy)methyl)benzimidazole.

The chemical shift of this product is consistent with the formation of ${}^n\text{BuPPh}_2$,^[140] and its formation is perhaps assisted by the chelating nature of the phosphite precursor. At this point, it was decided, largely due to time constraints, to abandon these initiatives in order to explore further variations of the groups attached to the phosphorus donor atom of **1a** and **1a'**.

In the course of studying the synthesis of $[\text{Li}(\text{THF})_2][\text{P}^{\text{Ph}}\text{NBPh}_4]$, it was found that the general synthetic method could be adapted to include other PR_2Cl phosphine reagents. Specifically, the use of $\text{P}^{\text{iPr}}_2\text{Cl}$ and PCy_2Cl provided access to the ligands $[\text{Li}(\text{THF})_2][\text{P}^{\text{iPr}}\text{NBPh}_4]$, **1b**, and $[\text{Li}(\text{THF})_4][\text{P}^{\text{Cy}}\text{NBPh}_4]$, **1c** (Figure 19),

albeit in only moderate yields compared to **1a**. It was found that **1c** was isolated as the $\text{Li}(\text{THF})_4^+$ salt (as opposed to $\text{Li}(\text{THF})_2^+$ for **1a** and **1b**) likely due to the increased size of the anion of **1c**. In light of the cost of the reagents used in these syntheses, optimization of the reaction conditions to produce **1b** and **1c** were explored. Aspects of the final lithiation step were first investigated. For

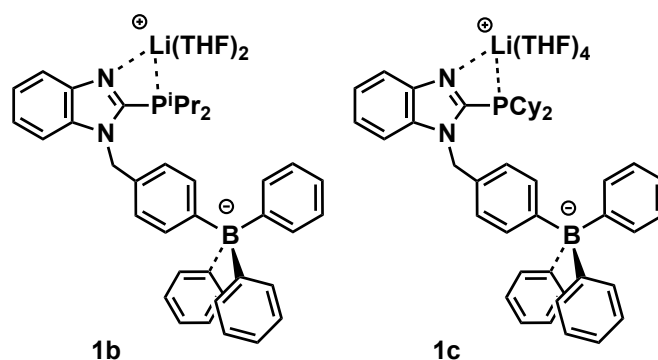


Figure 19. Molecular structures of $[\text{Li}(\text{THF})_2][\text{P}^{\text{iPr}}\text{NBPh}_4]$ (**1b**) and $[\text{Li}(\text{THF})_4][\text{P}^{\text{Cy}}\text{NBPh}_4]$ (**1c**).

example, increasing the molar ratio of $^t\text{BuLi}$ (up to two equivalents) had little effect on the yields. Although reducing the addition rate of the boron reagent for the production of ligand **1a** had a significant effect on the yield of this reaction, an even further

reduction in the addition rate of BPh_3 for the synthesis of ligands **1b** and **1c** had little effect. The only parameter that seemed to provide an increase in yield was the temperature at which the BPh_3 was added. In fact, lowering the temperature below $-100\text{ }^\circ\text{C}$ provided optimal yields of ligands **1b** and **1c**. Interestingly, a

much more pronounced effect regarding the phosphine-lithium interaction was observed in these ligands. For instance, the $^{31}\text{P}\{^1\text{H}\}$ NMR signal pertaining to ligand **1b** was significantly broadened compared to that of ligand **1a** whereas the corresponding signal generated by **1c** was, at times, difficult to distinguish from the baseline. However, removal of Li^+ via salt metathesis with PPh_4Cl (or by reaction with ruthenium precursors, *vide infra*) resolved this issue (generating ligands $[\text{PPh}_4][\text{P}^{\text{iPr}}\text{NBPh}_4]$, **1b'**, and $[\text{PPh}_4][\text{P}^{\text{Cy}}\text{NBPh}_4]$, **1c'**), producing sharp $^{31}\text{P}\{^1\text{H}\}$ NMR signals (Figure 20). Parallel to the observations for **1a**, there is an absence of phosphorus-lithium coupling in the ^7Li NMR spectra for **1b** and **1c**. As expected, spectroscopic details for **1b** and **1c** were similar to those of **1a**, including single $^{31}\text{P}\{^1\text{H}\}$ (CD_2Cl_2) NMR spectra peaks resonating at δ -8.0 ppm (**1b**) and δ -19.7 ppm (**1c**), and sharp ^{11}B NMR spectra peaks around -6.7 ppm. Furthermore, two sets of overlapping four-line multiplets are observed in the ^{13}C NMR spectra pertaining to the *ipso* carbons of the two different B-Ph linkages.

In addition to the anionic (phosphino)benzimidazole ligands, neutral variants of ligand **1a** were synthesized for comparative purposes (*vide infra*). Similar to the synthesis of **1a**, benzimidazole was first alkylated at N-1 using either benzyl bromide^[141] or methyl iodide to produce 1-benzyl- or 1-methylbenzimidazole, respectively (see Scheme 14). Each N-alkylbenzimidazole

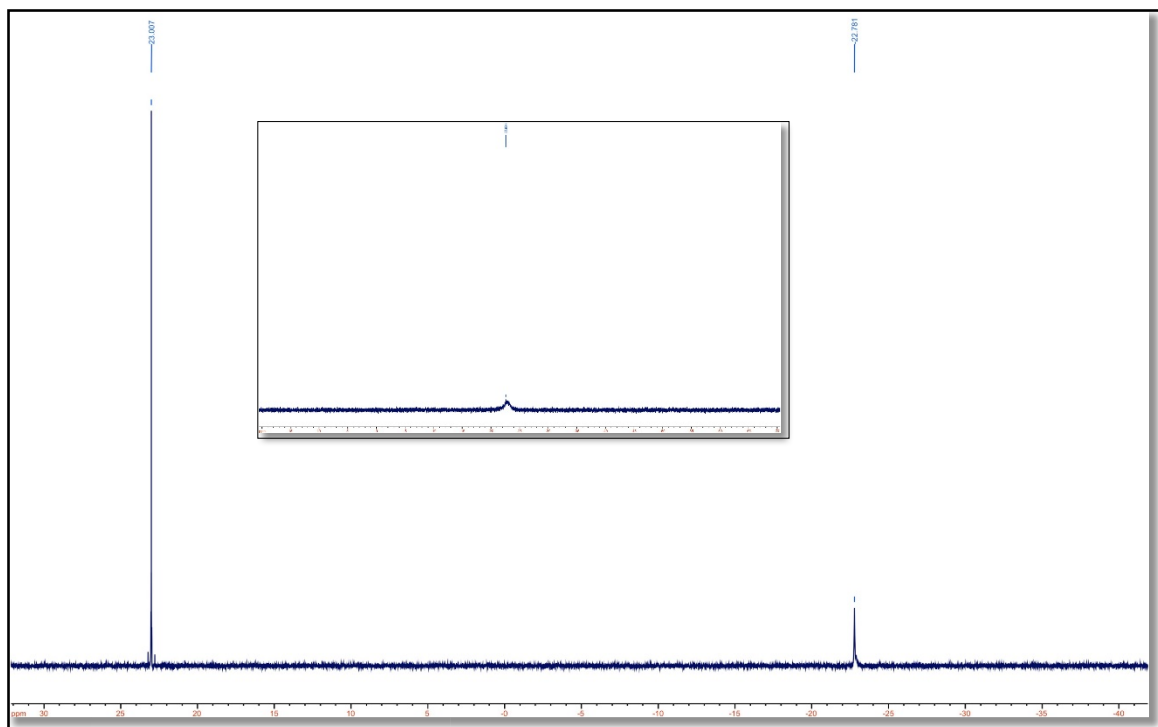
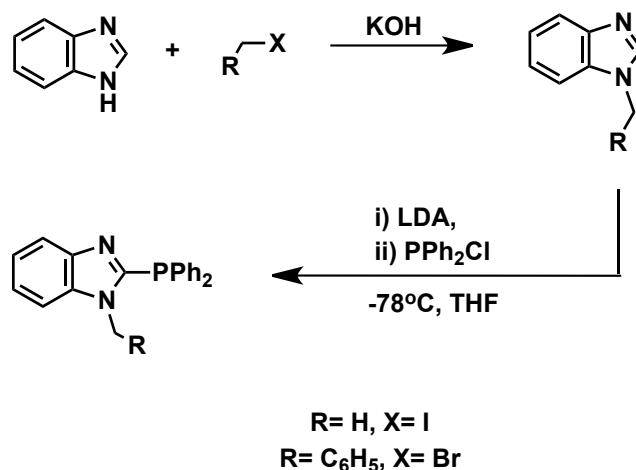


Figure 20. $^{31}\text{P}\{^1\text{H}\}$ NMR spectra highlighting the effect of cation exchange for ligand **1c**. The PPh_4^+ resonates at 23.0 ppm whereas the anion of ligand **1c'** appears at -22.8 ppm. Inset is the spectrum of the $\text{Li}(\text{THF})_4^+$ salt appearing as a broad signal at -22.6 ppm.

was then phosphinated using the same procedure described for **1a**, yielding 1-benzyl-2-(diphenylphosphino)benzimidazole (abbreviated as $[\text{PN}^{\text{Bz}}]$) and 1-methyl-2-(diphenylphosphino)benzimidazole (abbreviated as $[\text{PN}^{\text{Me}}]$).



Scheme 14. Synthesis of neutral homologues of **1a**.

3.5. Electron Donating Power: Assessment via ^{31}P - ^{77}Se Coupling Constants

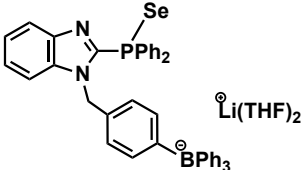
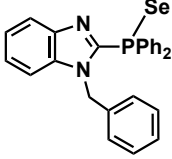
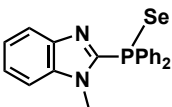
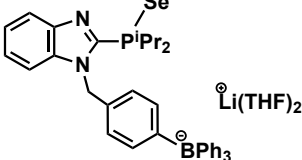
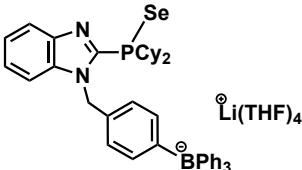
Probing the electronic character of phosphine ligands through the measurement of ^{31}P - ^{77}Se coupling constants has gained popularity recently due to the simplistic nature of this method compared to traditional techniques.^[56,126,142-148] Indeed, the selenide method for measuring the basicity of phosphines coincides well with measuring this property using IR spectroscopic stretching frequencies of metal carbonyl compounds,^[56,145] but perhaps represents a more convenient alternative method. A decrease in the magnitude of the $^1J_{\text{PSe}}$ coupling constant of a P-Se bond of R_3PSe corresponds to an increase in the σ -donating ability of R_3P (*i.e.*, lower degree of *s*-character of the parent phosphine). For example, when the Ph groups of PPh_3 are sequentially replaced by Cy groups in the series PPh_3 , PPh_2Cy , PPhCy_2 , PCy_3 the $^1J_{\text{PSe}}$ coupling constant of the

corresponding phosphine selenides decrease in magnitude (Table 1).^[146] The trend is fairly consistent except for phosphorus environments of extreme steric bulk such as that found in P^tBu_3 .^[144]

Facile generation of the selenides of ligands **1a-c**, as well as the neutral ligands $[\text{PN}^{\text{Bz}}]$ and $[\text{PN}^{\text{Me}}]$, was achieved by heating the ligands in the presence of a slight excess of elemental selenium. Measurement of the ^{31}P - ^{77}Se coupling constants allowed for the comparison of the electronic properties of the different phosphine ligands. The results are summarized in Table 1. Interestingly, the presence of the borate in the structure of **1a** does not seem to have a significant effect on the electronic nature of the phosphine group since the $^1J_{\text{PSe}}$ of the selenide for this system is very similar to those of the neutral analogues $[\text{PN}^{\text{Bz}}]$ and $[\text{PN}^{\text{Me}}]$. This is not surprising given that the borate is far removed from the phosphorus donor and is in agreement with related systems comparing the effect of borate proximity on the Lewis basicity of the phosphorus.^[56] The relative donor strengths of the anionic ligands follows the trend of **1a** < **1b** < **1c**, and suggests the cyclohexyl analogue **1c** is the most powerful donor phosphine of the series, while the phenyl analogue **1a** is the weakest. These observations are consistent with the traditional tertiary phosphines PPh_3 , PMe_3 , and PCy_3 as illustrated in Table 1.^[144,146] In this series, when the substituents on the phosphorous become better electron donors (ie. $\text{Ph} < \text{Me} < \text{Cy}$) the direct spin-spin coupling constant of the corresponding phosphine selenide decreases.^[146]

With reliable ligand syntheses in hand, we next turned our attention towards their coordination behavior in ruthenium half-sandwich chemistry.

Table 1. $^{31}\text{P}\{^1\text{H}\}$ NMR data for the phosphine selenides in CDCl_3 .

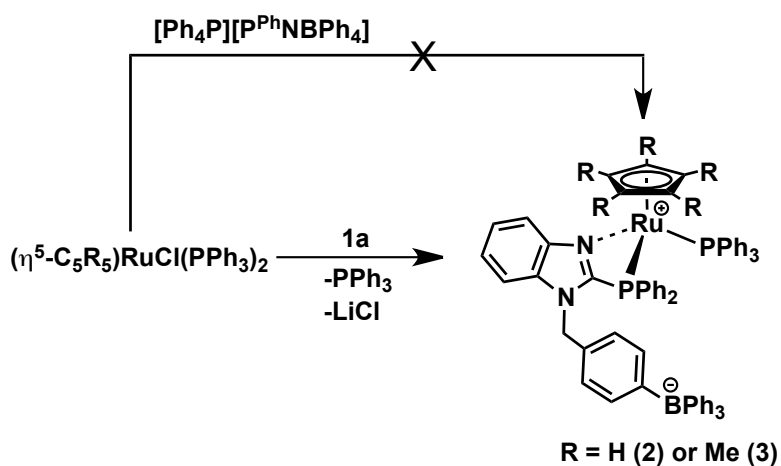
Selenide	$^{31}\text{P}\{^1\text{H}\}$ (δ/ppm)	$^1J_{\text{PSe}}$ (Hz)
	20.3 ^a	741 ^a
	20.4 ^a	742 ^a
	20.4 ^a	742 ^a
	51.0 ^a	712 ^a
	42.6 ^a	704 ^a
$\text{Ph}_3\text{P}-\text{Se}$	36.8 ^b	730 ^b
$(\text{Ph})_2\text{CyP}-\text{Se}$	46.3 ^b	725 ^b
$\text{Ph}(\text{Cy})_2\text{P}-\text{Se}$	55.9 ^b	701 ^b
$\text{Cy}_3\text{P}-\text{Se}$	59.2 ^b	673 ^b
$\text{Me}_3\text{P}-\text{Se}$	-	684 ^b

^a Data from this work. ^b Taken from references. ^[144, 146]

Chapter Four: Coordination Chemistry

4.1. Ligand Complexation Involving Ruthenium-Cp and Ruthenium-Cp* Precursors

Our initial efforts focused on reacting ligand **1a** and **1a'** with ruthenium-cyclopentadienyl precursors (Scheme 15). For example, stirring an equimolar mixture of $\text{CpRuCl}(\text{PPh}_3)_2$ and ligand **1a** in refluxing 1,2-dichloroethane leads to the substitution of the chloride ligand and one PPh_3 ligand, and yields the yellow, air-stable, chelated zwitterionic complex **2**. The corresponding reaction with



Scheme 15. Synthesis of complexes **2** and **3**. The presence of Li^+ is crucial for the formation of these species, as evidenced by the absence of reaction when the precursor is mixed with ligand **1a'**.

$\text{Cp}^*\text{RuCl}(\text{PPh}_3)_2$ occurs under milder conditions (*i.e.*, at room temperature), and produces yellow-orange complex **3**. The difference in reactivity between the Cp and Cp^* complexes is likely a result of the increased electronic and steric profiles of the Cp^* ligand, factors that would help facilitate labilization of the PPh_3 ligands.^[149-154]

These results are in contrast most other reactions between $(\text{C}_5\text{R}_5)\text{RuCl}(\text{PPh}_3)_2$ (R= H or Me) and neutral bidentate phosphine ligands, where often both PPh_3 ligands are displaced, and the chloride is retained as a ligand in the product.^[155-157] The $^{31}\text{P}\{^1\text{H}\}$ NMR spectra of **2** and **3** each reveal two doublets of an AX pattern corresponding to the PPh_3 ligand (δ_{A} 49.7 ppm for **2**, δ_{A} 50.1 ppm for **3**) and the $-\text{PPh}_2$ group (δ_{X} 17.6 ppm for **2**, δ_{X} 20.1 ppm for **3**) of the chelated anion of ligand **1a**, with *cis* $^2J_{\text{PP}}$ coupling constants of 36 Hz and 33 Hz, respectively. The chiral ruthenium centres (since they lack an improper rotation symmetry element, S_n) of **2** and **3** cause the protons of the ligand's bridging methylene group to be diastereotopic, with each group appearing as two doublets of an AB spin pattern (δ_{A} 5.09 ppm and δ_{B} 4.71 ppm for **2**, δ_{A} 5.00 ppm and δ_{B} 4.57 ppm for **3**, both with $^2J_{\text{HH}} = 16$ Hz) in their respective ^1H NMR spectra (Figure 21).

In situ monitoring of each reaction by $^{31}\text{P}\{^1\text{H}\}$ NMR spectroscopy at regular intervals showed only a steady increase in the concentrations of either **2** or **3**, along with free PPh_3 in each case, and a decrease in concentrations of the parent ruthenium complexes $\text{CpRuCl}(\text{PPh}_3)_2$ or $\text{Cp}^*\text{RuCl}(\text{PPh}_3)_2$. No monodentate

intermediates were observed, suggesting chelation rapidly occurs following initial ligand displacement in the formation of **2** and **3**. For comparison, reactions between $\text{CpRuCl}(\text{PPh}_3)_2$ and either 2-(diphenylphosphino)pyridine^[158] or 4-(diphenylphosphino)-2-isopropylimidazole^[124] result in the displacement of only

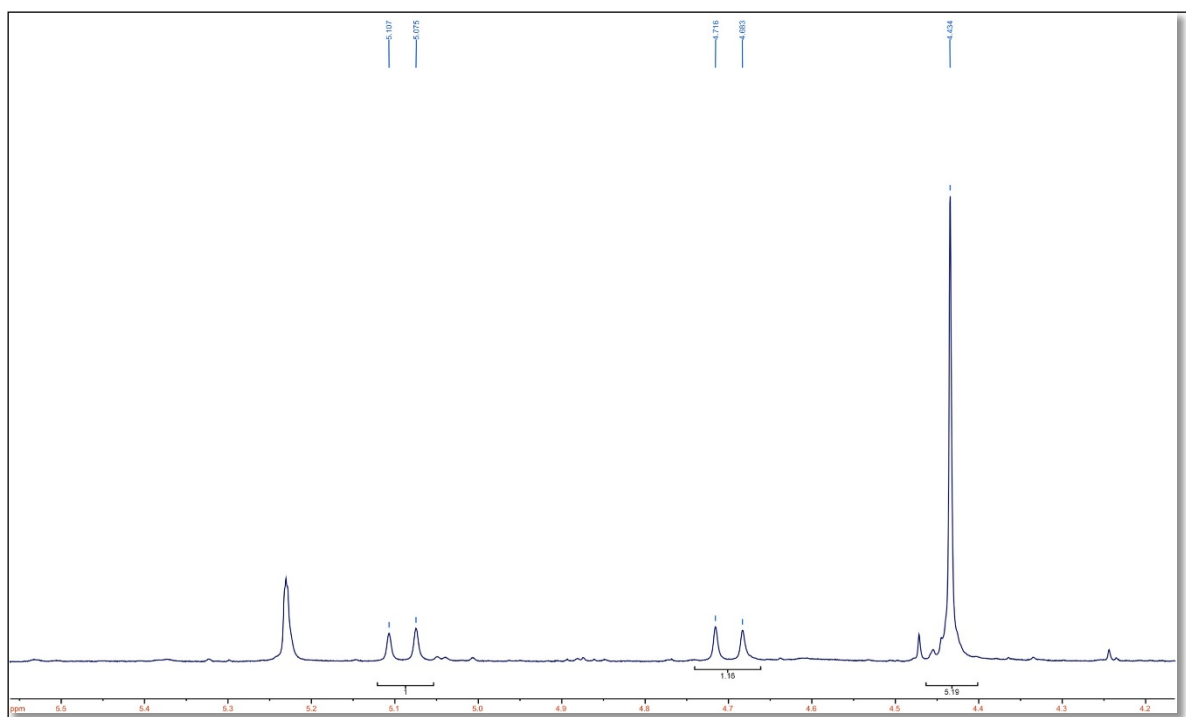


Figure 21. ^1H NMR spectrum (CD_2Cl_2) of complex **2** showing the two doublets generated by the diastereotopic protons of the bridging $-\text{CH}_2-$ group (δ 5.09 ppm and 4.70 ppm) of $[\text{P}^{\text{Ph}}\text{NBPh}_4]^-$ and the singlet pertaining to the $\eta^5\text{-Cp}$ ligand (δ 4.43 ppm). The signal at δ 5.23 ppm is from CH_2Cl_2 .

one PPh_3 ligand, to yield the monodentate products; ring-closing only occurs once a halide abstractor has been added. Thus, in these cases, formation of the

strained four-membered chelate ring only occurs on irreversible removal of a ligand, in this case the chloride.

This also seems to be the case for **2** and **3** since both PPh₃ and LiCl are formed as by-products. Interestingly, when either CpRuCl(PPh₃)₂ or Cp*RuCl(PPh₃)₂ was mixed with **1a'** in 1,2-dichloroethane, no reaction was observed, even under reflux conditions. Indeed, LiCl is much less soluble in 1,2-dichloroethane than PPh₄Cl, and these results suggest halide displacement is likely the first step in the reaction towards the formation of **2**, and not the displacement of triphenylphosphine. In support of this, refluxing the neutral ligand [PN^{Me}] and CpRuCl(PPh₃)₂ together in MeOH for 19 hours yields only starting materials. However, the chelated complex [CpRu(PPh₃)(κ²P,N-PN^{Me})]BPh₄ could be obtained when NaBPh₄ was added to assist in chloride abstraction.

Crystals of **2**·2CH₂Cl₂·(CH₃CH₂)₂O suitable for a crystallographic study were obtained via slow diffusion of diethyl ether into a concentrated CH₂Cl₂ solution of **2**. Selected bond lengths and angles are provided in Figure 22 along with a partially labelled structure (a more complete crystallographic data set is provided in the Experimental section). X-ray data for complex **2** was collected and refined by Dr. Hilary Jenkins at the McMaster Analytical X-Ray Diffraction Facility. The solid-state structure reveals several interesting features. As expected, complex **2** adopts a three-legged piano-stool structure typically observed for η⁵-Cp and -Cp* complexes of ruthenium, with the remaining octahedral sites occupied by a PPh₃ ligand, and the κ²-P^{Ph}NBPh₄ ligand. Several structural

features of the κ^2 -P,N ligand clearly show the strain of the chelate. The angles around the C(6) carbon atom of the benzimidazole moiety bearing the -PPh₂ group

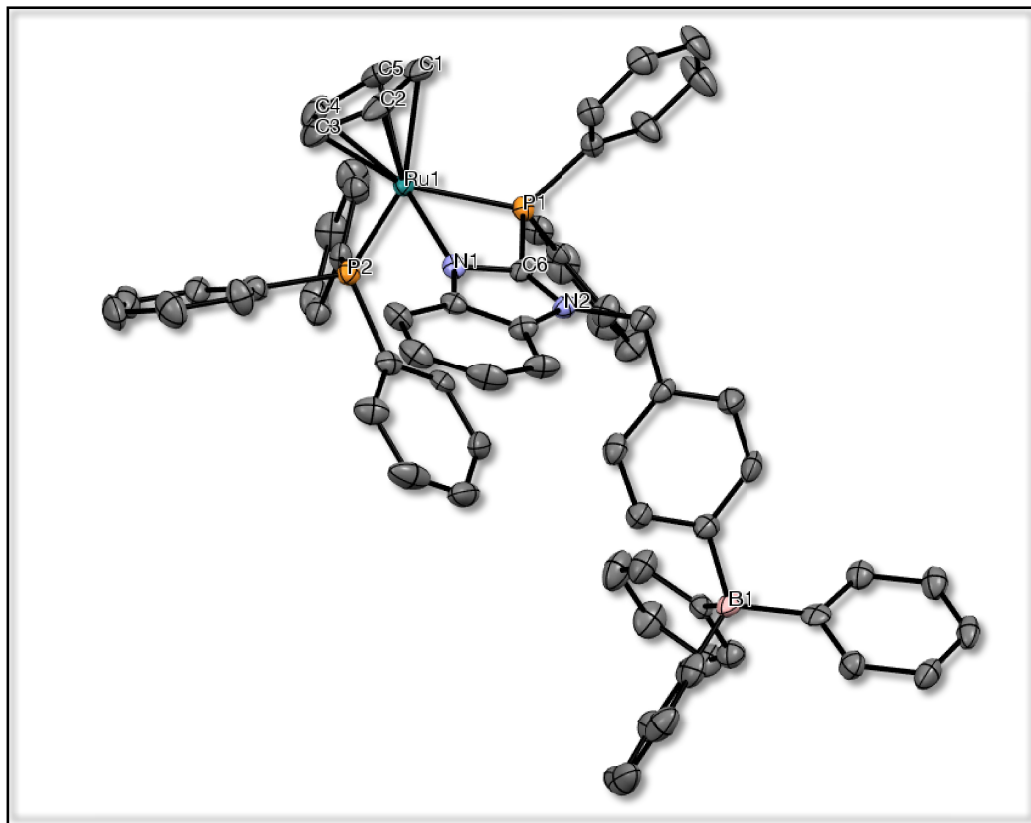


Figure 22. Crystallographic representation of complex **2** (hydrogen atoms and solvent molecules have been omitted for clarity). Selected bond lengths (Å) and angles (°): Ru(1)-P(1), 2.342(2); Ru(1)-P(2), 2.316(2); Ru(1)-N(1), 2.164(4); Ru(1)-C(1), 2.233(7); Ru(1)-C(2), 2.217(7); Ru(1)-C(3), 2.178(8); Ru(1)-C(4), 2.167(8); Ru(1)-C(5), 2.193(6); P(1)-C(6), 1.824(6); P(1)-C(6)-N(1), 104.4(4); P(1)-C(6)-N(2), 142.0(4); N(1)-Ru(1)-P(1), 67.6(1); P(2)-Ru(1)-N(1), 90.9(1); P(2)-Ru(1)-P(1), 97.89(5).

reveal a substantial amount of bending in order to accommodate the strained chelate (*i.e.*, P(1)-C(6)-N(1) = 104.4(4)° vs. P(1)-C(6)-N(2) = 142.0(4)°). Moreover,

the -PPh₂ group is pulled out of the plane of the planar benzimidazole group by about 13°. The N(1)-Ru(1)-P(1) chelate bite angle of 67.6(1)° is small, but not unusual.^[159] The distance between the ruthenium and the -PPh₂ group (Ru(1)-P(1) = 2.342(2) Å) is slightly longer than that observed between the ruthenium and the PPh₃ ligand (Ru(1)-P(2) = 2.316(2) Å), and this is undoubtedly attributed to the strained chelate. The different ruthenium-phosphorus distances seem to impact the distances between the ruthenium and the carbon atoms of the cyclopentadienyl ligand. For example, the PPh₃ ligand adopts a position that is roughly *trans* to the C(1)-C(2) bond of the cyclopentadienyl ligand, with the plane containing the ruthenium-PPh₃ vector Ru(1)-P(2) approximately bisecting C(1)-C(2). The ruthenium-carbon distances here are the longest (Ru(1)-C(1) = 2.233(7) Å and Ru(1)-C(2) = 2.217(7) Å). In contrast, the position of the -PPh₂ moiety is roughly *trans* to the C(3)-C(4) bond of the cyclopentadienyl ligand, with the Ru(1)-P(1) plane approximately bisecting C(3)-C(4). Here, the ruthenium-carbon distances are the shortest (Ru(1)-C(3) = 2.178(8) Å and Ru(1)-C(4) = 2.167(8) Å). The remaining Ru(1)-C(5) distance (2.193(6) Å) is intermediate between the two sets. Perhaps these differences in Ru-C(cyclopentadienyl) distances may be linked to the inability of the -PPh₂ group to exert its *trans* influence to the same extent as the PPh₃ ligand as a result of the strained metallacycle.

Structurally similar products were observed when ligands **1b** and **1c** were reacted with CpRuCl(PPh₃)₂ resulting in the isolation of complexes **4** and **5** respectively (Figure 23). Both of these complexes show similar NMR

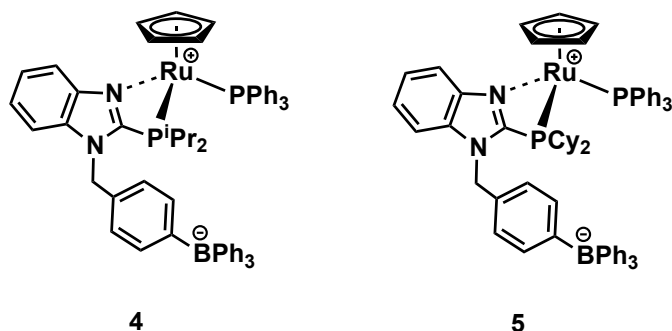


Figure 23. Structure of complex **4** and **5**.

spectroscopic details compared to complexes **2** and **3** (Table 2). Complexes **4** and **5** both display a set of doublets in the ^{31}P NMR spectrum arising from the chelated anions of ligands **1b** or **1c** coupling with the adjacent PPh₃ ligand. The $^{31}\text{P}\{^1\text{H}\}$ NMR chemical shift pertaining to the PPh₃ signal for complexes **2-5** were all close in magnitude, resonating downfield from the chelated anions of ligands **1a-c**. The $^{31}\text{P}\{^1\text{H}\}$ NMR generated by the coordinated (phosphino)borate ligands varied in these complexes. The -PⁱPr₂ donor group of complex **4** produced the furthest downfield $^{31}\text{P}\{^1\text{H}\}$ NMR shift (δ 46.0 ppm), whereas the -PPh₂ donor of complex **2** displayed a signal the furthest upfield ^{31}P NMR shift (δ 17.9 ppm). The proton NMR spectra of complexes **4** and **5** displayed diastereotopic -CH₂- signals pertaining to the coordinated anions of ligands **1b-c** and these signals were similar to those observed for **2** and **3** providing evidence for a chiral metal centre for these complexes. In addition, $^{13}\text{C}\{^1\text{H}\}$ NMR spectra for these complexes each showed

two sets of quartets pertaining to the two chemically inequivalent B-C bonds of the borate groups.

Table 2. Summary of key spectroscopic data for complexes **2-5**.

Complex	³¹ P (ppm)			¹ H (ppm) ^a			¹³ C (ppm)	
	δ _A ^b	δ _X ^c	² J _{PP} (Hz)	δ _A	δ _B	² J _{HH} (Hz)	δ	¹ J _{BC} (Hz)
2	49.8	17.9	36	5.09	4.70	16	165.9 ^e 164.0 ^f	49 ^e 49 ^f
3	50.1	20.1	33	4.99	4.58	16	166.2 ^e 163.6 ^f	49 ^e 50 ^f
4	47.7	46.0	34	5.32	5.14	16	166.5 ^e 163.9 ^f	48 ^e 50 ^f
5	48.3	37.3	35	5.11	5.04	16	164.7 ^e 162.6 ^f	48 ^e 49 ^f

^a Chemical shifts refer to the methylene linker of the anions of ligands **1a-c**. ^b Chemical shift of the PPh₃ ligand. ^c Chemical shift of the -PPh₂ moiety of coordinated anions of ligands **1a-c**. ^e Chemical shift of the benzyl C^{4'}-B of coordinated anions of ligands **1a-c** (See experimental for ligand numbering scheme). ^f Chemical shift of the *ipso* C of B-Ph of coordinated anions of ligands **1a-c**.

Even though the Lewis basicity of the phosphorus donor groups was found to increase across the ligand series (**1a** < **1b** < **1c**), the presence of Li⁺ to effectively abstract a chloride ligand was essential to the formation of these complexes. For example, no reaction was observed when CpRuCl(PPh₃)₂ was mixed with **1c'** under refluxing conditions in 1,2-dichloroethane, indicating that the basicity of the phosphine is not likely the prohibitive factor for PPh₃ or chloride substitution in these reactions.

Crystals of complex **4** (as **4**•CH₂Cl₂) suitable for X-ray structural analysis were obtained via slow diffusion of diethyl ether into a concentrated CH₂Cl₂ solution of **4**. Selected bond lengths and angles are provided in Figure 24 along with a partially labelled structure (a more complete crystallographic data set is provided in the Experimental section). X-ray data for complex **4** was collected and refined by Dr. Hilary Jenkins at the McMaster Analytical X-Ray Diffraction Facility. A comparison of the crystal structures of complexes **2** and **4** reveals several structural differences about the metal framework as a result of changing the substituents at the phosphorus donor atoms on ligands **1a** and **1b**. As anticipated, the general form of the solid state structure of complex **4** was analogous to complex **2**. However, there are a few interesting differences. For instance, the increased steric bulk of ligand **1b** did not have a significant effect on the bite angle of the chelate (N(1)-Ru(1)-P(1)= 67.5(1)° for **4** vs. 67.6(1)° for **2**). Perhaps the most interesting differences between the two structures was the variance in the respective Ru-P(1) and Ru-N(1) bond lengths. Although, the -PⁱPr₂ group has enhanced electron releasing power compared to -PPh₂, the Ru-P(1) bond distance for complex **4** (where Ru(1)-P(1)= 2.3824(15) Å) is actually longer in comparison to the analogous bond of complex **2** (where Ru(1)-P(1)= 2.342(2) Å). Furthermore, one might expect that the Ru-N(1) bond might be lengthened for complex **4** compared to complex **2** due to the increased electron density and steric profile at the ruthenium centre. However, the opposite was observed (where Ru(1)-N(1)= 2.136(4) Å for complex **4** and Ru(1)-N(1)= 2.164(4) Å for complex **2**).

These structural differences may simply be linked to the increased steric bulk of the $-P^iPr_2$ group in **4**, which repels itself from the metal centre (and thus leads to a lengthening of the Ru-P(1) bond), and provides more space within the coordination sphere of the metal for the Ru-N(1) interaction. Another possible

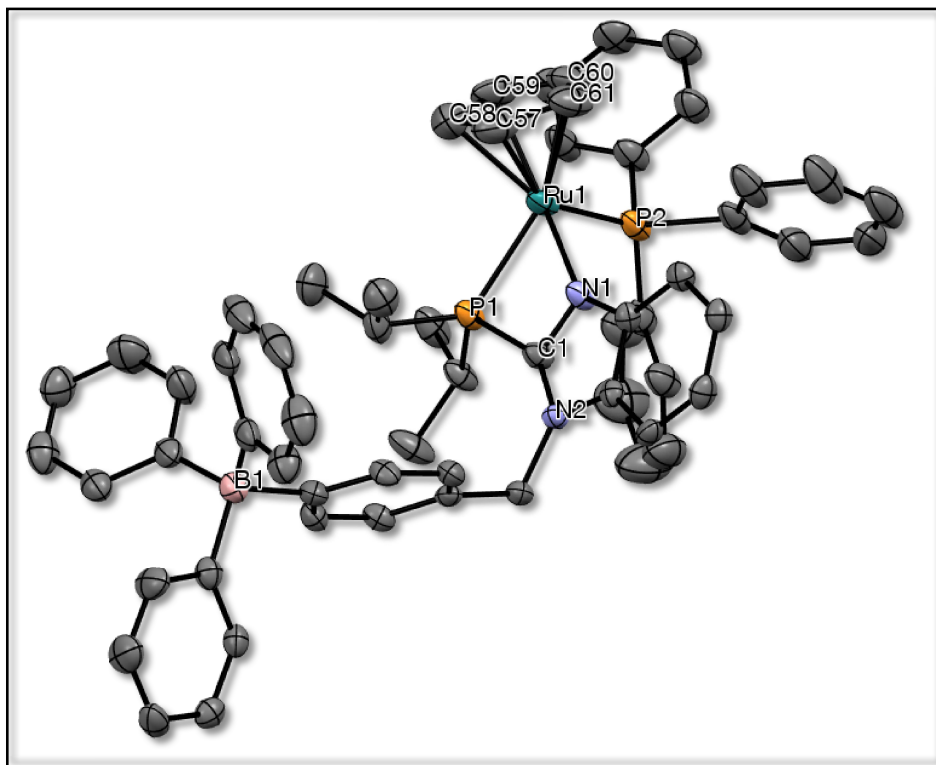
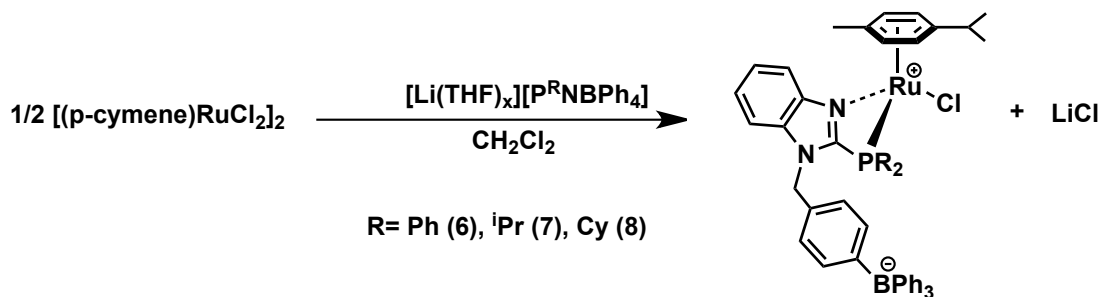


Figure 24. Molecular structure of complex **4** (hydrogen atoms omitted for clarity). Selected bond lengths (Å) and angles (°) are provided: Ru(1)-P(1), 2.3824(15); Ru(1)-P(2), 2.3227(19); Ru(1)-N(1), 2.136(4); Ru(1)-C(57), 2.231(8); Ru(1)-C(58), 2.216(7); Ru(1)-C(59), 2.198(6); Ru(1)-C(60), 2.202(6); Ru(1)-C(61), 2.214(7); P(1)-C(1), 1.840(6); P(1)-C(1)-N(1), 102.9(4); P(1)-C(1)-N(2), 145.2(4); N(1)-Ru(1)-P(1), 67.5(1); P(2)-Ru(1)-N(1), 91.79(14); P(2)-Ru(1)-P(1), 98.15(6).

explanation could be that placing a more electron-rich group on the 2-position of the benzimidazole ring may increase the Lewis basicity of the coordinating nitrogen, through delocalization or inductive electron attraction,^[160] thereby shortening the Ru-N(1) bond in complex **4** as compared to that of complex **2**. If this was the case, it would be expected that the P-C bond distance between R₂P- and the apical C of the benzimidazole ring (C6 for Figure 22 and C1 in Figure 24) would be smaller for complex **4** compared to that of complex **2**. However, the opposite is observed. Since these phenomena arise from the comparison of a pair of crystal structures, a larger population of analogous crystal structures would certainly prove insightful with regards to the true nature of these observations.

4.2. Ligand Complexation Involving [(p-cymene)RuCl₂]₂

In light of the success of ligands **1a-c** to provide chelated products when reacted with ruthenium-Cp precursors, we next turned our attention towards reacting these ligands with [(p-cymene)RuCl₂]₂. These efforts afforded the isolation of complexes **6**, **7** and **8**, as illustrated in Scheme 16.



Scheme 16. Synthesis of complexes **6**, **7**, and **8**.

Reaction of the ligands **1a-c** with $[(p\text{-cymene})\text{RuCl}_2]_2$ in CH_2Cl_2 in a 2:1 ratio results in cleavage of the chloride bridges of the parent dimer, and provides the chelated products **6-8**. Downfield shifts of the $^{31}\text{P}\{^1\text{H}\}$ NMR signals pertaining to complexes **6**, **7** and **8** (δ -6.43 ppm, 38.0 ppm and 26.8 ppm, respectively, in CDCl_3) were observed compared to those of the free phosphine ligands. Indeed, this trend parallels that observed for the $^{31}\text{P}\{^1\text{H}\}$ NMR resonances obtained for **2**, **4** and **5**, with the $-\text{P}^i\text{Pr}_2$ donor providing the furthest downfield shift and the $-\text{PPh}_2$ resonating the furthest upfield. Another revealing spectroscopic feature of complexes **6-8** are the set of doublets observed mid-field in each of the respective ^1H NMR spectra (for example, see Figure 25) arising from the diastereotopic protons of the bridging methylene group of these ligands. Similar spectroscopic features were observed for complexes **2-5**, and reveal the chirality of the ruthenium centre in each complex (see section 4.1). The asymmetry of the chiral ruthenium centre also gives rise to four distinct doublets pertaining to the aryl protons of the *p*-cymene group (see Figure 25). Indeed, these spectroscopic details are observed in similar systems.^[103]

Despite many attempts, a suitable single crystal for X-ray structural analysis of **6**, **7** or **8** could not be obtained. Complex **6**, in particular, displayed low solubility in most of the common solvents, and consequently crystallized out as powders in all attempts. Although crystals of moderate quality of complexes **6** and **8** were examined on one occasion by Dr. Hilary Jenkins at the McMaster Analytical

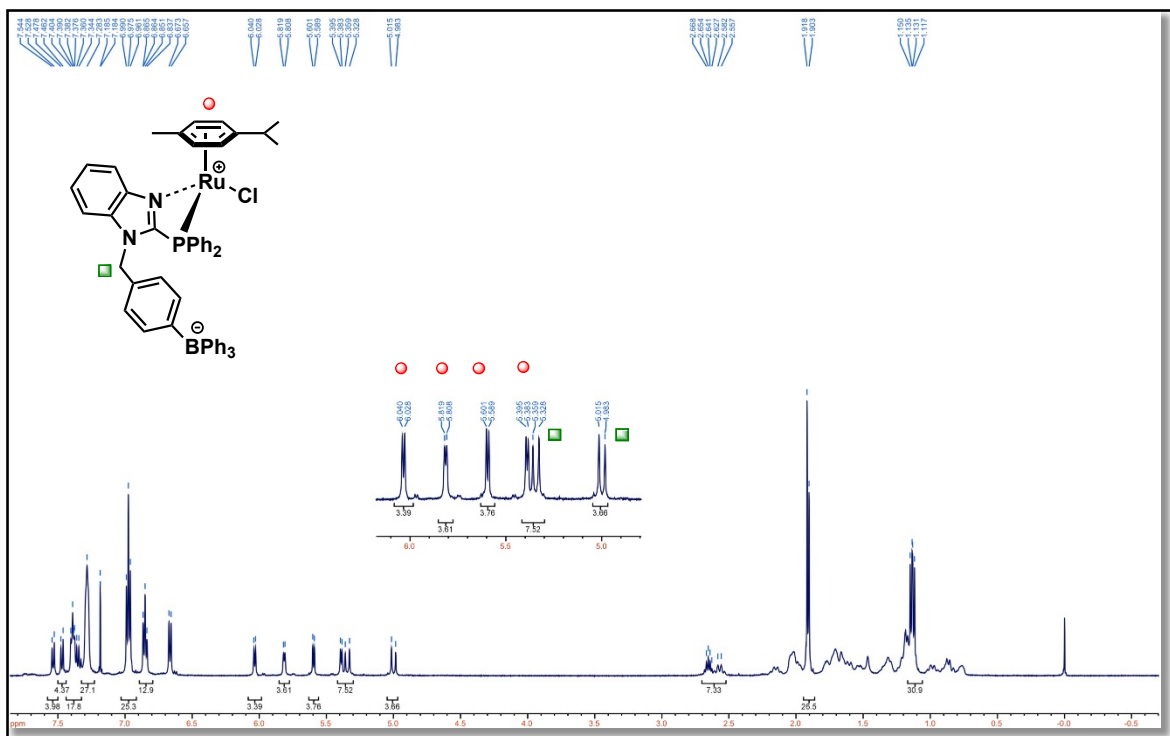
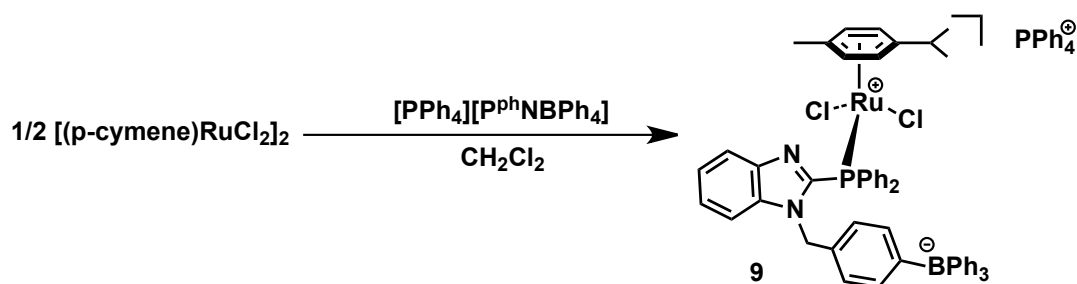


Figure 25. Proton NMR spectrum of complex **6** (acetone- d_6). Inset is the region displaying the four *p*-cymene signals (red circles) and the two methylene signals (green squares). The additional signals in the upfield region are due to residual hexanes used as a precipitating solvent.

X-Ray Diffraction Facility, they suffered from substantial solvent disorder and thus could not be solved. Attempts to produce crystals of X-ray quality for these complexes were eventually abandoned.

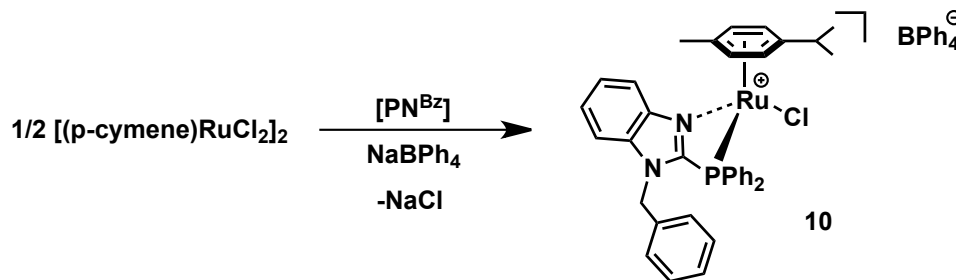
The identity of the ligand cation was, once again, important to the outcomes of the reactions with $[(p\text{-cymene})\text{RuCl}_2]_2$. For example, the reaction of $[(p\text{-cymene})\text{RuCl}_2]_2$ with **1a'** gives rise to a different $^{31}\text{P}\{^1\text{H}\}$ NMR signal resonating

downfield at δ 8.55 ppm, compared to that of the chelated complex **6** (δ -6.43 ppm). This new signal was evidence for the formation of the monodentate complex **9** (Scheme 17). In fact, it is typical for bidentate phosphines which can form strained four-membered metallacycles to display $^{31}\text{P}\{^1\text{H}\}$ resonances further upfield compared to the $^{31}\text{P}\{^1\text{H}\}$ resonances of the phosphine adopting a monodentate mode.^[103,161-163] This shielding effect observed for strained 4-membered phosphine metallacycles is a result of diminished electron donation capability from the phosphorus to the metal centre arising from the phosphine adopting a strained chelate structure, thus the lone pair of electrons provide greater shielding of the phosphorus nucleus in a strained chelate compared to a monodentate binding mode. The ^1H NMR spectrum of this complex also supports the proposed structure since only two signals, each with an integration of 2 H, arise from aryl protons of the symmetric *p*-cymene ring. Furthermore, the methylene spacer of the [P,N] ligand appears as a single peak, instead of a set of



Scheme 17. Synthesis of complex **9**. This reaction exemplifies the effect of changing the cation of the ligand on chelation.

diastereotopic doublets for chelate complex **6**, indicating symmetry at the Ru atom in **9** as opposed to chiral Ru atom in **6**. Indeed, complex **9** was easily converted to **6** by adding AgBF_4 to remove a chloride ligand. Similarly, the cationic complex **10** can be generated by reacting the neutral ligand $[\text{PN}^{\text{Bz}}]$ with $[(p\text{-cymene})\text{RuCl}_2]_2$ in the presence of NaBPh_4 (Scheme 18).

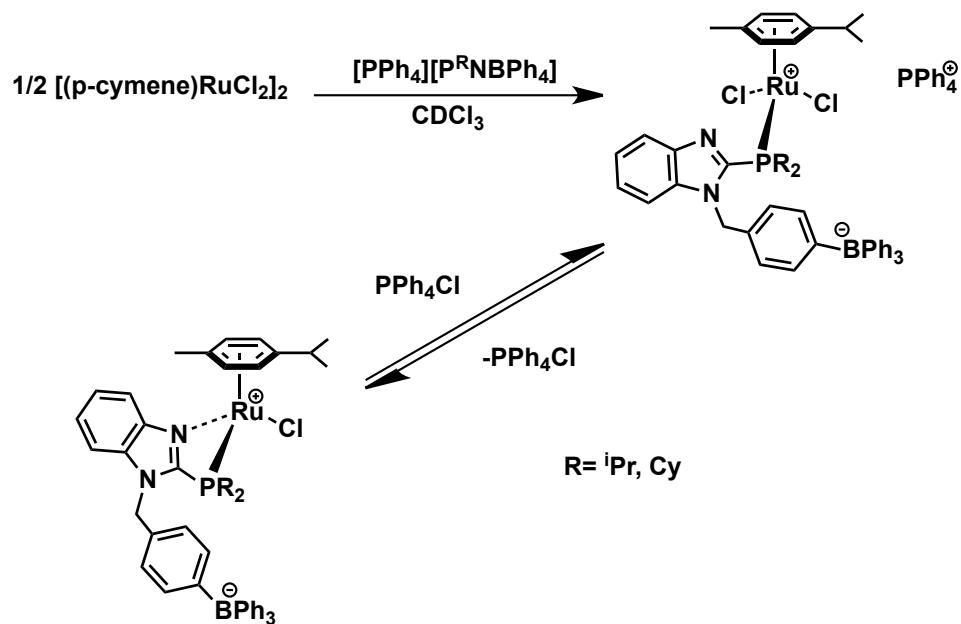


Scheme 18. Synthesis of cationic complex **10**.

Interestingly, ligands **1b'** and **1c'** showed different behaviours in these reactions involving $[(p\text{-cymene})\text{RuCl}_2]_2$. *In situ* monitoring via $^{31}\text{P}\{^1\text{H}\}$ NMR spectroscopy showed that when **1b'** or **1c'** were combined with the $[(p\text{-cymene})\text{RuCl}_2]_2$ precursor, equilibria were established between the $\kappa^1\text{-P}$ and the $\kappa^2\text{-P,N}$ complexes over time. In each case, disappearance of the $^{31}\text{P}\{^1\text{H}\}$ NMR signal pertaining to the anion of the free ligand was observed, and was accompanied by the rapid formation of downfield signals at δ 29.2 ppm and δ 22.4 ppm for the reactions involving **1b'** and **1c'**, respectively. However, in contrast to

the analogous reaction with **1a'**, new $^{31}\text{P}\{^1\text{H}\}$ NMR signals slowly begin to form downfield at δ 37.7 ppm and δ 26.9 ppm for the reactions involving **1b'** and **1c'**, respectively, corresponding to the κ^2 -*P,N* complexes **8** and **9**.

Indeed, the most likely explanation for the generation of the first peak in these reactions is that the PPh_4^+ salts rapidly cleave the Ru dimer forming the κ^1 -*P* complexes. Whereas the Li^+ cation is able to facilitate chelation by the abstraction of a chloride ligand from the metal complex and precipitate LiCl , the PPh_4^+ cation is less efficient at the removal of the chloride ligand from the system enabling equilibrium conditions between the κ^1 -*P* and the κ^2 -*P,N* complexes (Scheme 19).



Scheme 19. Reaction ligands **1b'** and **1c'** with $[(\textit{p}\text{-cymene})\text{RuCl}_2]_2$.

Evidence to support the formation of the κ^1 -*P* complexes was also provided by periodic monitoring of the reaction mixtures by ^1H NMR spectroscopy. The C_s symmetric κ^1 -*P* complex provides a simpler ^1H NMR signature for the arene ligand compared to the κ^2 -*P,N* complexes, which have a chiral Ru centre. Although the arene signals for both complexes overlap and made full assignment difficult, some distinguishing features were at least discernible. For example, in reactions of ligand **1b'** with $[(p\text{-cymene})\text{RuCl}_2]_2$, three signals with similar integrations may be identified. Two of these signals are doublets pertaining to two chemically inequivalent sets of arene protons on the *p*-cymene ring of $[\text{Ph}_4\text{P}][(\eta^6\text{-}p\text{-cymene})\text{RuCl}_2(\kappa^1\text{P}, \text{P}^{\text{iPr}}\text{NBPh}_4)]$ (indicated by green squares in Figure 26), while the third may be assigned to the $-\text{CH}_2-$ group that tethers the borate functionality to the benzimidazole (indicated by yellow square in Figure 26). The chemical shifts of these ^1H NMR resonances are also similar to those observed for complex **9** which also contains monodentate **1a'**. Among these signals, the arene and methylene signals of the chelated complex $[(\eta^6\text{-}p\text{-cymene})\text{RuCl}(\kappa^2\text{P}, \text{N}-\text{P}^{\text{iPr}}\text{NBPh}_4)]$ can also be identified. Thus, four distinct doublets are observed for the η^6 -*p*-cymene ring coordinated to the chiral centre of $[(\eta^6\text{-}p\text{-cymene})\text{RuCl}(\kappa^2\text{P}, \text{N}-\text{P}^{\text{iPr}}\text{NBPh}_4)]$ (indicated by red circles in Figure 26), while two distinct doublets are observed for the methylene spacer (indicated by blue circles in Figure 26).

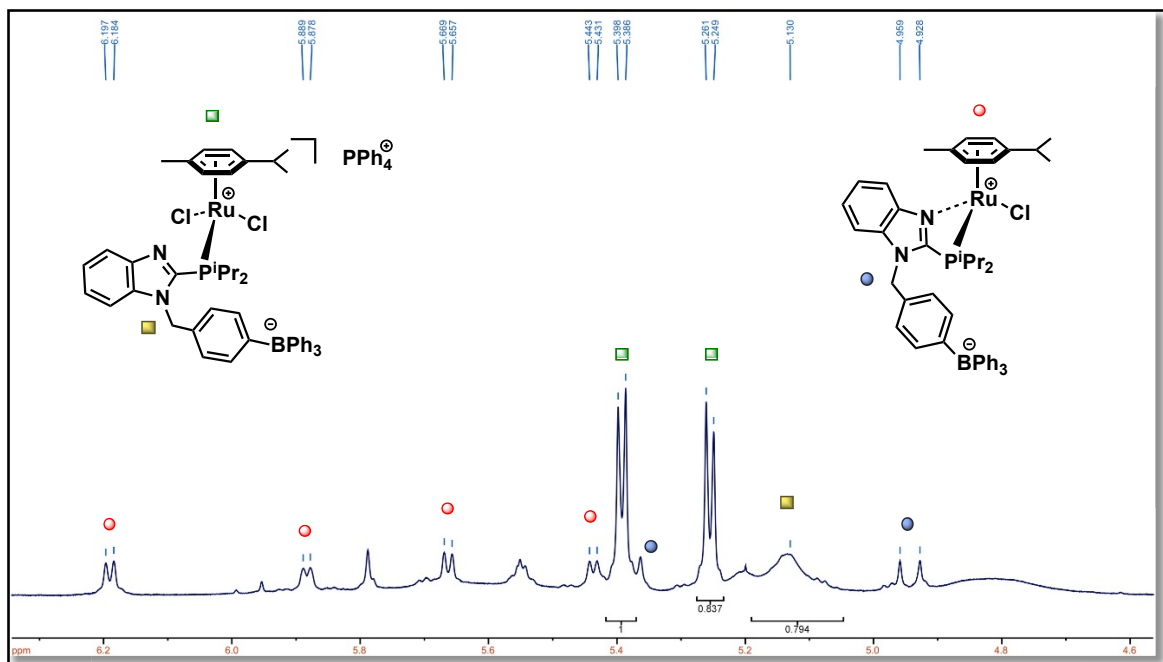


Figure 26. Proton NMR spectrum 30 minutes after reacting **1b'** with $[(p\text{-cymene})\text{RuCl}_2]_2$.

Interestingly, the positions of the equilibria differed for each of the reactions involving **1b'** and **1c'**. For instance, with **1b'**, equilibrium was reached within 4 hours at room temperature and consisted of an approximately 1:1 mixture of the $\kappa^1\text{-P}$ and $\kappa^2\text{-P,N}$ complexes, as revealed by ^{31}P NMR spectroscopy. In similar reactions involving **1c'**, however, chelation appears to occur much more rapidly, and an approximately 3:7 mixture of the $\kappa^1\text{-P,N}$ and $\kappa^2\text{-P,N}$ complexes is observed, respectively, within 4 hours under the same conditions; at equilibrium, a 1:3 mixture of the $\kappa^1\text{-P,N}$ and $\kappa^2\text{-P,N}$ complexes is observed for the cyclohexyl analogue. Prolonged heating of this mixture did not have an effect on the ratio of the two species in solution. The equilibria observed in these reactions might result from the electronic differences between the phosphines. For example, the greater

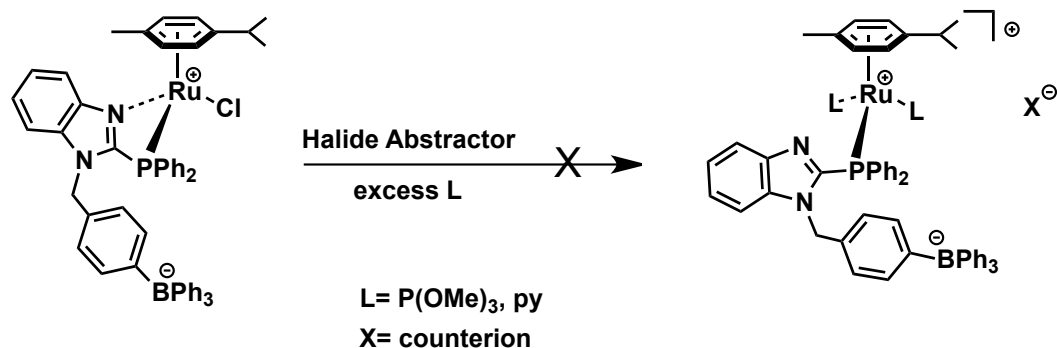
electron donating ability of the $-PCy_2$ group in ligand **1c'**, compared to the other ligands of this series, could promote dissociation of the chloride ligand thereby facilitating a vacant site on the metal available for chelation. Indeed, the poorest donor of the series, **1a'**, is unable to facilitate chloride loss to any significant extent, and thus chelation is not observed at all. Similar results were observed for other ruthenium-chlorido half-sandwich complexes containing $[PR_2(p\text{-}Ph_3BC_6H_4)]^-$ ligands (where R= Ph, ⁱPr, Cy).^[76] In these systems, the phosphines with the better donor groups (*i.e.*, ⁱPr and Cy) seemed to promote chloride dissociation more readily than did the Ph analogues.^[76]

Chapter Five: Reactions of Ruthenium-(Phosphino)benzimidazole Complexes with Small Molecules

5.1. Reactions with MeCN: Evidence for Hemilability

One of the objectives of this investigation was to establish whether the new (phosphino)borate ligands could display hemilability. One method used to explore this feature involved reacting the chelated complexes **2-8** with small coordinating ligands in order to see if ring opening of the metallacycle would occur. Indeed, the earlier studies involving the synthesis of the $\kappa^1\text{-P,N}$ and $\kappa^2\text{-P,N}$ Ru-arene complexes provided information on the relative NMR signatures for both the ring-opened and ring-closed forms of the ligands involved in this study.

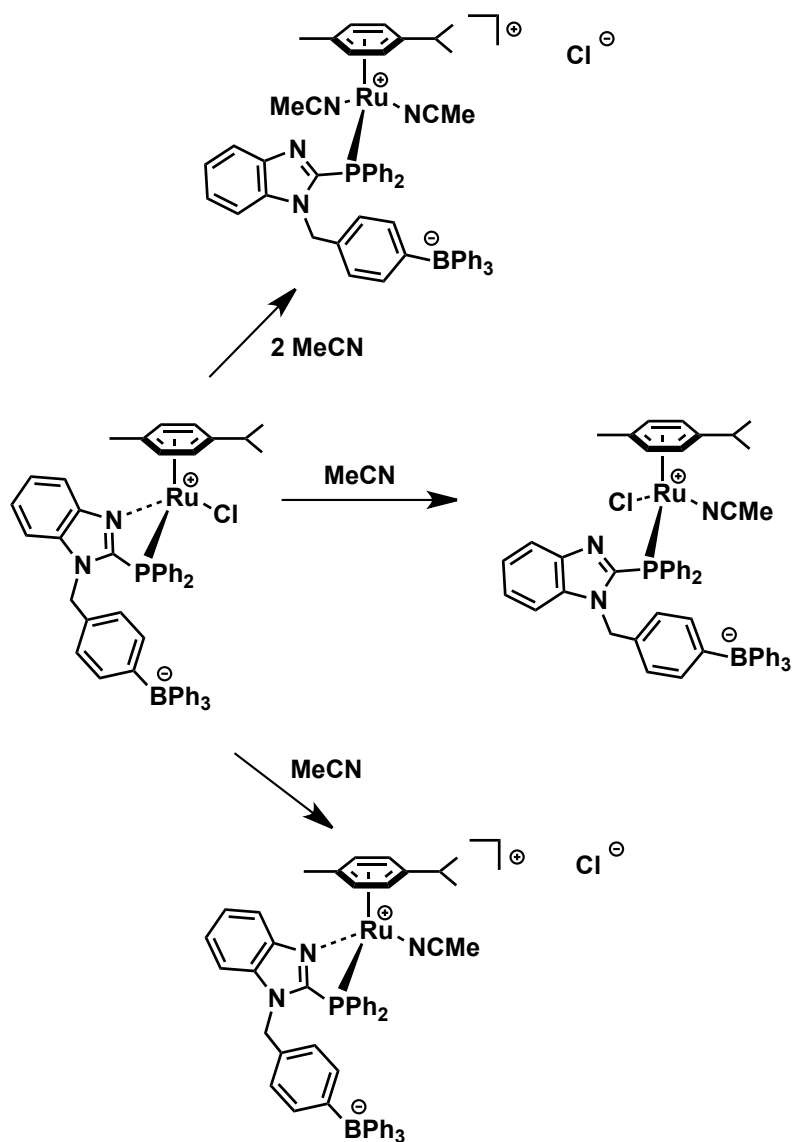
During initial studies, a number of sterically small coordinating molecules were reacted with complex **6** in an effort to force the displacement of the benzimidazole portion of the chelated anion of ligand **1a** from the metal. Interestingly (and, quite surprisingly), preliminary reactions of **6** with slight excesses of pyridine or P(OMe)_3 produced unappealing mixtures of products, as determined by $^{31}\text{P}\{^1\text{H}\}$ NMR spectroscopy. In an effort to enhance the selectivity of these reactions, and remove any complicating issues which might arise as a result of chloride dissociation, these reactions were repeated using various chloride abstracting reagents, including AgX ($\text{X} = \text{BF}_4$ or OTf), or MeOTf (Scheme 20). Unfortunately, mixtures of products were again observed by NMR spectroscopy.



Scheme 20. Attempted derivatization of complex **6**.

Interestingly, and in significant contrast to pyridine and $\text{P}(\text{OMe})_3$, MeCN alone proved to be more selective in its reaction with complex **6**. When complex **6** was heated in MeCN, only two $^{31}\text{P}\{^1\text{H}\}$ NMR signals were observed in a 1:1 ratio, a signal pertaining to complex **6** and a new peak resonating at δ 19.4 ppm. The downfield position of this new signal (relative to complex **6**) suggested a ring-opened structure of this product.^[164] However, it was uncertain whether MeCN was displacing the benzimidazole nitrogen, the chloride ligand, or both (Scheme 21). Indeed, the ^1H NMR spectrum of this mixture revealed interesting details regarding this reaction.

Perhaps the most revealing regions of the proton NMR spectrum generated by this mixture are in the arene region where the signals of the coordinated *p*-cymene ligand appear, and the aliphatic region where both the ^iPr protons of the *p*-cymene ligand and the MeCN protons appear (Figure 27).



Scheme 21. Some possible products formed by **6** in the presence of MeCN.

Features of the ¹H NMR spectrum that support the presence of complex **6** and the formation of a complex where the benzimidazole nitrogen of complex **6** has been displaced from the Ru centre by MeCN include eight sets of *p*-cymene arene signals between δ 6.23-5.29 ppm (there is overlap of two arene signals at δ 5.78

ppm as well as overlap between an arene signal and a $-\text{CH}_2-$ signal at δ 5.27 ppm) and four sets of *p*-cymene isopropyl signals between δ 1.23-1.08 ppm. These

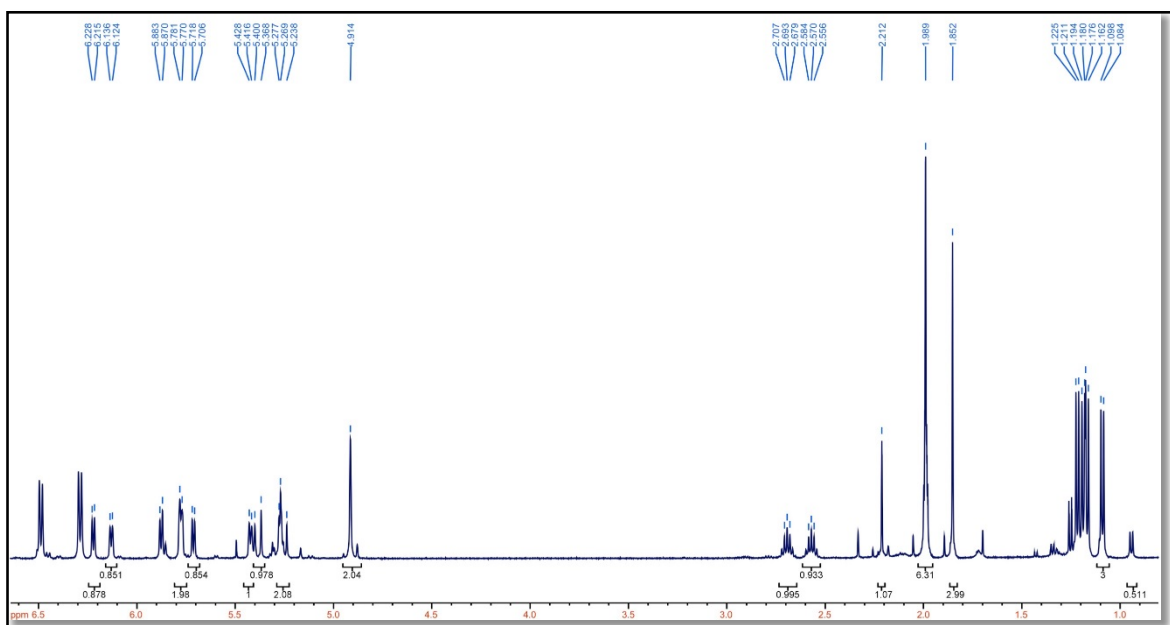


Figure 27. Proton NMR Spectrum of complex **6** in CD_3CN .

features substantiate the presence of two complexes containing chiral Ru centres. This evidence seems to suggest that the complex in Scheme 21 containing two coordinated acetonitrile ligands is not formed under these conditions since it is of C_s symmetry and would generate a less complex proton NMR signature. Indeed, the signal at δ 2.21 ppm could be due to coordinated MeCN as this shift is close to those found in similar systems,^[165,166] however, the integration of the MeCN signal would be unreliable since the reaction was performed in CD_3CN . Interestingly, prolonged heating of the solution to try and isolate the new species

did not seem to have an effect on the ratio of the two peaks suggesting that an equilibrium may be present where the ligand is operating in a hemilabile fashion. Further investigation involving systematic variance with respect to the concentration of MeCN and Cl⁻ would provide insight into whether the system is operating under equilibrium conditions.

Although the downfield shift in the ³¹P{¹H} spectrum of the new complex compared to complex **6** (δ -6.43 ppm) is consistent with the disruption of a strained 4-membered chelate,^[103,161-163] the formation of the cationic complex formed by substitution of the Cl⁻ ligand with MeCN, where the metallacycle remains intact (Scheme 20), cannot be ruled out and therefore only tentative assignment of the structure can be made as the ring-opened zwitterion. Another aspect of the reaction that prevents a definitive structure assignment is the presence of only one distinguishable set of -CH₂- doublets in the ¹H NMR spectrum. There is a signal at δ 4.91 ppm that has an expected integration of 2 H; nevertheless, this signal appears as a singlet as opposed to the anticipated set of AB doublets due to the chiral metal centre. Indeed, further characterization of this complex would be required for a more confident structure assignment.

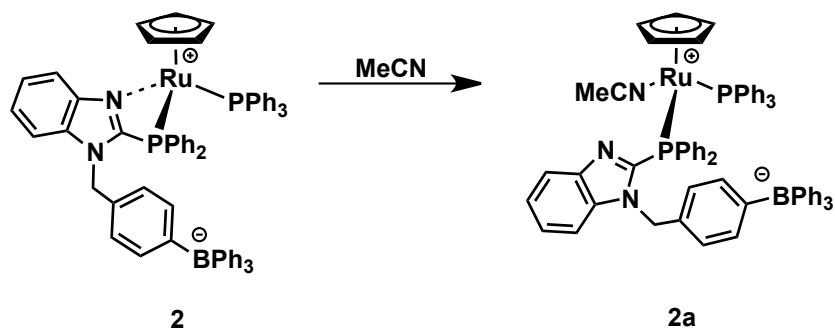
Solution studies of cationic complex **10** (see Scheme 18) as well as complex **8** (see Scheme 16) in the presence of MeCN provided interesting results for comparison. It was found that when the cationic complex **10** was placed in acetonitrile and monitored via ³¹P{¹H} NMR spectroscopy, a similar spectrum to that obtained for the analogous reaction involving complex **6** was generated in and

was comprised of two resonance signals. One of the peaks corresponded to unreacted complex **10** whereas the other signal was located downfield (δ 19.8 ppm) with a similar $^{31}\text{P}\{^1\text{H}\}$ NMR shift to that of the product generated from the reaction involving complex **6** and MeCN (δ 19.4 ppm). Interestingly, the mixture consisted of a 1:3 ratio of complex **10** to the new product indicating that more of the starting material had been consumed in this reaction compared to the analogous reaction involving complex **6**. The ratio of the two species did not change over time suggesting that equilibrium conditions may be operating in this case as well, with the position of the equilibrium shifted to the formation of the ring opened species.

The identity of the $-\text{PR}_2$ group in these reactions with MeCN had a more dramatic effect on the outcome of the reaction. When complex **8**, containing $-\text{PCy}_2$ as opposed to $-\text{PPh}_2$, was dissolved in MeCN and monitored over time under the same conditions, no change in the $^{31}\text{P}\{^1\text{H}\}$ NMR spectrum was observed. Interestingly, this suggests that the metallacycle in this complex does not undergo ring opening as readily as those in complexes **6** and **10**. Heating the reaction mixture in this case resulted in only degradation as evidenced by unidentified multiple phosphorus NMR signals.

The reactions with MeCN were also extended to include complexes **2**, **4** and **5**. For example, heating complex **2** at 55 °C for 10 minutes in MeCN results in the clean conversion of **2** to a new species **2a** (Scheme 22), as determined by $^{31}\text{P}\{^1\text{H}\}$ NMR spectroscopy. Thus, the pair of doublets pertaining to complex **2** (at

δ 49.8 ppm and δ 17.9 ppm) disappear, and are accompanied by the appearance of a new pair of doublets at δ 43.1 ppm and δ 30.5 ppm. Interestingly, after work-up, an examination of the ^{31}P NMR spectrum of the product in CDCl_3 had revealed



Scheme 22. Synthesis of complex **2a** via displacement of the coordinated benzimidazole N in complex **2**.

substantial reversion back to complex **2** (Figure 28). The ^1H NMR spectrum of the mixture also revealed signals confirming the almost complete reformation of complex **2**. After 18 hours, NMR spectroscopy revealed complete reversion back to **2**, along with the presence of free MeCN in solution (^1H NMR). The accumulated

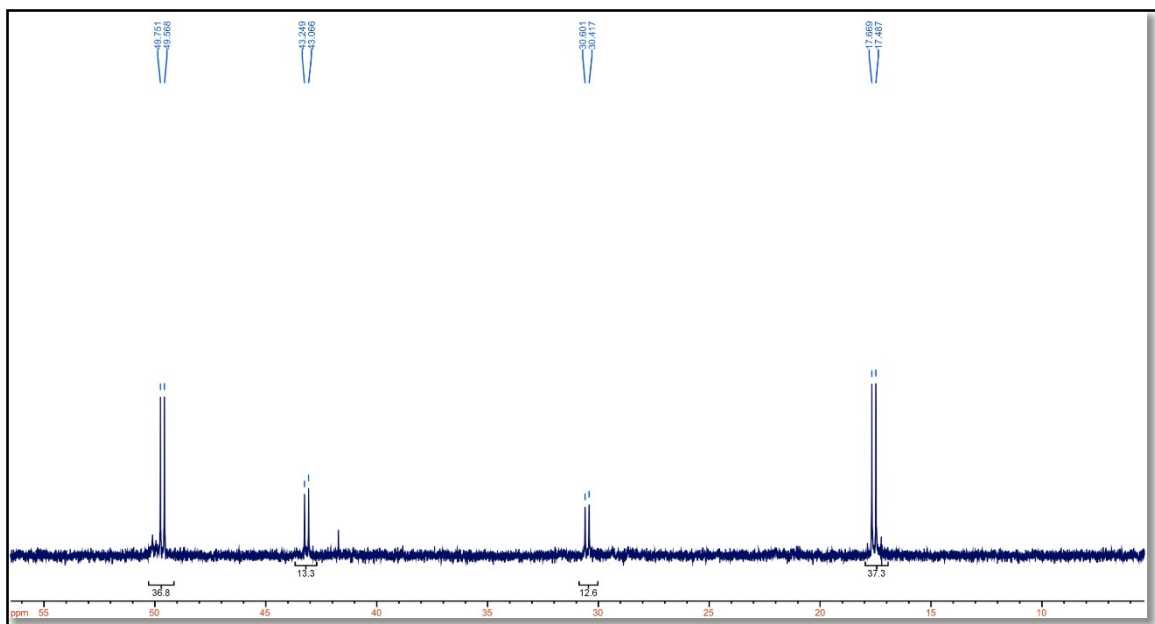


Figure 28. $^{31}\text{P}\{^1\text{H}\}$ NMR spectrum of complex **2a** reverting back to the parent complex **2** after dissolving in CDCl_3 .

evidence suggests complex **2a** is quite labile in solution. Interestingly, when the product was dissolved in a mixture of $\text{CD}_2\text{Cl}_2/\text{CD}_3\text{CN}$ (~ 3.8 M CD_3CN), no reversion to complex **2** was observed. Thus, the $^{31}\text{P}\{^1\text{H}\}$ NMR spectrum revealed only the doublets pertaining to **2a** at δ 43.1 ppm and δ 30.5 ppm. The ^1H NMR spectrum of the product dissolved in the $\text{CD}_2\text{Cl}_2/\text{CD}_3\text{CN}$ mixture revealed a pair of doublets of an AB spin pattern in close proximity (δ_{A} 4.72 ppm and δ_{B} 4.68 ppm) pertaining to the methylene unit of monodentate $\kappa^1\text{-P}^{\text{Ph}}\text{NBPh}_4$ (Figure 29), and revealing the presence of a chiral metal centre. A Cp ligand peak was also present at δ 4.37 ppm. A peak slightly downfield from free MeCN was present at δ 1.97 ppm and may be generated by coordinated MeCN.^[167] When the complex is

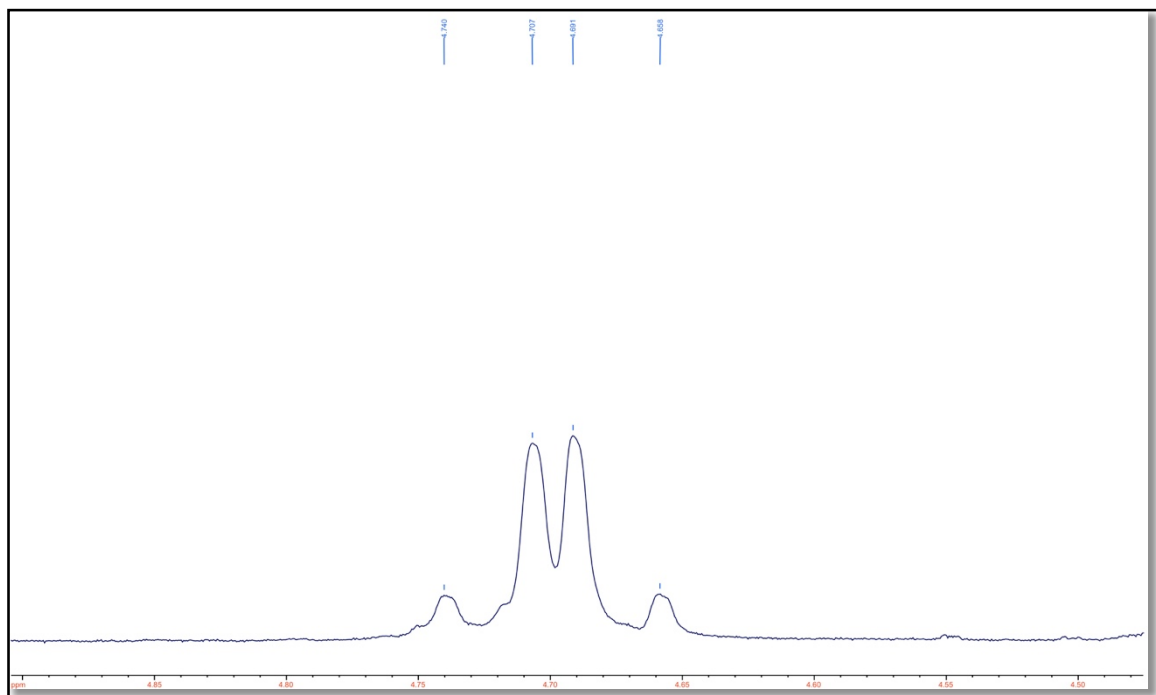


Figure 29. ^1H NMR of the benzyl $-\text{CH}_2-$ signal generated by **2a**.

dissolved in neat CD_3CN the coordinated MeCN signal is unobstructed, residing at δ 2.51 ppm, and coincides with the corresponding signal found in similar systems.^[167,168] However, due to $\text{CD}_3\text{CN}/\text{CH}_3\text{CN}$ exchange, the integration of these peaks would be unreliable and would appear lower in magnitude. Furthermore, a peak at 14.5 ppm, likely pertaining to coordinated MeCN , is visible in the $^{13}\text{C}\{^1\text{H}\}$ NMR spectrum.

The data collected for this transformation likely pertains to displacement of the benzimidazole nitrogen by MeCN forming complex **2a**. Perhaps most fascinating is the observation of this product reverting back to complex **2**. Indeed,

this evidence points to an elegant example of the $[\text{P}^{\text{Ph}}\text{NBPh}_4]^-$ ligand demonstrating hemilability.

Interestingly, very different results were obtained when these reactions were extended to include either complex **4** or **5** (see Figure 23). In fact, no reaction was observed when either **4** or **5** was treated with excess MeCN. Moreover, heating the reaction mixtures only led to decomposition, as determined by $^{31}\text{P}\{^1\text{H}\}$ NMR spectroscopy. These results mirror those found for the *p*-cymene complexes, where changing the groups attached to the phosphine donor centres influenced the ability of the complex to undergo ring-opening of the chelate. In general, it seems substituting for a better donor group inhibits the hemilability of these ligand systems.

5.2. Reactions with CO: Evidence for Hemilability

In parallel studies, CO was also examined for its ability to force ring-opening of the chelated products.^[169] For example, when either complex **2** or **3** was treated with excess CO, either at room temperature or at reflux ($\text{C}_2\text{H}_4\text{Cl}_2$, 80° , up to 24 hours), NMR spectroscopy of the product mixtures revealed a number of compounds had formed, including free PPh_3 . Considering the complexity of the NMR spectra, and the production of PPh_3 , the formation of ring-opened, including bridged-species cannot be ruled out in these reactions.^[124,159] In contrast (but perhaps not unexpected), refluxing either complex **4** or **5** with excess CO in 1,2-dichloroethane for 24 hours resulted in no reaction, as evidenced by $^{31}\text{P}\{^1\text{H}\}$ NMR spectroscopy of the reaction solutions which revealed only the presence of either

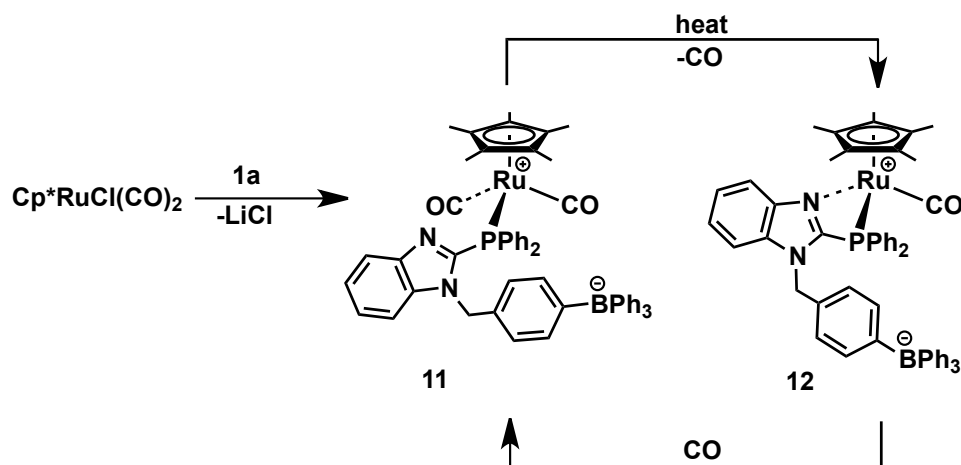
4 or **5**. These reactions provide further proof of the strength of the metallacycle in the complexes bearing stronger phosphorus donor centres.

Since the synthesis of complexes **2-5** likely proceed via initial halide displacement, it was reasoned that the complex $\text{Cp}^*\text{RuCl}(\text{CO})_2$ ^[155] would be a good candidate to examine in reactions with ligands **1a-c**.

When equimolar amounts of $\text{Cp}^*\text{RuCl}(\text{CO})_2$ and ligand **1a** are refluxed together in 1,2-dichloroethane over 24 hours (Scheme 23), a mixture of the monodentate (**11**) and ring-closed (**12**) zwitterionic complexes are formed in an approximately 3:2 ratio. *In situ* monitoring of the reaction progress at regular intervals by $^{31}\text{P}\{^1\text{H}\}$ NMR spectroscopy revealed complex **11** forms first, and it is slowly converted to the chelated complex **12** before ligand **1a** is completely consumed. Unfortunately, complex **12** slowly decomposes with prolonged heating (*i.e.*, to ensure complete conversion from complex **11**), and this prevented its isolation in pure form. Complex **11** exhibits a singlet at δ 36.1 ppm in the $^{31}\text{P}\{^1\text{H}\}$ NMR spectrum, while the singlet for **12** appears at δ 19.4 ppm. Again, these results are consistent with the large chemical shift differences observed between chelated phosphine ligands forming four-membered rings with a metal, and their corresponding ring-opened structures.^[164] Consistent with the chirality of **12**, two distinct doublets of an AB spin pattern (δ_{A} 5.15 ppm and δ_{B} 4.99 ppm) are observed, which correspond to the diastereotopic protons of the methylene group bridging the BPh_4 group to the phosphinobenzimidazole moiety. In contrast, C_s

symmetric **11** displays a singlet at δ 4.75 ppm for the bridging methylene group of the κ^1 -ligand.

Importantly, Scheme 23 illustrates the hemilabile nature of the anion of ligand **1a** as part of complexes **11** and **12**. Thus, pure complex **11** in CH_2Cl_2 slowly evolves CO when heated, and undergoes ring-closing to produce complex **12**. When complex **12** is dissolved in CH_2Cl_2 and allowed to stir under CO, it undergoes ring opening and adds a second CO ligand to yield the monodentate complex **11**.



Scheme 23. Reversible displacement of the benzimidazole nitrogen by CO in the interconversion of complexes **11** and **12** reveals the hemilability of $[\text{P}^{\text{Ph}}\text{NBPh}_4]^-$.

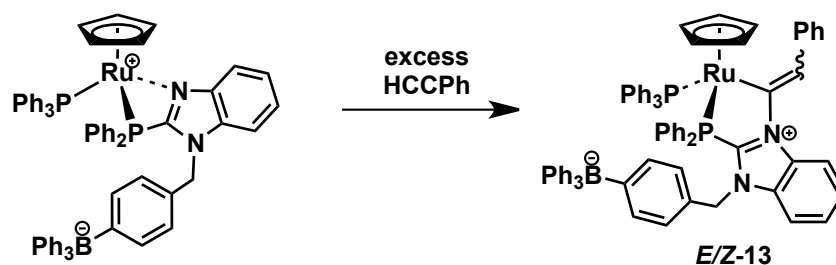
Chapter Six: Reactions of Ruthenium-(Phosphino)

benzimidazole Complexes with Alkynes

6.1. Attempted Syntheses of Ruthenium Vinylidenes: Insertion of Alkynes into Ru-N bonds

We have had a long-standing interest in the synthesis and chemistry of ruthenium-vinylidene and higher-cumulene complexes, mainly because they may be employed as precursors to ruthenium carbyne complexes.^[119] Encouraged by our observations from the reactions of **2-8** with CO and MeCN, as well as the hemilabile properties displayed by **2** and **11**, it was wondered if the chelated complexes **2-8** might serve as suitable precursors to vinylidene complexes if they, too, could undergo ring-opening in the presence of alkyne substrates.^[105,170-173]

As illustrated in Scheme 24, when complex **2** is stirred with a 10-fold excess of phenylacetylene in CH₂Cl₂ over 24 hours, a dark red-orange solution is



Scheme 24. Reaction of complex **2** with phenylacetylene forming *E/Z*-**13**.

produced from which a microcrystalline red-orange solid is obtained upon work-up. NMR spectroscopic analysis of the solid reveals the clean formation of a mixture of the *E*- and *Z*-isomers of the vinylidene insertion product [CpRu(PPh₃)(κ²C,*P*-(CCHPh)-P^{Ph}NBPh₄)], **13**, in approximately a 4:1 ratio. The ³¹P{¹H} and ¹H NMR spectra clearly show that **13** contains inequivalent phosphine ligands and a chiral metal centre. For example, the major isomer displays two doublets of an AX pattern in the ³¹P{¹H} NMR spectrum corresponding to the PPh₃ ligand (δ_A 69.0 ppm) and the -PPh₂ group (δ_X 49.1 ppm) of the anion of **1a** (²J_{PP} = 35 Hz), and two doublets of an AB pattern (δ_A 4.89 ppm, δ_B = 4.71 ppm, ²J_{HH} = 16 Hz) in the ¹H NMR spectrum corresponding to the protons of the methylene tether of the [P^{Ph}NBPh₄]⁻ ligand. The corresponding data for the minor isomer are very similar (³¹P: δ_A = 69.6 ppm, δ_X = 50.8, ²J_{PP} = 35 Hz; ¹H: δ_A 5.15 ppm, δ_B = 4.98 ppm, ²J_{HH} = 16 Hz). The ¹³C{¹H} NMR spectrum of **13** perhaps offers the most compelling evidence for insertion, and shows two sets of overlapping doublets at δ 159.6 ppm (major, ²J_{PC} = 18 Hz, ²J_{PC} = 17 Hz) and δ 155.0 ppm (minor, ²J_{PC} = 22 Hz, ²J_{PC} = 12 Hz) corresponding to C_α of the alkenyl ligands coupling with the PPh₃ ligand and -PPh₂ portion of coordinated anion of ligand **1a**.^[170] Interestingly, when this reaction was repeated but instead using excess 1-hexyne, only one isomer of [CpRu(PPh₃)(κ²C,*P*-(CCHBu)-P^{Ph}NBPh₄)], **14**, is produced. Moreover, the reactions between complex **3** and either excess phenylacetylene or 1-hexyne also preferentially produced only one isomer, the complexes

[Cp*Ru(PPh₃)(κ²C,*P*-(CCHPh)-P^{Ph}NBPh₄)], **15**, and [Cp*Ru(PPh₃)(κ²C,*P*-(CCHBu)-P^{Ph}NBPh₄)], **16**, respectively. See Table 3 for a summary of key NMR spectroscopic data.

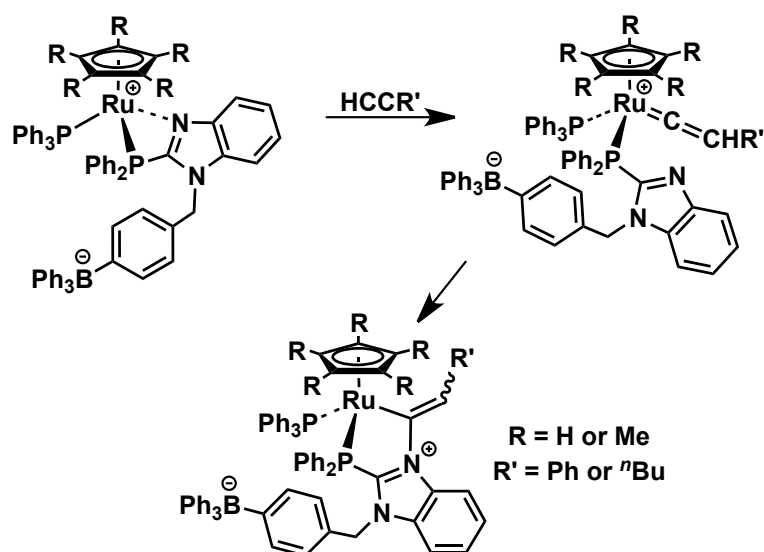
Table 3. Summary of key spectroscopic data for complexes **13-16**.

Complex	³¹ P (ppm)			¹ H (ppm) ^a			¹³ C (ppm) ^b
	δ _A ^c	δ _X ^d	² J _{PP} (Hz)	δ _A	δ _B	² J _{HH} (Hz)	δ _{Cα}
13	69.0 ^e	49.1 ^e	35 ^e	4.89 ^e	4.71 ^e	16 ^e	159.6 ^e
	69.6 ^f	50.8 ^f	35 ^f	5.15 ^f	4.98 ^f	16 ^f	155.0 ^f
14	69.0	52.2	34	5.02	4.88	15	154.7
15	67.1	51.9	32	5.05	4.74	15	162.2
16	66.5	52.5	33	5.05	4.68	15	153.3

^a Chemical shifts refer to the methylene linker of ligand **1a**. ^b Chemical shifts correspond to C_α of the alkenyl ligand. ^c Chemical shift of the PPh₃ ligand. ^d Chemical shift of the -PPh₂ moiety of coordinated ligand **1a**. ^e Major isomer. ^f Minor isomer.

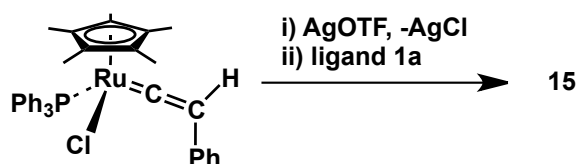
Although the full assignment of complexes **13-16** as either *E* or *Z* was not pursued using solution methods, a partial X-ray structure determination of complex **15** by Dr. Hilary Jenkins at the McMaster Analytical X-Ray Diffraction Facility not only confirmed that ring-opening had occurred to form the five-membered ring vinylidene insertion product, but also that the connectivity about the double bond was, in fact, *E*. Unfortunately, extensive solvent disorder prevented the complete refinement of the solid state structure.

Scheme 25 illustrates a plausible mechanism by which the vinylidene insertion complexes **13-16** may form.^[105,170,171] The precursors **2** or **3** first undergo ring-opening to yield unsaturated $\kappa^1\text{-P}^{\text{Ph}}\text{NBPh}_4$ intermediates that rapidly coordinate and isomerize the alkyne to an intermediate vinylidene complex. The vinylidene intermediate then undergoes attack at strongly electrophilic C_α by the pendant, nucleophilic benzimidazole nitrogen of the $\kappa^1\text{-P}^{\text{Ph}}\text{NBPh}_4$ ligand to yield the ring-closed product. The ring-closing process would be especially facile since the nucleophilic attack occurs in an intramolecular, chelate-assisted fashion. Certainly, the relief in ring-strain upon switching from the 4-membered to the 5-



Scheme 25. Possible mechanism for the synthesis of complexes **13-16**.

membered metallacycle assists this process. Attempts were made to detect the ring-opened, vinylidene intermediates via *in situ* monitoring of the reactions by NMR spectroscopy, however evidence of their formation was not observed. To establish the likelihood of this intermediate, the complex $\text{Cp}^*\text{RuCl}(\text{CCHPh})(\text{PPh}_3)$,^[174] which contains a preformed vinylidene ligand, was reacted sequentially with AgOTf and ligand **1a** in THF (Scheme 26). NMR spectroscopic analysis of the red solid isolated from the reaction showed clean conversion to complex **15**, suggesting the vinylidene intermediate in Scheme 23 is plausible.



Scheme 26. Alternate synthetic route to complex **15**.

Considering the comparatively more robust metallacycles observed for complexes **4** and **5** in previous reactions with small molecules, it was reasoned that perhaps these complexes might be less prone to ring-opening in their corresponding reactions with 1-alkynes, and thus vinylidene insertion products might be avoided. In general, complexes **4** and **5** were, in fact, found to be more resistant towards reactions with 1-alkynes compared to complexes **2** and **3**. However, under forcing conditions (excess alkyne reagent, prolonged heating at

80 °C for up to 10 days) , insertion was observed to occur, but only to a limited extent. For example, heating either complex **4** or **5** in the presence of a 10-fold excess of phenylacetylene over 24 hours in 1,2-dichloroethane shows small conversions to the vinylidene insertion products, as evidenced by the presence of two new sets of doublets of an AX spin pattern consistent with the formation of the *E*- and *Z*-product isomers, along with substantial amounts of starting complex in each case. Unfortunately, prolonged heating over extended periods only resulted in significant decomposition, as revealed by $^{31}\text{P}\{^1\text{H}\}$ NMR spectroscopy, and thus the insertion products in these reactions could not be isolated and fully characterized.

The corresponding *p*-cymene chelate complexes **6-8** were also reacted with 1-alkyne reagents. It was hoped that the Cl ligand in these complexes would be sufficiently labile to afford the corresponding vinylidene complexes and ring-opening of the phosphinobenzimidazole chelates would be avoided.

When complex **6** was reacted with 1 molar equivalent of 1-phenylacetylene in an NMR tube (CD_2Cl_2 , heated at 60°C for 24 hours), disappearance of the $^{31}\text{P}\{^1\text{H}\}$ signal of **6** was accompanied by the formation of a set of peaks at δ 55.4 ppm and δ 53.4 ppm in an approximate ratio of 9:1 respectively (Figure 30). Similar results were obtained for reacting complex **6** with 1-hexyne under the same conditions. Again, the $^{31}\text{P}\{^1\text{H}\}$ NMR of the product revealed that the starting material had been completely consumed and two different phosphorus-containing compounds had been generated with resonances at δ 54.2 ppm and δ 53.9 ppm

in a 4:1 ratio respectively (Figure 31). Unfortunately, a peak far downfield in the $^{13}\text{C}\{^1\text{H}\}$ NMR spectrum, a region where the $\text{C}\alpha$ of Ru-vinylidene complexes typically resonates, ^[117-119,175,176] was absent for the products formed by reacting complex **6** with the 1-phenylacetylene or 1-hexyne. In light of the formation of the

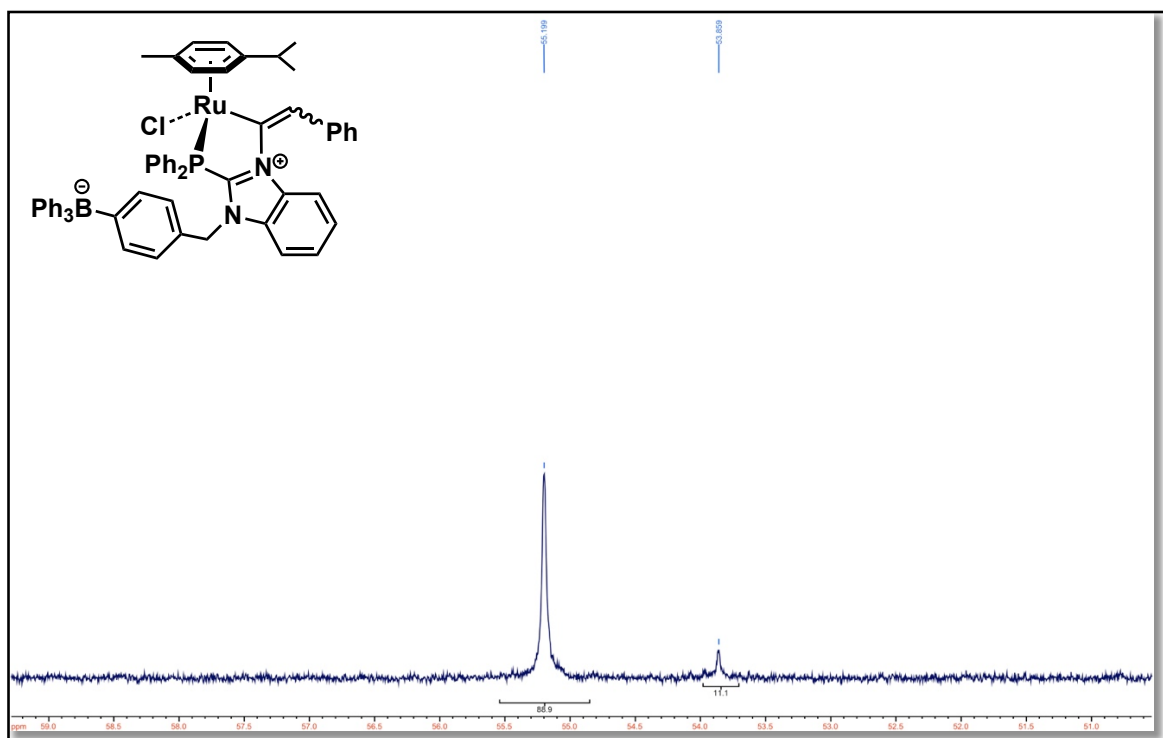


Figure 30. $^{31}\text{P}\{^1\text{H}\}$ NMR spectrum of the products obtained by reacting complex **6** with 1-phenylacetylene. The proposed isomeric structure of the products is displayed illustrating the insertion of the alkyne into the Ru-N bond.

alkyne insertion products **13-16** by reacting complex **2** with the 1-alkyne reagents, it was suspected that alkyne insertion was occurring in the reactions involving complex **6** as well (Figure 30). Furthermore, similar results were

obtained when a halide abstracting agent was used in these reactions. For example, the addition of NaBPh₄ or NaPF₆ to complex **6** in the presence of 1-phenylacetylene or 1-hexyne under various conditions (e.g., CH₂Cl₂ vs. THF, increased molar ratio of halide abstractor, room temperature vs. 60°C) resulted in the same products

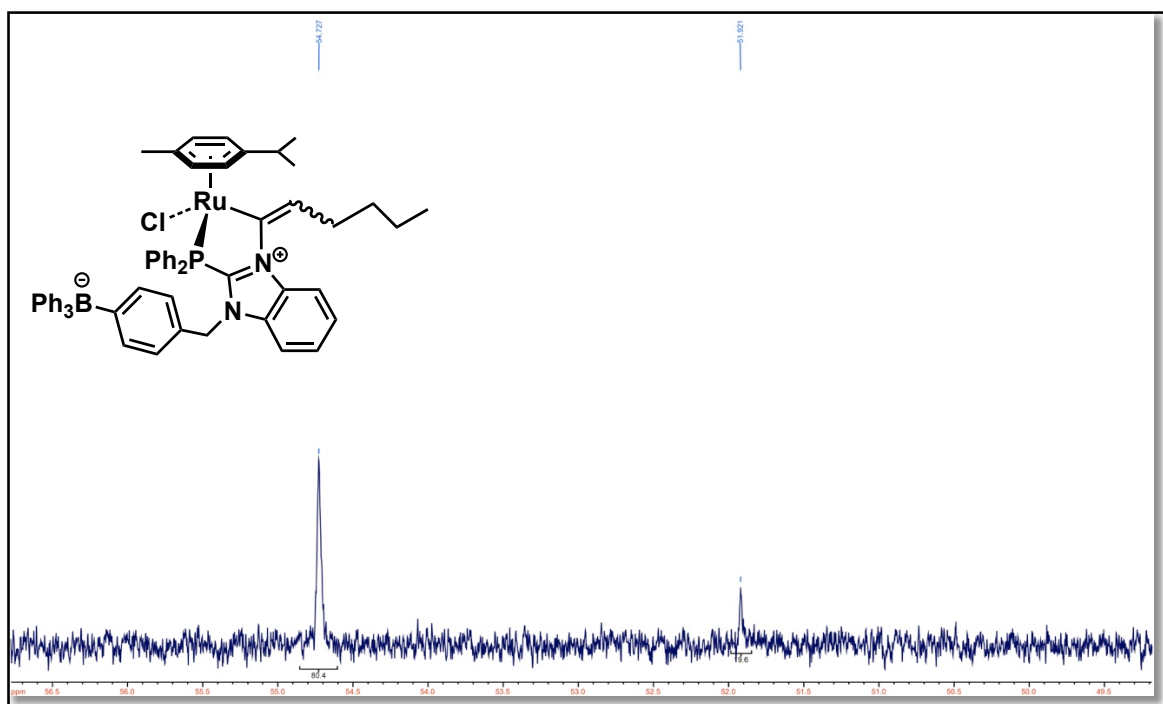


Figure 31. ³¹P NMR spectrum of the products generated from the reaction of complex **6** with 1-hexyne. The proposed isomeric structure of the products is displayed illustrating the insertion of the alkyne into the Ru-N bond.

being formed as obtained in the absence of these salts. Since the insertion products were not the desired products (as was the case with complexes **13-16**)

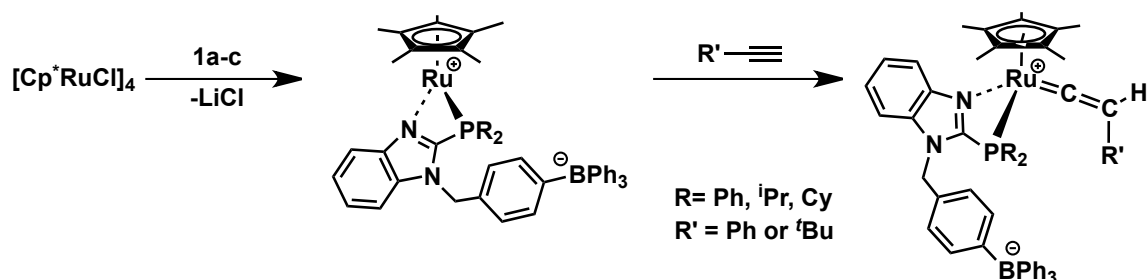
for additional investigation, efforts to further characterize these complexes were abandoned.

The corresponding *p*-cymene chelate complexes **7** and **8** showed poor reactivity and/or selectivity towards 1-alkyne reagents. Complex **7**, when heated in 1,2-dichloroethane in the presence of excess phenylacetylene, only yielded unappealing mixtures of products, as determined by $^{31}\text{P}\{^1\text{H}\}$ NMR spectroscopy. Complex **8**, under similar conditions, showed no reactivity at all; it was the only product observed in the reaction mixture ($^{31}\text{P}\{^1\text{H}\}$ NMR) after refluxing with a 10-fold excess of phenylacetylene in 1,2-dichloroethane over 12 hours. Attempts to facilitate these reactions by using chloride abstracting reagents (e.g., NaBPh_4 , AgBF_4 , AgOTf , or MeOTf) only lead to mixtures containing a substantial number of different products ($^{31}\text{P}\{^1\text{H}\}$ NMR).

6.2. Reaction of Ligand **1c** with $[\text{Cp}^*\text{RuCl}]_4$ and 1-Phenylacetylene: The Formation of Ruthenium Vinylidenes

Given the difficulties experienced in attempting to generate distinct ruthenium vinylidene complexes beginning with complexes **2-8**, a different approach was sought. The ruthenium, cubane-like complex $[\text{Cp}^*\text{RuCl}]_4$ ^[177] is a proven source of the “ Cp^*RuCl ” building block.^[177-179] Since ligands **1a-c** were shown to facilitate removal of chloride ligands from ruthenium-chloro precursors during the initial coordination chemistry studies, it was reasoned that perhaps, in a similar manner, **1a-c** will react with $[\text{Cp}^*\text{RuCl}]_4$ to form the 16-electron complexes of the general type $\text{Cp}^*\text{Ru}(\kappa^2\text{P}, N\text{-P}^{\text{R}}\text{NBPh}_4)$. It was also reasoned that

such unsaturated complexes might readily isomerize 1-alkynes to the corresponding vinylidenes (Scheme 27).



Scheme 27: Proposed synthetic route to Cp*Ru vinylidenes beginning with $[Cp^*RuCl]_4$ and ligands **1a-c**.

Preliminary studies involved monitoring reaction solutions containing $[Cp^*RuCl]_4$ and one equivalent of either **1a** or **1b** via NMR spectroscopy, and revealed surprisingly complex mixtures. None of the products formed in these mixtures could be confidently identified. Perhaps the lack of selectivity in these initial reactions might be traced to inadequate steric and/or electronic profiles of ligands **1a** and **1b** in these reactions, both of which are critical to the formation of unsaturated 16-electron ruthenium complexes.^[180-182]

In stark contrast to the reactions with **1a** and **1b**, when four molar equivalents of ligand **1c** are mixed with $[Cp^*RuCl]_4$, the solution turns deep dark blue in colour – an observation that is characteristic of unsaturated 16-electron Cp*RuCl(L) (L = monodentate ligand, e.g., PR₃) complexes – and a broad signal

at δ 53.3 ppm is observed in the $^{31}\text{P}\{^1\text{H}\}$ NMR spectrum. Completely characterizing this complex proved to be challenging, as all attempts to isolate it, either as a bulk product or as single crystals, resulted in the formation of orange solutions containing mixtures of unidentified products (NMR). However, upon adding four equivalents of phenylacetylene to the blue solution, a progressive change in colour was observed from dark blue to finally dark orange-red. *In situ* monitoring of the solution via $^{31}\text{P}\{^1\text{H}\}$ NMR spectroscopy during the very early stages of the reaction revealed two signals, one at δ 14.4 ppm, the other at δ 29.5 ppm soon after the alkyne was added. Over time, the signal at δ 14.4 ppm disappears, and is accompanied by an increase in the intensity of the signal at δ 29.5 ppm. It is proposed that the signal at δ 29.5 ppm is attributed to the target vinylidene complex of $\text{Cp}^*\text{RuCl}(\text{CCHPh})(\kappa^2\text{P},\text{N}-\text{P}^{\text{Cy}}\text{NBPh}_4)$ (**18**) (*vide infra*), however the short-lived species producing the signal at δ 14.4 ppm is intriguing. The isomerization of 1-alkynes about ruthenium often proceed through η^2 -alkyne intermediates.^[175,176] It is thought that perhaps the short-lived species at δ 14.4 ppm might be attributed to the formation of the intermediate η^2 -alkyne species.

The reaction solutions containing **18** were often accompanied by the presence of an unknown impurity which produced a very broad $^{31}\text{P}\{^1\text{H}\}$ NMR signal at approximately δ 54 ppm (Figure 32). This unidentified product persisted through the various purification steps, and consequently complicated all attempts to isolate **18** as a pure material. Nonetheless, the ^1H NMR spectrum of **18** reveals, among other signals, an AB spin pattern attributed to the methylene linker of the

coordinated anion of **1c** ligand (δ_A 5.38 ppm and δ_B 5.18 ppm, $^2J_{HH} = 16$ Hz), suggesting a chiral Ru centre. The proton on C_β of the vinylidene ligand

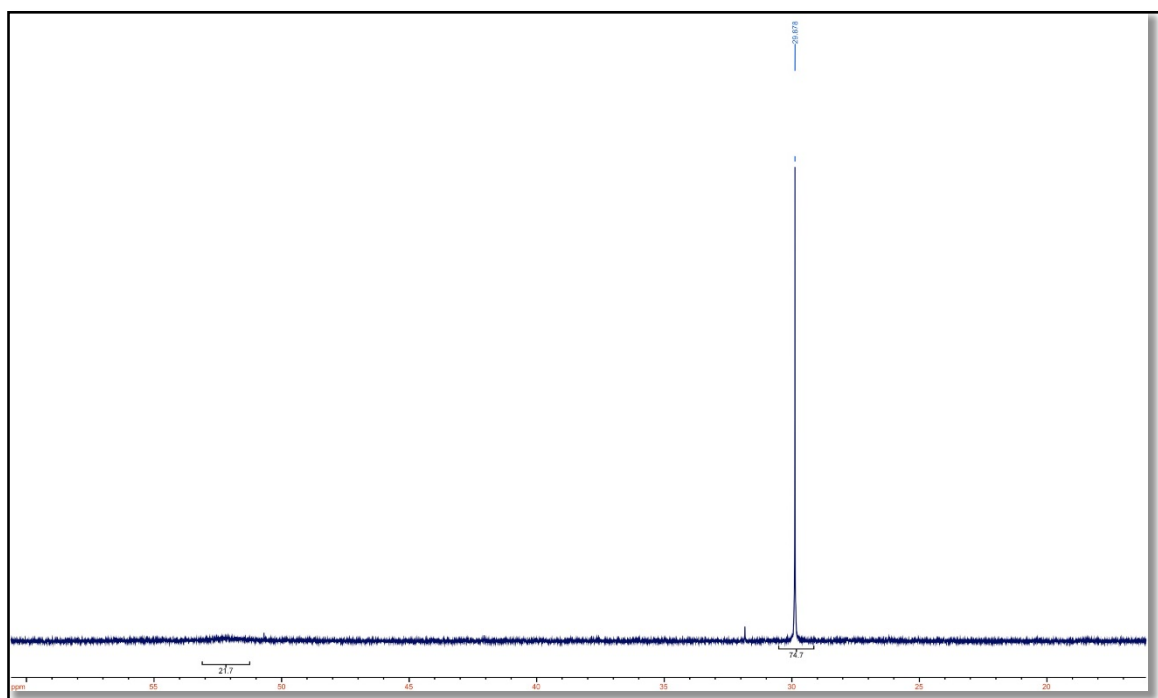


Figure 32. $^{31}\text{P}\{^1\text{H}\}$ NMR spectrum of crude $\text{Cp}^*\text{RuCl}(\text{CCHPh})(\kappa^2\text{P},\text{N}-\text{P}^{\text{Cy}}\text{NBPh}_4)$.

appears as a doublet at δ 4.86 ppm ($^4J_{\text{PH}} = 2$ Hz), consistent with other related ruthenium-vinylidene complexes.^[117-119,175,176] Perhaps the most convincing evidence for the presence of the vinylidene ligand in **18** is the doublet resonance located substantially downfield at δ 345.4 ppm ($^2J_{\text{PC}} = 13$ Hz) in its $^{13}\text{C}\{^1\text{H}\}$ NMR spectrum (Figure 33), again consistent with related systems.^[117-119,175,176]

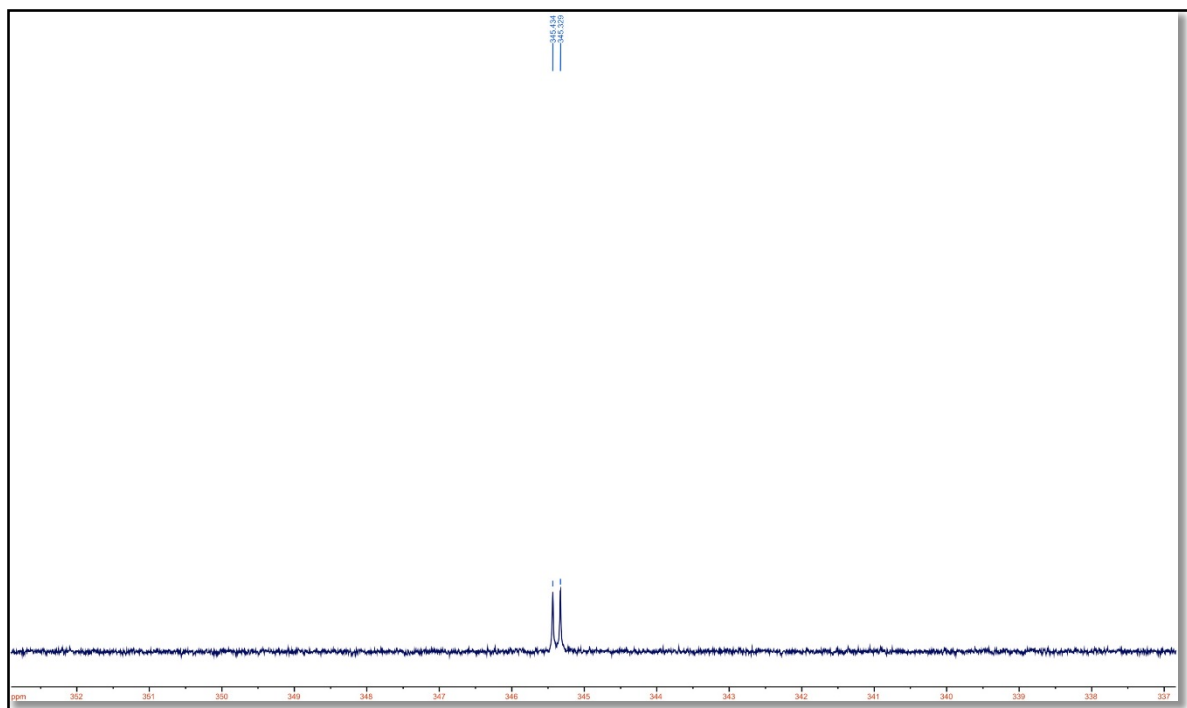


Figure 33. $^{13}\text{C}\{^1\text{H}\}$ NMR spectrum (C_α region only) of $\text{Cp}^*\text{RuCl}(\text{CCHPh})(\kappa^2\text{P},\text{N}-\text{P}^{\text{Cy}}\text{NBPh}_4)$.

Extending this reaction to include *tert*-butylacetylene as the vinylidene source allowed for the production of the analogous vinylidene complex $\text{Cp}^*\text{RuCl}(\text{CCH}^t\text{Bu})(\kappa^2\text{P},\text{N}-\text{P}^{\text{Cy}}\text{NBPh}_4)$, **19**. The $^{31}\text{P}\{^1\text{H}\}$ NMR spectrum of the crude material reveals a strong singlet at δ 30.7 (Figure 34). As was the case for the phenyl vinylidene complex **18** an impurity at ~ 54 ppm ($^{31}\text{P}\{^1\text{H}\}$ NMR) frustrated all

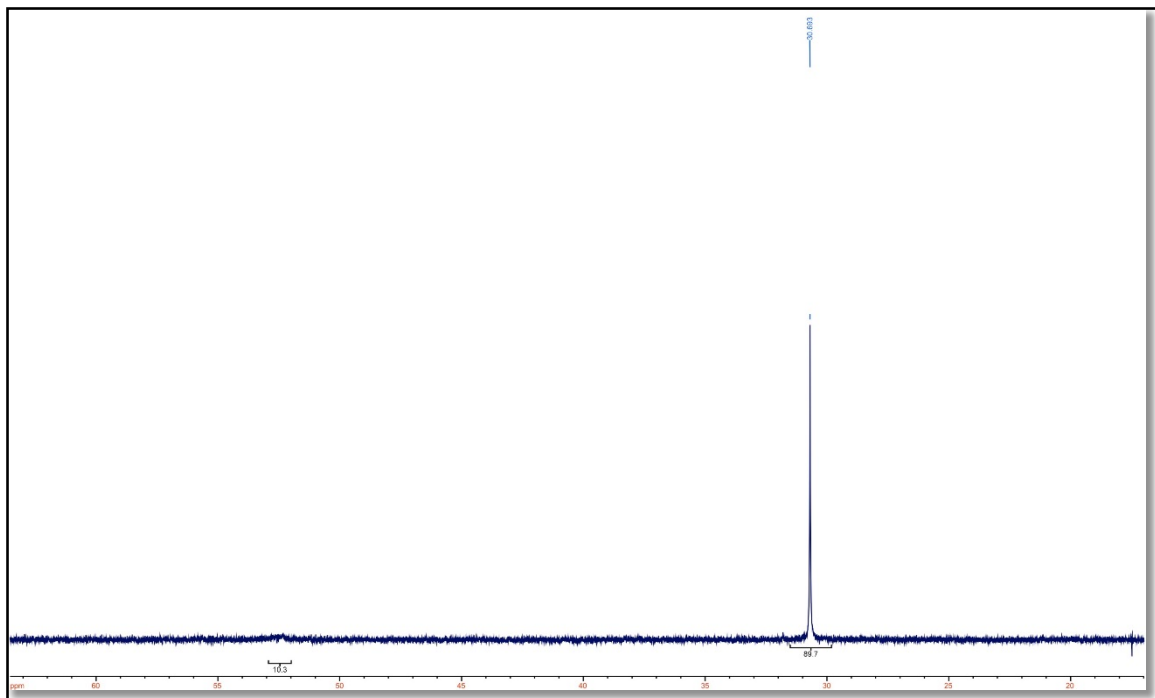


Figure 34. $^{31}\text{P}\{^1\text{H}\}$ NMR spectrum of $\text{Cp}^*\text{RuCl}(\text{CCH}^t\text{Bu})(\kappa^2\text{P},\text{N}-\text{P}^{\text{Cy}}\text{NBPh}_4)$ revealing a signal at δ 30.7 ppm pertaining to the vinylidene product and a broad impurity peak at approximately δ 54 ppm.

attempts at isolating **19** in analytically pure form. Regardless, the accumulated key NMR evidence is consistent with its formulation: a set of diastereotopic protons (δ_{A} 5.42 ppm and δ_{B} 5.35 ppm, $^2J_{\text{HH}} = 16$ Hz) attributed to the methylene linker of the ligand; a signal at δ 3.77 ppm assigned to the $\text{C}_{\beta}\text{-H}$ of the vinylidene ligand in the ^1H NMR spectrum; and, a doublet in the $^{13}\text{C}\{^1\text{H}\}$ NMR spectrum located substantially downfield at δ 340.0 ppm ($^2J_{\text{PC}} = 14$ Hz) attributed to C_{α} of the vinylidene ligand (Figure 35).

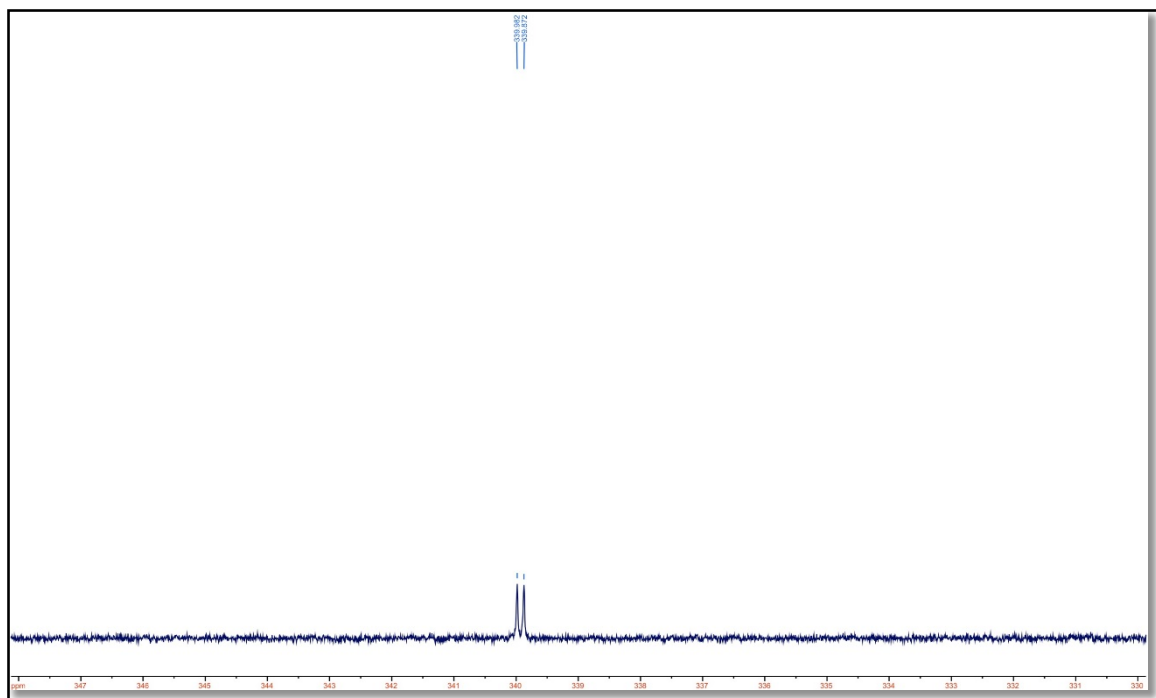


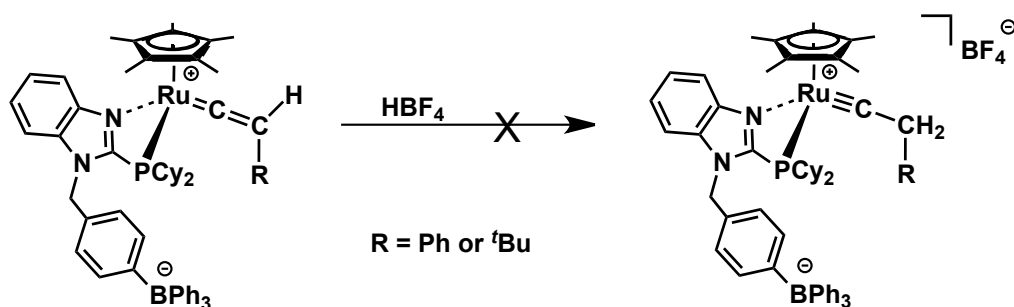
Figure 35. $^{13}\text{C}\{^1\text{H}\}$ NMR spectrum (C_α region only) of $\text{Cp}^*\text{RuCl}(\text{CCH}^t\text{Bu})(\kappa^2\text{P},\text{N}-\text{P}^{\text{Cy}}\text{NBPh}_4)$, **19**.

6.3. Attempted Synthesis of Ruthenium-Carbyne Complexes

As mentioned previously in the Introduction of this work, the explosive development of well-defined and highly efficient catalysts for olefin metathesis has been accompanied by a rapid expansion in applications of these catalysts in a variety of C-C bond forming reactions in organic and polymer synthesis. Undeniably, many of the greatest advances in this area have involved the Grubbs'-class of ruthenium carbene catalysts. Surprisingly, despite the tremendous

interest in refining and applying these catalysts, considerably less attention has been given to the development of their ruthenium-carbon triple bond counterpart. Conceivably, ruthenium-carbyne complexes may possess similar properties to the ruthenium carbenoid complexes, and possibly demonstrate novel reactivity patterns and substantial promise as catalysts (*e.g.*, as alkyne metathesis initiators).

Perhaps the more convenient method of preparing ruthenium-carbynes is via regioselective protonation of suitable ruthenium-vinylidene precursors.^[117-119,175,176] It was therefore reasoned that the new ruthenium-vinylidene complexes described in the previous section might also allow access to ruthenium-carbyne complexes (Scheme 28). The carbyne targets described in Scheme 25 are certainly worthy of pursuit from a more practical perspective since the chelating



Scheme 28. Proposed strategy for synthesizing ruthenium-carbyne complexes from ruthenium-vinylidene precursors.

κ^2 -*P,N* ligand could potentially furnish a vacant site adjacent to the carbyne ligand by reversibly dissociating the benzimidazole arm from the metal during catalysis (e.g., alkyne metathesis). Unfortunately, the addition of $\text{HBF}_4 \cdot \text{Et}_2\text{O}$ to CD_2Cl_2 solutions of either **18** or **19**, even at low temperatures ($-70\text{ }^\circ\text{C}$), led to complete decomposition of the parent vinylidenes, as determined by variable temperature NMR spectroscopy. Interestingly, the ^{11}B NMR spectra of these reactions show the complete disappearance of the signal attributed to the tetraphenylborate moiety (~ -6 ppm) of the coordinated κ^2 *P,N*- $\text{P}^{\text{Cy}}\text{NBPh}_4$, suggesting this anionic centre of the molecule might affect the regioselectivity of the protonation reactions, and thus play a role in the decomposition of the parent vinylidene complexes.

Chapter Seven: Summary, Conclusions and Future

Prospects

The results presented in this body of research provide insight regarding the fundamental properties of the borate-functionalized (phosphino)benzimidazole ligands **1a-c** and their coordination behavior in ruthenium half-sandwich chemistry. The synthesis of ligands **1a-c** were found to be particularly sensitive towards reaction conditions, especially the final step involving the installation of the borate group. Indeed, competing reactions between the metalated intermediate and the benzimidazole nitrogen (*i.e.*, N-3) can complicate their syntheses. The presence of the borate group does not seem to impact the donor power of the anionic (phosphino)benzimidazole ligands, based on comparative spectroscopic (NMR) studies of their selenide derivatives with neutral analogues. However, these same studies do support the expected trend in donor power among the anionic phosphines **1a-c** (*i.e.*, **1a** < **1b** < **1c**), and that the cyclohexyl-substituted ligand **1c** is the strongest donor ligand in the series.

There was a significant difference in coordination behaviour among the anionic (phosphino)benzimidazole ligands depending of the form of the salt (*i.e.*, lithium vs. tetraphenylphosphonium). In general, ligands **1a-c** assist in the coordination and chelation of these ligands to ruthenium-chloro precursors via LiCl elimination. In contrast, ligands **1a'-c'** in the presence of the same metal precursors, either produced monodentate (*i.e.*, ring-opened) complexes, a mixture of both monodentate and chelate complexes, or didn't react at all, suggesting

chloride abstraction was key to the success behind the synthesis of a number of the complexes described herein.

The substituents on the phosphorus centres (*i.e.*, Ph vs. ⁱPr vs. ^tBu) of the anionic (phosphino)benzimidazole ligands were observed to influence strongly the strength of the metallacycle in many of the chelated (*i.e.*, κ^2 -P,N-P^RNBPh₄) complexes examined as part of this work. In several instances, the anion of ligand **1a** (phenyl substituents on phosphorus) displayed an ability to adopt both monodentate and chelate coordination modes, in some cases interchangeably (hemilabile behaviour) in the presence of labile molecules (*e.g.*, MeCN or CO). In contrast, ligands **1b** and **1c** showed a strong propensity to chelate to ruthenium, and were observed to be resilient towards ring-opening, even under forcing conditions.

Ultimately, there was a greater interest to examine the use of the anions of **1a-c** as supporting ligands in ruthenium-carbyne chemistry and to assess the capability of these complexes to initiate alkyne metathesis. However, these efforts were initially frustrated by the synthesis of ruthenium-vinylidene precursors. Interestingly (and consistent with observations made in earlier studies involving small molecules), several ruthenium complexes containing the chelated [P^{Ph}NBPh₄]⁻ ligand readily underwent ring-opening in the presence of 1-alkynes to yield (very short-lived) ruthenium-vinylidene intermediates. However, the electrophilic character of C_α of the vinylidene ligand promoted nucleophilic attack by the resulting pendant benzimidazole moiety leading to vinylidene

insertion (*i.e.*, alkenyl) products. Undoubtedly, these insertion reactions are also driven in part by a relief in ring-strain upon going from 4-membered ring to a 5-membered ring in the insertion product. In contrast, similar reactions involving analogous ruthenium precursors containing the anion of either **1b** or **1c** were much more sluggish, and only proceeded to comparatively smaller extents (compared with the anion of **1a**), even under forcing conditions.

Distinct ruthenium-vinylidene complexes containing at least the anion of **1c** could be prepared using a slightly different strategy, specifically one where the target vinylidene is constructed sequentially beginning with a simple ruthenium building block. For example, beginning with the convenient precursor $[\text{Cp}^*\text{RuCl}]_4$, sequential addition of ligand **1c** followed by a 1-alkyne (via a proposed coordinatively unsaturated, 16-electron intermediate $\text{Cp}^*\text{Ru}(\kappa^2\text{P},\text{N}-\text{P}^{\text{Cy}}\text{NBPh}_4)$) successfully leads to the formation of the vinylidene complexes $\text{Cp}^*\text{RuCl}(\text{CCHR})(\kappa^2\text{P},\text{N}-\text{P}^{\text{Cy}}\text{NBPh}_4)$ (R = alkyl or aryl). We were especially interested in such complexes because it was expected that they might serve as convenient precursors to ruthenium-carbyne complexes. Unfortunately, the coordinated anion of ligand **1c** proved to be sensitive towards the acidic conditions required to manufacture the target ruthenium-carbyne. Perhaps the anionic borate moiety tethered to the (phosphino)benzimidazole framework of the coordinated anion of ligand **1c** complicates the regioselectivity of these reactions. However, further investigation is required to provide insight to the nature of these reactions.

Numerous avenues for future work regarding heterobidentate (phosphino)borate ligands have been paved by this study. For example, one of the motivations of tethering a tetraphenylborate group to the [P,N] ligand structure was to potentially increase the electron donor-power of the phosphine group. However, segregating the negative charge of the borate from the phosphine group seemed to have negligible effects on the donor capacity of the phosphine atom. It would be interesting to formulate a design strategy that placed the borate group closer to the phosphine atom (in a similar fashion compared to other (phosphino)borate systems^[76]) as an attempt to increase the electron donating capacity of the ligand.

Another structural feature of the anionic [P,N] ligands described in this work was the incorporation of a benzimidazole group with the intention that it would operate in a hemilabile fashion. However, it was found that the pendant groups on the phosphorous greatly impacted the ability of the metallacycles formed by these ligands to undergo ring-opening. Extending this class of ligand to include phosphorous groups with different steric/electronic characteristics (ie. $-\text{P}(\text{OMe})_2$, $-\text{P}(\text{Me})_2$, $-\text{P}(\text{tBu})_2$) and comparing their effect on the lability of the coordinated benzimidazole nitrogen may shed light on the origin of the difference in hemilability of the ligands presented in this work.

In addition to altering the identity of the phosphorous moiety of the [P,N] hybrid ligands, other methods that could be utilized to tune hemilability include changing the identity of the nitrogen donor and/or extending the bite angle of the

chelate. For example, changing the N donor atom to an O donor would influence the hemilability of the system. Although attempts to widen the bite angle of ligands **1a-c** were unsuccessful, changing the basic ligand scaffold could afford access to a larger metallacycle and therefore provide a means to influence the hemilability of the ligand.

Indeed, these generalized structural modifications could lead to a plethora of ligand designs for future study. An example of a potential ligand where some of these alterations are present is illustrated in Figure 36. This ligand structure

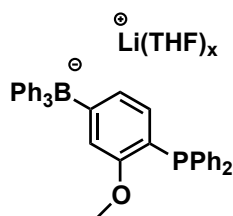


Figure 36. A potential ligand design incorporating a larger bite angle and closer proximity of the borate to the phosphine group compared to ligands **1a-c**, as well as an oxygen donor atom.

contains an oxygen donor as opposed to a nitrogen donor, it places the anionic borate functionality close to the phosphorus donor and would form a five-membered metallacycle when chelated to a metal. Furthermore, derivatization of the pendant group attached to the oxygen donor (Me group in Figure 36) would provide a means to tune the electronic and steric effects of the ligand.

Another structural feature of ligands **1a-c** that could be modified is the identity of the borate group. It was found that the borate of the anion of **1c** in complex **18** and **19** was sensitive to the presence of HBF_4 . Perhaps using a different borate such as a $-\text{BF}_3$ group would circumvent this issue and provide access to the target carbyne complexes.

Furthermore, the incorporation of two borate groups into the ligand architecture would be an intriguing ligand design. For example, the $-\text{PR}_2$ donor could incorporate borate groups thereby placing the anionic borate in close proximity to the phosphine (left in Figure 37) or the borates could be integrated into a heteroscorpionate-type structure (right in Figure 37). An advantage of these designs is that they have the potential to form charge-neutral Ru(II) zwitterions in the absence of other charged ligands (ie. halide, Cp, Tp).

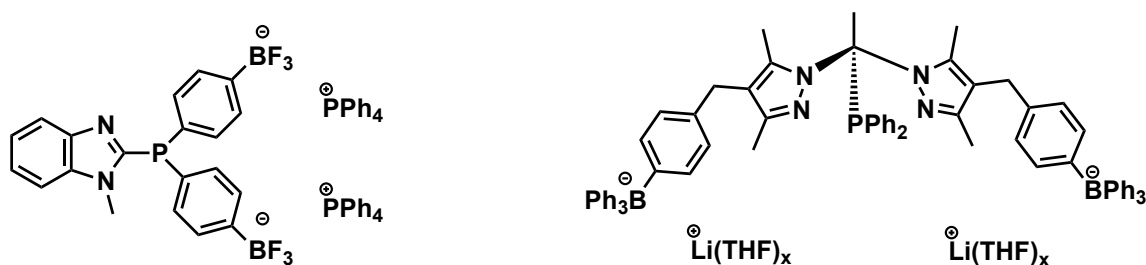


Figure 37. Examples of dianionic (phosphino)borate ligand structures.

The relative scarcity of (phosphino)borate ligands in the literature renders this class of ligand a wide open field for exploration. The few examples that have been studied to date have revealed some interesting and divergent properties of the metal complexes that contain them (compared to complexes that contain

neutral analogues). Without a doubt, anionic (phosphino)borate ligands will remain a fascinating area of ligand design.

Chapter Eight: Experimental

8.1. General Experimental Details

All experiments and manipulations were conducted under an inert atmosphere of pre-purified nitrogen using standard Schlenk techniques. Hexanes, CH_2Cl_2 and 1,2-dichloroethane were pre-dried over activated 4 Å molecular sieves, passed through a column of alumina, purged with N_2 and stored over 4 Å molecular sieves in bulbs with Teflon taps.^[183] Diethyl ether and THF were freshly distilled from sodium metal under N_2 . Acetone was stored under an atmosphere of N_2 and used without further purification. CDCl_3 (dried over anhydrous CaCl_2) and CD_2Cl_2 (dried over CaH_2) were vacuum distilled, freeze-pump-thaw degassed three times, and stored in bulbs with Teflon taps. NMR spectra (^1H , $^{13}\text{C}\{^1\text{H}\}$, $^{31}\text{P}\{^1\text{H}\}$, $^{11}\text{B}\{^1\text{H}\}$ and ^7Li) were obtained using a Varian Unity INOVA 500 MHz spectrometer, with chemical shifts (in ppm) referenced to residual solvent peaks (^1H and ^{13}C), external 85% H_3PO_4 (^{31}P), external $\text{BF}_3\cdot\text{OEt}_2$ solution (^{11}B), or external LiCl in D_2O . Infrared spectra were acquired using a Nicolet 380 FT-IR spectrometer. Elemental analyses were obtained from the Lakehead University Instrumentation Laboratory. 1-(4-Bromobenzyl)-2-(hydroxymethyl)benzimidazole was prepared using a modified literature preparation.^[139] 1-(benzyl)benzimidazole,^[184] $\text{CpRuCl}(\text{PPh}_3)_2$,^[185] $\text{Cp}^*\text{RuCl}(\text{PPh}_3)_2$,^[186] $\text{Cp}^*\text{RuCl}(\text{CO})_2$,^[155] $\text{Cp}^*\text{RuCl}(\text{CCHPh})(\text{PPh}_3)$,^[174] and $[\text{Cp}^*\text{RuCl}]_4$ ^[177] were synthesized using previously reported procedures. Ligands **1a-c** were synthesized (*vide infra*) and sufficiently pure for further use. Variable solvent

content made the acquisition of combustion data difficult; however, the comparison of data to similar neutral systems that have been previously reported allowed for the confident characterization of ligands **1a-c** via NMR spectroscopy.

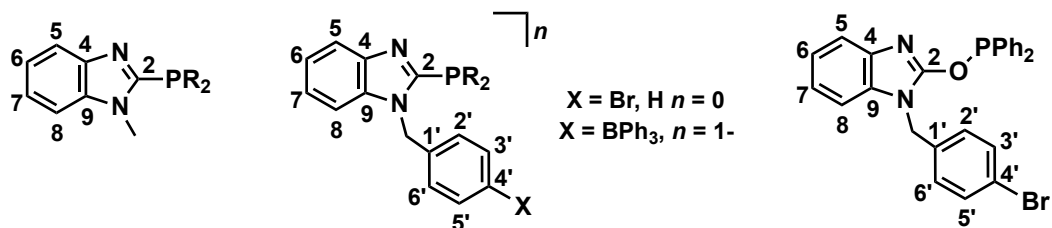


Figure 38. Ligand numbering scheme for characterization.

8.2. Synthesis of 1-(4-bromobenzyl)benzimidazole

The following is a modification of the literature procedure.^[127] Benzimidazole (4.00 g, 33.9 mmol), 4-bromobenzyl bromide (8.46 g, 33.86 mmol) and KO^tBu (4.00 g, 35.6 mmol) were combined and dissolved in THF (70 mL). The cloudy, colourless mixture was stirred at reflux for 8 hours before the volatiles were removed under reduced pressure. The product was then dissolved in CH₂Cl₂ (100 mL) and filtered through a small pad of silica. An additional volume of CH₂Cl₂ (100 mL) was used to quantitatively transfer the product through the filtration apparatus. The volatiles were removed from the clear, colourless filtrate yielding a colourless crystalline solid. The solid was used without further purification. Yield: 6.90 g (71%). The ¹H NMR spectral data were in agreement with the previously published data for this compound.

8.3. Synthesis of 1-(4-bromobenzyl)-2-(diphenylphosphino)benzimidazole

Lithium diisopropylamide (LDA) was first synthesized by adding ⁿBuLi (4.40 mL of a 1.6 M solution in hexanes, 6.97 mmol) to diisopropylamine (976 μ L, 6.97 mmol) in THF (5 mL) at -78 °C. After 1 hour at -78 °C, the LDA solution was then added via cannula to a THF (30 mL) solution of 1-(4-bromobenzyl)benzimidazole (2.00 g, 6.97 mmol) pre-cooled to -78 °C. The bright orange solution was stirred at -78 °C for 1 hour. Next, PPh₂Cl (1.25 mL, 6.97 mmol) was added to the cooled orange solution via syringe. The mixture was left in the cooling bath and allowed to warm slowly to room temperature over 2 hours. After this time, the volatiles were removed under reduced pressure to yield a tacky orange solid. The solid was extracted into CH₂Cl₂ (5 x 10 mL) and filtered through Celite. Removal of the volatiles under reduced pressure yielding a pale yellow solid. The solid was used without further purification. Yield: 3.16 g (96%). ¹H NMR (500 MHz, 22 °C, CDCl₃): 7.85 (d, 1 H, ²J_{HH} = 8.5 Hz, C⁸H), 7.50-7.19 (overlapping m, 15H, Ph of -PPh₂, C⁵H-C⁷H, C³H and C⁵H), 6.80 (d, 2H, ²J_{HH} = 8.5 Hz, C²H, C⁶H), 5.55 (d, 2H, ⁴J_{PH} = 3 Hz, -CH₂-). ¹³C{¹H} NMR (125 MHz, 22°C, CDCl₃): 154.4 (d, ¹J_{PC} = 9 Hz, C²), 144.6-128.4 (Ph, C¹-C⁶ and C⁴, C⁹), 123.5, 122.4 (both s, C⁶ and C⁷), 120.8 (s, C⁵), 110.0 (s, C⁸), 47.8 (d, ³J_{PC} = 15 Hz, -CH₂-). ³¹P{¹H} NMR (202 MHz, 22 °C, CDCl₃): -28.3 (s, -PPh₂).

8.4. Synthesis of 1-(4-bromobenzyl)-2-(diisopropylphosphino)benzimidazole

LDA was first generated by adding ${}^n\text{BuLi}$ (1.96 mL, of a 1.6 M solution in hexanes, 3.14 mmol) to a THF (10 mL) solution of diisopropylamine (440 μL , 3.14 mmol) at $-80\text{ }^\circ\text{C}$. After stirring at $-80\text{ }^\circ\text{C}$ for 1 hour the LDA solution was added via cannula to a solution of 1-(4-bromobenzyl)benzimidazole (902 mg, 3.14 mmol) dissolved in THF (20 mL). The dark red-orange solution was stirred at $-80\text{ }^\circ\text{C}$ for 1 hour before $\text{P}^i\text{Pr}_2\text{Cl}$ (500 μL 3.14 mmol) was added dropwise. The light yellow solution was allowed to warm to room temperature and then was stirred for 17 hours. The volatiles were removed from the orange-yellow solution and the residue was redissolved in CH_2Cl_2 . After filtration through a small plug of silica, the volatiles were removed from the bright yellow filtrate yielding a yellow oil which solidified upon prolonged exposure to reduced pressure. The solid was used without further purification. Yield: 1.13 g (89%). ${}^1\text{H}$ NMR (500 MHz, $22\text{ }^\circ\text{C}$, CDCl_3): 7.81 (d, 1H, ${}^2J_{\text{HH}} = 8.5\text{ Hz}$, C^8H), 7.33 (d, 2H, ${}^3J_{\text{HH}} = 8\text{ Hz}$, C^3H and C^5H), 7.22-7.11 (overlapping m, 3H, $\text{C}^5\text{H}-\text{C}^7\text{H}$) 6.90 (d, 2H, ${}^3J_{\text{HH}} = 8.5\text{ Hz}$, C^2H , C^6H), 5.59 (d, 2H, ${}^4J_{\text{PH}} = 3\text{ Hz}$, $-\text{CH}_2-$) 2.44-2.38 (m, 2H, $-\text{CH}(\text{CH}_3)_2$), 1.06 (dd, 6H, ${}^3J_{\text{PH}} = 15\text{ Hz}$, ${}^3J_{\text{HH}} = 7.3\text{ Hz}$, $-\text{CH}(\text{CH}_3)(\text{CH}_3)$), 0.94 ((dd, 6H, ${}^3J_{\text{PH}} = 13\text{ Hz}$, ${}^3J_{\text{HH}} = 7\text{ Hz}$, $-\text{CH}(\text{CH}_3)(\text{CH}_3)$) ${}^{13}\text{C}\{{}^1\text{H}\}$ NMR (125 MHz, $22\text{ }^\circ\text{C}$, CDCl_3): 155.1 (d, ${}^1J_{\text{PC}} = 21\text{ Hz}$, C^2), 144.3-128.3 (Ph, C^1-C^6 and C^4 , C^9), 123.2, 122.5 (both s, C^6 and C^7), 120.2 (s, C^5), 110.4 (s, C^8), 47.8 (d, ${}^3J_{\text{PC}} = 16\text{ Hz}$, $-\text{CH}_2-$), 24.7 (d, ${}^1J_{\text{PC}} = 7.6\text{ Hz}$, $-\text{CH}(\text{CH}_3)_2$), 20.0 (d, ${}^2J_{\text{PC}} = 17.5\text{ Hz}$, $-\text{CH}(\text{CH}_3)(\text{CH}_3)$) 19.8 (d, ${}^2J_{\text{PC}} = 9.1\text{ Hz}$, $-\text{CH}(\text{CH}_3)(\text{CH}_3)$). ${}^{31}\text{P}\{{}^1\text{H}\}$ NMR (202 MHz, $22\text{ }^\circ\text{C}$, CDCl_3): -14.4 (s, $-\text{P}^i\text{Pr}_2$).

8.5. Synthesis of 1-(4-bromobenzyl)-2-(dicyclohexylphosphino)benzimidazole

All flasks were flame-dried prior to use. LDA was first synthesized by adding $^n\text{BuLi}$ (2.83 mL of a 1.6 M solution in hexanes, 4.53 mmol) to diisopropylamine (634 μL , 4.52 mmol) in THF (10 mL) at $-80\text{ }^\circ\text{C}$. After 1 hour at $-80\text{ }^\circ\text{C}$, the LDA solution was then added via cannula to a THF (20 mL) solution of 1-(4-bromobenzyl)benzimidazole (1.30 g, 4.53 mmol) pre-cooled to $-80\text{ }^\circ\text{C}$. The resulting bright orange-red solution was stirred for 1 hour at $-80\text{ }^\circ\text{C}$ and then PCy_2Cl (1.00 mL, 4.53 mmol) was added dropwise producing a bright yellow solution. The mixture was warmed to room temperature and stirred for 17 hours. The volatiles were removed from the yellow solution and the foamy residue was redissolved in 20 mL of CH_2Cl_2 . The solution was filtered through Celite and the volatiles were removed from the filtrate yielding a bright yellow solid. The solid was used without further purification. Yield: 1.99 g (91%). ^1H NMR (500 MHz, $22\text{ }^\circ\text{C}$, CDCl_3): 7.82 (d, 1 H, $^2J_{\text{HH}} = 8\text{ Hz}$, C^8H), 7.32 (d, 2H, $^3J_{\text{HH}} = 8.5\text{ Hz}$, C^3H and C^5H), 7.21-7.10 (overlapping m, 3H, $\text{C}^5\text{H}-\text{C}^7\text{H}$) 6.88 (d, 2H, $^3J_{\text{HH}} = 8.5\text{ Hz}$, C^2H , C^6H), 5.56 (d, 2H, $^4J_{\text{PH}} = 3.5\text{ Hz}$, $-\text{CH}_2-$), 2.25-2.20 (m, 2H, C_6H_{11}), 1.84-1.81 (m, 2H, C_6H_{11}), 1.67-1.64 (m, 2H, C_6H_{11}), 1.57-1.47 (m, 6H, C_6H_{11}), 1.28-1.01 (overlapping m, 5H, C_6H_{11}). $^{13}\text{C}\{^1\text{H}\}$ NMR (125 MHz, $22\text{ }^\circ\text{C}$, CDCl_3): 154.9 (d, $^1J_{\text{PC}} = 20.5\text{ Hz}$, C^2), 144.4-128.3 (Ph, C^1-C^6 and C^4 , C^9), 123.0, 122.3 (both s, C^6 and C^7), 120.1 (s, C^5), 110.3 (s, C^8), 47.5 (d, $^3J_{\text{PC}} = 16.5\text{ Hz}$, $-\text{CH}_2-$), 33.9 (d, $J_{\text{PC}} = 7.8\text{ Hz}$, C_6H_{11}), 30.2 (d, $J_{\text{PC}} = 15.6\text{ Hz}$, C_6H_{11}), 29.4 (d, $J_{\text{PC}} = 7.5\text{ Hz}$, C_6H_{11}), 26.9 (d,

$J_{PC} = 12.5$ Hz, C_6H_{11}), 26.7 (d, $J_{PC} = 8.5$ Hz, C_6H_{11}), 26.2 (s, C_6H_{11}). $^{31}P\{^1H\}$ NMR (202 MHz, 22 °C, $CDCl_3$): -22.9 (s, $-P(Cy)_2$).

8.6. Synthesis of 1-(4-bromobenzyl)-2-((diphenylphosphino)methoxy)-benzimidazole

1-(4-Bromobenzyl)-2-(hydroxymethyl)benzimidazole was placed in a flask. The flask was briefly flame-dried before THF (20 mL) was added followed by Et_3N (233 μ L, 1.67 mmol). The mixture was stirred at room temperature for 30 minutes turning cloudy-orange. The solution was cooled to 0 °C, PPh_2Cl was added dropwise over 10 minutes, and then the mixture was stirred at 0 °C for 3 hours. The volatiles were removed from the grey-green solution and the residue was dissolved in C_6D_6 (20 mL). The resulting solution was filtered through Celite using C_6D_6 (2 x 5 mL) to quantitatively transfer the product through the frit. The volatiles were removed from the clear grey filtrate yielding a residue of similar colour that solidified after being stored under vacuum for 19 hours. The solid was used without further purification. Yield: 795 mg (95 %). 1H NMR (500 MHz, 22 °C, $CDCl_3$): 1H NMR (500 MHz, 22 °C, $CDCl_3$): 7.72 (d, 1 H, $^2J_{HH} = 8$ Hz, C^8H), 7.21-7.10 (overlapping m, 15 H, Ph, C^5H-C^7H , C^3H , C^5H) 6.73 (d, 2 H, $^3J_{HH} = 8$ Hz, C^2H , C^6H). 5.21 (s, 2 H, $-CH_2-$), 4.97 (d, $^3J_{PH} = 8$ Hz, $-CH_2OPPh$). $^{13}C\{^1H\}$ NMR (125 MHz, 22 °C, $CDCl_3$): 154.9 (d, $^1J_{PC} = 20.5$ Hz, C^2), 144.4-128.3 (Ph, $C^{1'}$ - $C^{6'}$ and C^4 , C^9), 123.0, 122.3 (both s, C^6 and C^7), 120.1 (s, C^5), 110.3 (s, C^8), 47.5 (d,

$^3J_{PC} = 16.5$ Hz, $-\text{CH}_2^-$), 33.9 (d, $J_{PC} = 7.8$ Hz, C_6H_{11}), 30.2 (d, $J_{PC} = 15.6$ Hz, C_6H_{11}), 29.4 (d, $J_{PC} = 7.5$ Hz, C_6H_{11}), 26.9 (d, $J_{PC} = 12.5$ Hz, C_6H_{11}), 26.7 (d, $J_{PC} = 8.5$ Hz, C_6H_{11}), 26.2 (s, C_6H_{11}). $^{31}\text{P}\{^1\text{H}\}$ NMR (202 MHz, 22 °C, CDCl_3): -22.9 (s, $-\text{P}(\text{Cy})_2$).

8.7. Synthesis of $[\text{Li}(\text{THF})_2][\text{P}^{\text{Ph}}\text{NBPh}_4]$, (**1a**)

The compound 1-(4-bromobenzyl)-2-(diphenylphosphino)benzimidazole (1.00 g, 2.13 mmol) was dissolved in THF (30 mL) and the solution was cooled to -80 °C (isopropanol/ LN_2). Next, $^i\text{BuLi}$ (1.25 mL of 1.7 M solution in pentane, 2.13 mmol) was added dropwise via syringe to the cooled solution over about 2 minutes yielding a dark orange solution. The solution was stirred and kept between -80 °C and -90 °C for 1 hour. The solution was maintained at -90 °C, and then BPh_3 (0.516 g, 2.13 mmol) in THF (8 mL) was added very slowly dropwise via syringe over 30 minutes. The orange solution was stirred at -90 °C for 2 hours, and then it was allowed to warm slowly to room temperature overnight while in the cooling bath. The next day, excess hexanes (~ 100 mL) were added to the light orange solution producing an orange oil. The mixture was allowed to stand for about 3 hours, and then the supernatant was decanted. The remaining orange oil was washed with hexanes (2 x 20 mL) and then dried under reduced pressure to yield a powdery pale yellow solid. The solid was used without further purification. Yield: 1.20 g (73%). ^1H NMR (500 MHz, 22 °C, CDCl_3): 7.62 (d, 1H, $^2J_{\text{HH}} = 8$ Hz, C^8H), 7.47-6.89 (overlapping m, 30H, Ph of $-\text{PPh}_2$ and BPh_3 , $\text{C}^5\text{H}-\text{C}^7\text{H}$ and C^3H , C^5H), 6.79 (d, 2 H, $^2J_{\text{HH}} = 8$ Hz, C^2H , C^6H), 5.31 (s, 2H, $-\text{CH}_2^-$), 3.60 (m, 8H, THF), 1.79 (m, 8H, THF). $^{13}\text{C}\{^1\text{H}\}$ NMR (125 MHz, 22 °C, CDCl_3): 165.0 (q, $^1J_{\text{BC}} = 48$ Hz, C^4),

163.9 (q, $^1J_{BC} = 50$ Hz, *ipso* C of B-Ph), 155.7 (d, $^1J_{PC} = 16$ Hz, C^2), 142.7-123.3 (Ph, C^1 - C^3 , C^5 , C^6 , C^4 and C^9), 121.9 (s, C^6 , C^7), 117.9 (s, C^5), 112.5 (s, C^8), 88.7 (s, C_5Me_5), 68.6 (s, THF), 50.0 (s, $-CH_2-$), 25.5 (s, THF). $^{31}P\{^1H\}$ NMR (202 MHz, 22 °C, $CDCl_3$): -24.1 (s, $-PPh_2$). $^{11}B\{^1H\}$ NMR (160 MHz, 22 °C, $CDCl_3$): -6.7 (s). 7Li NMR (195 MHz, 22 °C, $CDCl_3$): -0.35 (s).

8.8. Synthesis of $[Li(THF)_2][P^{iPr}NBPh_4]$, (**1b**)

The compound 1-(4-bromobenzyl)-2-(diisopropylphosphino)benzimidazole (2.00 g, 4.95 mmol) was placed in a flask and dissolved in THF (40 mL). The solution was cooled to -80 °C (ethanol/ LN_2) and then $tBuLi$ (3.0 mL of a 1.7 M solution in pentane, 5.1 mmol) was added dropwise inducing a colour change to dark red. The mixture was stirred at -80 °C for 1 hour before being cooled to -110 °C. At this temperature, the BPh_3 (1.198 g, 4.95 mmol) in THF (16 mL) was added dropwise very slowly over 45 mins resulting in a bright orange-red solution. The mixture was stirred at -110 °C for 2 hours, allowed to warm to room temperature, and then stirred for an additional 17 hours. Excess hexanes (150 mL) were added to the solution precipitating a pale orange-yellow oil deposited on the walls of the flask. The mixture was kept at room temperature to allow the oil to settle. The supernatant was decanted and then the volatiles were removed from the oil under reduced pressure. The residue was taken up in CH_2Cl_2 (30 mL) and filtered through Celite containing a small amount of silica. CH_2Cl_2 (20 mL) was used to quantitatively transfer the product through the frit. The volatiles were removed from the filtrate yielding a pale yellow solid. The solid was used without further

purification. Yield: 2.376 g (67%). ^1H NMR (500 MHz, 22 °C, CD_2Cl_2): 7.47-7.42 (overlapping d, C^8H , C^5H), 7.26-6.77 (overlapping m, 20 H, Ph of $-\text{BPh}_3$, $\text{C}^6\text{H}-\text{C}^7\text{H}$ and C^3H , C^5H), 6.77 (d, 2H, $^2J_{\text{H-H}} = 7$ Hz, C^2H , C^6H), 5.31 (s, 2H, $-\text{CH}_2-$), 3.59-5.56 (m, 4 H, THF), 2.31-2.27 (m, 2H, $\text{CH}(\text{CH}_3)_2$), 1.78-1.76 (m, 4H, THF), 1.01-1.02 (overlapping d, 6H, $\text{CH}(\text{CH}_3)(\text{CH}_3)$), 0.82-0.78 (overlapping d, 6H, $\text{CH}(\text{CH}_3)(\text{CH}_3)$). $^{13}\text{C}\{^1\text{H}\}$ NMR (125 MHz, 22 °C, CD_2Cl_2): 165.1 (q, $^1J_{\text{BC}} = 49$ Hz, C^4), 163.9 (q, $^1J_{\text{BC}} = 49$ Hz, *ipso* C of B-Ph), 155.9 (d, $^1J_{\text{PC}} = 34$ Hz, C^2), 142.9-124.2 (Ph, C^1-C^3 , C^5 , C^6 , C^4 and C^9), 122.4 (s, C^6 , C^7), 117.5 (s, C^5), 112.8 (s, C^8), 68.8 (s, THF), 50.3 (d, $^3J_{\text{PC}} = 12$ Hz, $-\text{CH}_2-$), 25.7 (s, THF). 25.4 (d, $^1J_{\text{PC}} = 9.7$ Hz, $-\text{CH}(\text{CH}_3)_2$), 20.6-20.5 (overlapping m, $\text{CH}(\text{CH}_3)(\text{CH}_3)$). $^{31}\text{P}\{^1\text{H}\}$ NMR (202 MHz, 22 °C, CD_2Cl_2): -9.14 (s, $-\text{P}(\text{Pr})_2$). $^{11}\text{B}\{^1\text{H}\}$ NMR (160 MHz, 22 °C, CD_2Cl_2): -6.6 (s). ^7Li NMR (195 MHz, 22 °C, CD_2Cl_2): -3.02 (s).

8.9. Synthesis of $[\text{Li}(\text{THF})_4][\text{P}^{\text{Cy}}\text{NBPh}_4]$, (**1c**).

The procedure outlined for ligand **1a** was followed but instead using 1-(4-bromobenzyl)-2-(dicyclohexylphosphino)benzimidazole (2.060 g, 4.26 mmol) as the phosphine precursor. Yield: 2.342 g (58%). ^1H NMR (500 MHz, 22 °C, CDCl_3): 7.68 (overlapping , 2H, C^5H , C^8H), 7.48-6.90 (overlapping m, 22H, Ph of $-\text{PPh}_2$ and BPh_3 , C^6H , C^7H and $\text{C}^2\text{H}-\text{C}^6\text{H}$), 5.56 (s, 2 H, $-\text{CH}_2-$), 3.63-3.61 (m, 16 H, THF), 1.92-1.11 (m, 18H, THF, C_6H_{11}). $^{13}\text{C}\{^1\text{H}\}$ NMR (125 MHz, 22 °C, CDCl_3): 164.2-163.0 (overlapping q, C^4 , *ipso* C of B-Ph). 155. (d, $^1J_{\text{PC}} = 23$ Hz, C^2), 138.8-123.3 (Ph, C^1-C^3 , C^5 , C^6 , C^4 and C^9), 122.5 (s, C^6 , C^7), 118.3 (s, C^5), 112.4 (s,

C^8), 68.2 (s, THF), 49.6 (s, $-CH_2-$), 34.5 (d, $^1J_{PC} = 9.5$ Hz, C_6H_{11}), 30.9-30.8 (m, C_6H_{11}), 31.1-30.0 (m, C_6H_{11}), 26.6-26.2 (overlapping m, C_6H_{11}) 25.5 (s, THF). $^{31}P\{^1H\}$ NMR (202 MHz, 22 °C, $CDCl_3$): -18.56 (s, $-PCy_2$). $^{11}B\{^1H\}$ NMR (160 MHz, 22 °C, $CDCl_3$): -6.6 (s). 7Li NMR (195 MHz, 22 °C, $CDCl_3$): -3.13 (s).

8.10. Synthesis of 1-(benzyl)-2-(diphenylphosphino)benzimidazole, $[PN^{Bz}]$.

LDA was first generated by adding $nBuLi$ (1.60 mL of a 1.6 M solution in hexanes, 2.56 mmol) to diisopropylamine (357 μL , 2.56 mmol) in THF (5 mL) at -78 °C. After 1 hour at -78 °C, the LDA solution was then added via cannula to a THF (20 mL) solution of 1-(benzyl)benzimidazole (1.00 g, 2.55 mmol) pre-cooled to -78 °C. The bright orange-red solution was stirred at -78 °C for 1 hour. Next, PPh_2Cl (458 μL , 2.55 mmol) was added to the cooled orange solution via syringe inducing a colour change to dark yellow. The mixture was left in the cooling bath and allowed to warm slowly to room temperature over 3 hours. After this time, the volatiles were removed under reduced pressure to yield a tacky yellow solid. The solid was extracted into CH_2Cl_2 (20 mL) and filtered through Celite. Removal of the volatiles under reduced pressure yielded a yellow solid. The solid was used without further purification. Yield: 810 mg (81%). 1H NMR (500 MHz, 22 °C, $CDCl_3$): 7.83 (d, 1 H, $^2J_{HH} = 8$ Hz, C^8H), 7.52-7.16 (overlapping m, 15H, Ph of $-PPh_2$, C^5H-C^7H , C^3H and C^5H), 6.98 (d, 2H, $^2J_{HH} = 8$ Hz, C^2H , C^6H), 5.61 (d, 2H, $^4J_{PH} = 3$ Hz, $-CH_2-$). $^{31}P\{^1H\}$ NMR (202 MHz, 22 °C, $CDCl_3$): -28.6 (s, $-PPh_2$).

8.11. Synthesis of 1-(methyl)benzimidazole

The following is a modification of the literature procedure.^[187] KOH (12.0 g, 212 mmol) was crushed and dissolved in acetone (150 mL). Benzimidazole (5.00 g, 42.3 mmol) was added to the solution. The pale yellow solution was stirred for 10 minutes and then was placed in a cold water bath. MeI (6.5 mL, 127 mmol) was added and the resulting in a cloudy mixture was stirred for 1 hour. After this period, distilled deionized water was added and the acetone was removed under reduced pressure. The product was extracted into CH₂Cl₂ (2 x 100 mL) and the organic layers were collected and dried over NaSO₄. After filtration the volatiles were removed yielding a pale yellow liquid. The liquid was used without further purification. ¹H NMR (500 MHz, 22 °C, CDCl₃): 7.78-7.74 (m, 1 H, C⁸H), 7.73 (s, 1 H, C²H), 7.21-7.18 (m, 3 H, C⁵H-C⁷H), 3.64 (s, 3H, -CH₃) ppm. ¹³C{¹H} NMR (125 MHz, 22 °C CDCl₃): 143.5 (s, C²), 143.4 (s, C⁴), 134.3 (s, C⁹), 122.7, 121.4 (s, C⁶ and C⁷), 119.8 (s, C⁵), 109.6 (s, C⁸), 30.7 (s, -CH₃).

8.12. Synthesis of 1-(methyl)-2-(diphenylphosphino)benzimidazole, [PN^{Me}]

LDA was prepared by treating a THF (5 mL) solution of diisopropylamine (1060 μL, 7.57 mmol) with ⁿBuLi (4.73 mL of a 1.6 M solution in hexanes, 7.57 mmol) at -80 °C. After stirring at -80 °C for 1 hour, the LDA solution was added via cannula to a solution consisting of 1-(methyl)benzimidazole (1.00 g, 7.57 mmol) dissolved in THF (25 mL) at -80 °C. The resulting yellow solution was stirred at -80 °C for 1 hour before PPh₂Cl (1.36 mL, 7.57 mmol) was added dropwise and

the mixture turned almost colourless with a tinge of yellow. The solution was warmed to room temperature and stirred for 18 hours and then the volatiles were removed under reduced pressure yielding a sticky, foamy residue. The product was redissolved in CH_2Cl_2 (4 x 20 mL) and filtered through a small column containing Celite layered with silica. Removal of the volatiles from the filtrate yielded a sticky product. Trituration of the material with hexanes (10 mL) provided a colourless powder. The solid was used without further purification. Yield: 1.31 g (55%). ^1H NMR (500 MHz, 22 °C, CDCl_3): 7.82 (d, 1 H, $^2J_{\text{HH}} = 8$ Hz, C^8H), 7.50 (m, 3 H, $\text{C}^5\text{H}-\text{C}^7\text{H}$), 7.36 (m, 8 H, Ph), 7.30-7.23 (m, 2 H, Ph), 3.80 (s, 3 H, $-\text{CH}_3$). $^{13}\text{C}\{^1\text{H}\}$ NMR (125 MHz, 22 °C CDCl_3): 154.16 (d, $^1J_{\text{PC}} = 7$ Hz, C^2), 143.4 (d, $^3J_{\text{PC}} = 3$ Hz, C^4), 134.2, 134.1, 133.7, 129.5 (Ph), 123.0, 122.0 (s, C^6 and C^7), 120.6 (s, C^5), 109.2 (s, C^8), 30.8 (s, $-\text{CH}_3$). $^{31}\text{P}\{^1\text{H}\}$ NMR (202 MHz, 22 °C, CDCl_3): -25.7 (s, $-\text{PPh}_3$).

8.13. General procedure for the synthesis of phosphine selenides

An NMR tube was charged with the phosphine, excess selenium (10 molar equivalents) and CDCl_3 (0.5 mL). The mixture was heated at 60 °C for 2 hours before being cooled to room temperature and $^{31}\text{P}\{^1\text{H}\}$ NMR data acquisition. The results of the $^{31}\text{P}\{^1\text{H}\}$ NMR studies are presented in Table 1.

8.14. Synthesis of [CpRu(PPh₃)(κ²P,N-P^{Ph}NBPh₄)], (2)

CpRuCl(PPh₃)₂ (0.139 g, 0.191 mmol) and ligand **1** (0.150 g, 0.191 mmol) were combined and dissolved in 1,2-dichloroethane (10 mL). The orange mixture was refluxed for 24 hours. The next day, the cloudy orange-yellow mixture was allowed to cool to room temperature and then it was filtered through Celite. The volatiles were removed from the filtrate and the orange-yellow solid that remained was washed with diethyl ether (4 x 20 mL) to remove the PPh₃. The yellow-orange product was dried under reduced pressure. Yield: 0.178 g (88%). Recrystallization from CH₂Cl₂/diethyl ether yielded analytically pure samples. Anal. Calcd. for C₆₇H₅₅BN₂P₂Ru•0.5CH₂Cl₂: C, 73.4; H, 5.11; N, 2.54. Found: C, 73.8; H, 5.11; N, 2.62. ¹H NMR (500 MHz, 22 °C, CD₂Cl₂): 7.41-6.78 (overlapping m, 46H, Ph of -PPh₂, PPh₃ and BPh₃, C⁵H-C⁸H, and C³H, C⁵H), 6.42 (d, 2H, ²J_{HH} = 8 Hz, C²H, C⁶H), 5.09 (d, 2H, ²J_{HH} = 16 Hz, -CH_AH_B-), 4.70 (d, 1H, ²J_{HH} = 16 Hz, -CH_AH_B-), 4.43 (s, 5H, Cp). ¹³C{¹H} NMR (125 MHz, 22 °C, CD₂Cl₂): 165.9 (q, ¹J_{BC} = 49 Hz, C⁴), 164.0 (q, ¹J_{BC} = 49 Hz, ipso C of B-Ph), 156.6 (d, ¹J_{PC} = 31 Hz, C²), 143.4-124.3 (Ph, C¹-C³, C⁵, C⁶, C⁴ and C⁹), 122.5 (s, C⁶, C⁷), 117.6 (s, C⁵), 113.6 (s, C⁸), 78.7 (s, C₅H₅), 50.2 (s, -CH₂-). ³¹P{¹H} NMR (202 MHz, 22 °C, CD₂Cl₂): 49.8 (d, ²J_{PP} = 36 Hz, PPh₃), 17.9 (d, ²J_{PP} = 36 Hz, -PPh₂). ¹¹B{¹H} NMR (160 MHz, 22 °C, CD₂Cl₂): -6.6 (s).

8.15. Synthesis of [CpRu(MeCN)(PPh₃)(κ¹P-P^{Ph}NBPh₄)], (2a)

Complex **2** (60 mg, 0.060 mmol) was placed in a flask and dissolved in MeCN. The yellow solution was stirred at 55 °C for 10 minutes before being cooled to room temperature. Removal of the volatiles under reduced pressure afforded a bright yellow solid. The solid was washed with diethyl ether (2 x 10 mL) and then stored under vacuum for 3 days before NMR data were acquired. Reliable elemental analysis was not obtained for this complex due to time constraints. ¹H NMR (500 MHz, 22 °C, CD₂Cl₂/CD₃CN (4:1 v/v)): 7.61 (d, 1H, ³J_{HH} = 8 Hz, C⁸H), 7.48-6.83 (overlapping m, 30H, Ph of -PPh₂-BPh₃, C⁵H-C⁷H and C³H, C⁵H), 6.03 (d, 2H, ³J_{HH} = 8 Hz, C²H, C⁶H), 4.78 (d, 2H, ²J_{HH} = 8 Hz, C²H, C⁶H), 4.74 (d, 2H, ²J_{HH} = 16 Hz, -CH_AH_B-), 4.37 (s, 5H, Cp), 1.98 (s, MeCN). ¹³C{¹H} NMR (125 MHz, 22 °C, CD₂Cl₂/CD₃CN (4:1 v/v)): 163.13 (q, ¹J_{BC} = 49 Hz, *ipso* C of B-Ph), 162.81 (q, ¹J_{BC} = 50 Hz, C⁴), 150.1 (d, ¹J_{PC} = 61 Hz, C²), 142.3-122.0 (Ph, C¹-C³, C⁵, C⁶, C⁴ and C⁹), 121.3 (s, C⁶, C⁷), 119.6 (s, C⁵), 112.0 (s, C⁸), 82.8 (s, C₅H₅), 49.5 (s, -CH₂-), 14.5 (MeCN). ³¹P{¹H} NMR (202 MHz, 22 °C, CD₃CN): 43.3 (d, ²J_{PP} = 38 Hz, PPh₃), 31.5 (d, ²J_{PP} = 38 Hz, -PPh₂). ¹¹B{¹H} NMR (160 MHz, 22 °C, CD₂Cl₂/CD₃CN): -6.8 (s).

8.16. Synthesis of [Cp*^{Ru}(PPh₃)(κ²P,N-P^{Ph}NBPh₄)], (3)

Cp*^{Ru}Cl(PPh₃)₂ (0.100 g, 0.125 mmol) and ligand **1a** (0.099 g, 0.125 mmol) were combined and dissolved in CH₂Cl₂ (10 mL). The orange solution was allowed to stir for 24 hours. The next day, the hazy, light orange mixture was

filtered through Celite, and then the volatiles were removed from the filtrate under reduced pressure. The light orange solid was then washed with diethyl ether (4 x 20 mL) to remove the PPh₃. The yellow-orange product was dried under reduced pressure. Yield: 0.126 g (89%). Recrystallization from CH₂Cl₂/diethyl ether yielded analytically pure samples. Anal. Calcd. for C₇₅H₆₅BN₂P₂Ru•CH₂Cl₂: C, 74.1; H, 5.66; N, 2.38. Found: C, 74.4; H, 5.69; N, 2.54. ¹H NMR (500 MHz, 22 °C, CDCl₃): 7.72 (d, 1H, ²J_{HH} = 8 Hz, C⁸H), 7.51-6.73 (overlapping m, 45H, Ph of -PPh₂, PPh₃ and BPh₃, C⁵H-C⁷H, and C³H, C⁵H), 6.49 (d, 2H, ²J_{HH} = 8 Hz, C²H, C⁶H), 4.99 (d, 1H, ²J_{HH} = 16 Hz, -CH_AH_B-), 4.58 (d, 1H, ²J_{HH} = 16 Hz, -CH_AH_B-), 1.33 (s, 15 H, Cp*). ¹³C{¹H} NMR (125 MHz, 22 °C, CDCl₃): 166.2 (q, ¹J_{BC} = 49 Hz, C⁴), 163.6 (q, ¹J_{BC} = 50 Hz, ipso C of B-Ph), 156.4 (d, ¹J_{PC} = 33 Hz, C²), 142.2-124.1 (Ph, C¹-C³, C⁵, C⁶, C⁴ and C⁹), 121.8 (s, C⁶, C⁷), 116.8 (s, C⁵), 114.2 (s, C⁸), 88.7 (s, C₅Me₅), 51.0 (s, -CH₂-), 10.8 (s, -CH₃ of Cp*). ³¹P{¹H} NMR (202 MHz, 22 °C, CDCl₃): 50.1 (d, ²J_{PP} = 33 Hz, PPh₃), 20.1 (d, ²J_{PP} = 33 Hz, -PPh₂). ¹¹B{¹H} NMR (160 MHz, 22 °C, CDCl₃): -6.6 (s).

8.17. Synthesis of [CpRu(PPh₃)(κ²-P,N^{Me})] [BPh₄]

CpRuCl(PPh₃) (100 mg, 0.138 mmol) was placed in a flask followed by PN^{Me} (44 mg, 0.138 mmol) and NaBPh₄ (48 mg, 0.138 mmol). The components, dissolved in 1,2-dichloroethane (5 mL) and MeOH (5 mL), were stirred at reflux for 24 hours. The resulting bright yellow solution was allowed to cool to room temperature and then the volatiles were removed under reduced pressure. The

solid was extracted into CH_2Cl_2 (2 x 10 mL) and filtered through Celite. The volatiles were removed from the yellow filtrate yielding a yellow solid which was washed with diethyl ether (3 x 10 mL) before being dried under reduced pressure. The product was recrystallized using CH_2Cl_2 /hexanes and analytically pure orange-yellow crystals were obtained. Yield: 98 mg (67%). Anal. Calcd. for $\text{C}_{68}\text{H}_{64}\text{BN}_2\text{P}_2\text{Ru}$: C, 75.4; H, 5.96; N, 2.59. Found: C, 75.4; H, 5.53; N, 2.62. ^1H NMR (500 MHz, 22 °C, CDCl_3): 7.42-6.80 (overlapping m, 49H, Ph of PPh_3 , $-\text{PPh}_2$, BPh_4 , and $\text{C}^5\text{H}-\text{C}^8\text{H}$), 4.47 (s, 5H, C_5H_5), 2.96 (s, 3H, $\text{N}-\text{CH}_3$). $^{13}\text{C}\{^1\text{H}\}$ NMR (125 MHz, 22 °C, CDCl_3): 164.3 (q, $^1J_{\text{BC}} = 49$ Hz, *ipso* C of B-Ph), 155.6 (d, $^1J_{\text{PC}} = 32$ Hz, C^2), 142.3-124.9 (Ph, C^4 and C^9), 121.6 (s, C^6 , C^7), 116.7 (s, C^5), 112.1 (s, C^8), 78.0 (m, C_5H_5), 31.5 (s, $\text{N}-\text{CH}_3$). $^{31}\text{P}\{^1\text{H}\}$ NMR (202 MHz, 22 °C, CDCl_3): 51.2 (d, $^2J_{\text{PP}} = 37$ Hz, PPh_3), 16.8 (d, $^2J_{\text{PP}} = 37$ Hz, $-\text{PPh}_2$). $^{11}\text{B}\{^1\text{H}\}$ NMR (160 MHz, 22 °C, CDCl_3): -6.5 (s).

8.18. Synthesis of $[\text{CpRu}(\text{PPh}_3)(\kappa^2\text{P},\text{N}-\text{P}^{\text{iPr}}\text{NBPh}_4)]$, (**4**)

The same procedure outlined for complex **2** was followed except using $\text{CpRuCl}(\text{PPh}_3)$ (220 mg, 0.303 mmol) and ligand **1b** (261 mg, 0.303 mmol), yielding an analytically pure mustard-yellow solid. Yield after recrystallization (CH_2Cl_2 /diethyl ether): 168 mg (55%). Anal. Calcd. for $\text{C}_{61}\text{H}_{59}\text{BN}_2\text{P}_2\text{Ru}$: C, 73.7; H, 5.98; N, 2.82. Found: C, 73.4; H, 6.30; N, 2.52. ^1H NMR (500 MHz, 22 °C, CD_2Cl_2): 7.55-6.92 (overlapping m, 21H, Ph of PPh_3 and BPh_3 , $\text{C}^5\text{H}-\text{C}^8\text{H}$, and $\text{C}^{3'}\text{H}$, C^5H), 6.80 (d, 2H, $^2J_{\text{HH}} = 7.5$ Hz, C^2H , C^6H), 5.32 (d, 2H, $^2J_{\text{HH}} = 16$ Hz, $-\text{CH}_\text{A}\text{H}_\text{B}-$

), 5.14 (d, 1H, $^2J_{\text{HH}} = 15.5$ Hz, $-\text{CH}_\text{A}\text{H}_\text{B-}$), 4.78 (s, 5H, Cp), 2.89-2.81 (m, 1H, $\text{CH}(\text{CH}_3)_2$), 1.41 (dd, 3H, $^3J_{\text{PH}} = 18.5$ Hz, $^3J_{\text{HH}} = 7$ Hz, $-\text{CH}(\text{CH}_3)(\text{CH}_3)$) 1.20-1.10 (overlapping m, 6H, $\text{CH}(\text{CH}_3)(\text{CH}_3)$), 0.96-0.88 (m, 1H, $\text{CH}(\text{CH}_3)_2$), 0.69 (dd, 3H, $^3J_{\text{PH}} = 16.5$ Hz, $^3J_{\text{HH}} = 7$ Hz, $-\text{CH}(\text{CH}_3)(\text{CH}_3)$). $^{13}\text{C}\{^1\text{H}\}$ NMR (125 MHz, 22 °C, CD_2Cl_2): 166.2 (q, $^1J_{\text{BC}} = 48.5$ Hz, C^4), 163.6 (q, $^1J_{\text{BC}} = 49$ Hz, *ipso* C of B-Ph), 157.9 (d, $^1J_{\text{PC}} = 18$ Hz, C^2), 142.7-124.3 (Ph, C^1 - C^3 , C^5 , C^6 , C^4 and C^9), 122.3 (s, C^6 , C^7), 117.4 (s, C^5), 113.1 (s, C^8), 76.6 (s, C_5H_5), 50.1 (s, $-\text{CH}_2-$), 25.2 (d, $^1J_{\text{PC}} = 9.9$ Hz, $-\text{CH}(\text{CH}_3)_2$), 23.5 (d, $^1J_{\text{PC}} = 19.8$ Hz, $-\text{CH}(\text{CH}_3)_2$) 20.7 (d, $^2J_{\text{PC}} = 10.9$ Hz, $-\text{CH}(\text{CH}_3)(\text{CH}_3)$), 20.2 (d, $^2J_{\text{PC}} = 9.5$ Hz, $-\text{CH}(\text{CH}_3)(\text{CH}_3)$), 19.7 (d, $^2J_{\text{PC}} = 8.5$ Hz, $-\text{CH}(\text{CH}_3)(\text{CH}_3)$), 19.4 (d, $^2J_{\text{PC}} = 8.5$ Hz, $-\text{CH}(\text{CH}_3)(\text{CH}_3)$). $^{31}\text{P}\{^1\text{H}\}$ NMR (202 MHz, 22 °C, CD_2Cl_2): 47.7 (d, $^2J_{\text{PP}} = 34.1$ Hz, PPh_3), 46.0 (d, $^2J_{\text{PP}} = 34.1$ Hz, $-\text{P}(\text{IPr})_2$). $^{11}\text{B}\{^1\text{H}\}$ NMR (160 MHz, 22 °C, CD_2Cl_2): -6.7 (s).

8.19. Synthesis of $[\text{CpRu}(\text{PPh}_3)(\kappa^2\text{P}, \text{N}-\text{P}^{\text{Cy}}\text{NBPh}_4)]$, (**5**)

The same procedure outlined for complex **2** was followed except using $\text{CpRuCl}(\text{PPh}_3)$ (235 mg, 0.324 mmol) and ligand **1c** (305 mg, 0.324 mmol) yielding an analytically pure mustard-yellow solid. Yield after recrystallization (CH_2Cl_2 /diethyl ether): 162 mg (47%). Anal. Calcd. for $\text{C}_{67}\text{H}_{67}\text{BN}_2\text{P}_2\text{Ru}\cdot\text{CH}_2\text{Cl}_2$: C, 70.5; H, 6.00; N, 2.42. Found: C, 70.9; H, 5.85; N, 2.37. ^1H NMR (500 MHz, 22 °C, CD_2Cl_2): 7.39-6.78 (overlapping m, 21H, Ph of PPh_3 and BPh_3 , $\text{C}^5\text{H}-\text{C}^8\text{H}$, and C^3H , C^5H), 6.42 (d, 2H, $^2J_{\text{HH}} = 7.5$ Hz, C^2H , C^6H), 5.11 (d, 2H, $^2J_{\text{HH}} = 16$ Hz, $-\text{CH}_\text{A}\text{H}_\text{B-}$), 5.04 (d, 1H, $^2J_{\text{HH}} = 15.5$ Hz, $-\text{CH}_\text{A}\text{H}_\text{B-}$), 4.60 (s, 5H, Cp), 2.57-2.49 2.25-

2.20 (m, 1H, C₆H₁₁), 2.06-2.04 2.25-2.20 (m, 1H, C₆H₁₁), 1.79-0.34 (overlapping m, 20H, C₆H₁₁). ¹³C{¹H} NMR (125 MHz, 22 °C, CD₂Cl₂): 164.7 (q, ¹J_{BC} = 48 Hz, C⁴), 162.6 (q, ¹J_{BC} = 49 Hz, *ipso* C of B-Ph), 156.4 (d, ¹J_{PC} = 18 Hz, C²), 141.7-122.8 (Ph, C¹-C³, C⁵, C⁶, C⁴ and C⁹), 121.1 (s, C⁶, C⁷), 116.1 (s, C⁵), 112.2 (s, C⁸), 75.8 (s, C₅H₅), 49.4 (s, -CH₂-), 35.6 (d, J_{PC} = 8.5 Hz, C₆H₁₁), 33.1 (d, J_{PC} = 18.6 Hz, C₆H₁₁), 29.9-29.8 (overlapping d, C₆H₁₁), 28.6 (d, J_{PC} = 7.5 Hz, C₆H₁₁), 27.4 (s, C₆H₁₁), 25.8-25.3 (overlapping m, C₆H₁₁), 24.9 (s, C₆H₁₁), 24.3 (s, C₆H₁₁). ³¹P{¹H} NMR (202 MHz, 22 °C, CD₂Cl₂): 48.3 (d, ²J_{PP} = 34.5 Hz, PPh₃), 37.3 (d, ²J_{PP} = 34.5 Hz, -PCy₂). ¹¹B{¹H} NMR (160 MHz, 22 °C, CD₂Cl₂): -6.7 (s).

8.20. Synthesis of [(*p*-cymene)RuCl(κ²P,N-P^{Ph}NBPh₄)], (6)

[(*p*-cymene)RuCl₂]₂ (305 mg, 0.498 mmol) and **1a** (782 mg, 0.997 mmol) were placed in a flask and dissolved in dichloromethane (30 mL) The bright orange mixture was stirred at room temperature for 3 hours becoming cloudy with the precipitation of LiCl. The mixture was filtered through Celite and the volatiles were removed from the bright orange-red filtrate under reduced pressure yielding a solid of similar colour. The solid was washed with diethyl ether (3 x 20 mL) yielding analytically pure samples. Yield: 0.816 g (90%) Anal. Calcd. for C₅₄H₆₁BClN₂PRu•CH₂Cl₂: C, 66.0; H, 6.34; N, 2.80. Found: C, 66.1; H, 6.21; N, 2.73. ¹H NMR (500 MHz, 22 °C, CDCl₃): 8.04-8.00 (overlapping d, 2H), 7.81 (d, 1H, J = 6 Hz), 7.38 (d, 1H J = 8 Hz), 7.63 (m, 2H, -PPh₂), 7.53-7.43, (overlapping m, 8H, -PPh₂), 7.36-7.35 (m (br), 6H, ortho-BPh), 7.22-7.19 (m (br), 2H, C³H,

C^5H), 7.04-6.98 (m, 6H, *meta*-BPh), 6.90 (t, 3H $^3J_{HH} = 7$ Hz, *para*-BPh), 6.63 (d, 2H $^3J_{HH} = 8$ Hz, C^2H , C^6H), 5.80 (d, 1H, $^3J_{HH} = 6$ Hz, *p*-cym), 5.58 (d, 1H, $^3J_{HH} = 4$ Hz, *p*-cym), 5.45 (d, 1H, $^3J_{HH} = 6$ Hz, *p*-cym), 5.22 (d, 1H, $^2J_{HH} = 16$ Hz - CH_AH_B -), 4.72 (d, 1H, $^2J_{HH} = 16$ Hz, - CH_AH_B -), 4.55 (d, 1H, $^3J_{HH} = 6$ Hz, *p*-cym), 2.58-2.54 (m, 1H, - $CH(CH_3)_2$), 1.54 (s, 3H - CH_3) 1.15 (d, $^3J_{HH} = 7$ Hz, - $CH(CH_3)(CH_3)$), 1.09 (d, $^3J_{HH} = 7$ Hz, - $CH(CH_3)(CH_3)$). $^{13}C\{^1H\}$ NMR (125 MHz, 22 °C, $CDCl_3$): 164.7-162.8 (overlapping m, C^4 , *ipso* C of B-Ph), 153.5 (d, $^1J_{PC} = 45$ Hz, C^2), 140.1-122.8 (Ph, C^1 - C^3 , C^5 , C^6 , C^4 and C^9), 121.1 (s, C^6 , C^7), 116.9 (s, C^5), 113.2 (s, C^8), 106.2-80.9 (Ar, *p*-cym), 49.7 (s, - CH_2 -), 31.0 (s, - $CH(CH_3)_2$), 23.3 (s, - $CH(CH_3)(CH_3)$), 21.5 (s, - $CH(CH_3)(CH_3)$), 19.3 (CH_3 -*p*-cym). $^{31}P\{^1H\}$ NMR (202 MHz, 22 °C, $CDCl_3$): -6.43. $^{11}B\{^1H\}$ NMR (160 MHz, 22 °C, $CDCl_3$): -6.7 (s).

8.21. Synthesis of [(*p*-cymene)RuCl(κ^2P,N -P^{iPr}NBPh₄)], (**7**)

The same procedure outlined for complex **6** was followed using [(*p*-cymene)RuCl₂]₂ (179 mg, 0.292 mmol) and ligand **1b** (504 mg, 0.585 mmol), yielding a bright orange analytically pure solid. Yield: 444 mg (91%). Anal. Calcd. For C₅₄H₄₈BClN₂PRu•CHCl₃: C, 61.6; H, 5.70; N, 2.93. Found: C, 61.6; H, 5.75; N, 2.92. 1H NMR (500 MHz, 22 °C, CD_2Cl_2): 7.74 (m, 1H, $^3J_{HH} = 8$ Hz, C^8H), 7.81 (d, 1H, $J = 7$ Hz), 7.52-7.50 (overlapping d, 2H), 7.30-7.21 (overlapping m (br), 8H, *ortho*-BPh, C^3H , C^5H), 6.96 ((m, 6H, *meta*-BPh), 6.84 (t, 3H $^3J_{HH} = 7$ Hz, *para*-BPh), 6.63 (d, 2H $^3J_{HH} = 7$ Hz, C^2H , C^6H), 6.07 (d, 1H, $^3J_{HH} = 6$ Hz, *p*-cym), 5.81 (d, 1H, $^3J_{HH} = 6$ Hz, *p*-cym), 5.62 (d, 1H, $^3J_{HH} = 6$ Hz, *p*-cym), 5.42 (d, 1H, $^2J_{HH} =$

15 Hz $-CH_AH_B-$), 5.35 (d, 1 H, $^3J_{HH} = 6$ Hz, p-cym) 4.86 (d, 1H, $^2J_{HH} = 16$ Hz, $-CH_AH_B-$), 2.78-2.64 (overlapping m, 3H, $-CH(CH_3)_2$), 1.87 (s, 3H, $-CH_3$ -p-cym), 1.44-1.08 (overlapping m, 18H, $-CH(CH_3)(CH_3)$). Crystallization in the NMR tube produced low quality ^{13}C results, however, the following are selected features that could be observed. $^{13}C\{^1H\}$ NMR (125 MHz, 22 °C, CD_2Cl_2): 166.1 (q, $^1J_{BC} = 50$ Hz, $C^{4'}$), 162.5 (q, $^1J_{BC} = 49$ Hz, *ipso* C of B-Ph), 155.0 (d, $^1J_{PC} = 31$ Hz, C^2), 136.0-123.7 (Ph, C^1 - C^3 , C^5 , C^6 , C^4 and C^9) 121.3 (s, C^6 , C^7), 115.8 (s, C^5), 112.0 (s, C^8), 106.1-79.1 (Ar, p-cym), 49.5 (s, $-CH_2-$), 30.7-13.28 (p-cym, $-P^{iPr}$) $^{31}P\{^1H\}$ NMR (202 MHz, 22 °C, $CDCl_3$): 37.7. $^{11}B\{^1H\}$ NMR (160 MHz, 22 °C, $CDCl_3$): -6.6 (s).

8.22. Synthesis of $[(p\text{-cymene})RuCl(\kappa^2P,N\text{-}P^{Cy}NBPh_4)]$, (**8**)

The same procedure outlined for complex **6** was followed using $[(p\text{-cymene})RuCl_2]_2$ (325 mg, 0.529 mmol) and ligand **1c** (1.00 g, 1.06 mmol). A bright orange analytically pure solid was obtained. Yield: 903 mg (93%). Anal. Calcd. For $C_{54}H_{61}BClN_2PRu \cdot CH_2Cl_2$: C, 66.0; H, 6.34; N, 2.80. Found: C, 66.1; H, 6.21; N, 2.73. 1H NMR (500 MHz, 22 °C, $CDCl_3$): 7.54 (d, 1H, $^3J_{HH} = 8$ Hz, C^8H), 7.45-6.83 (overlapping m, 20H, Ph of $-BPh_3$, C^5H - C^7H and C^3H , C^5H), 6.65 (d, 2H, $^3J_{HH} = 8$ Hz, C^2H , C^6H), 6.00 (d, 1H, $^3J_{HH} = 6$ Hz, p-cym), 5.80 (d, 1H, $^3J_{HH} = 5$ Hz, p-cym) 5.57 (d, 1H, $^3J_{HH} = 6$ Hz, p-cym), 5.37 (d, 1H, $^3J_{HH} = 6$ Hz, p-cym), 5.32 (d, 2H, $^2J_{HH} = 16$ Hz, $-CH_AH_B-$), 5.00 (d, 2H, $^2J_{HH} = 16$ Hz, $-CH_AH_B-$) 2.67-0.73 (overlapping m, 32H, *iPr* and CH_3 of p-cym, $-P(C_6H_{11})$). $^{13}C\{^1H\}$ NMR (125 MHz, 22 °C, CD_2Cl_2): 165.5 (q, $^1J_{BC} = 48$ Hz, $C^{4'}$), 162.4 (q, $^1J_{BC} = 49$ Hz, *ipso* C of B-Ph), 154.9 (d, $^1J_{PC}$

= 32 Hz, C^2), 139.1-122.8 (Ph, $C^{1'-C^3'}$, $C^{5'}$, $C^{6'}$, C^4 and C^9), 121.2 (s, C^6 , C^7), 115.6 (s, C^5), 112.2 (s, C^8), 105.6-79.4 (Ar, p-cym), 49.5 (s, $-CH_2-$), 33.6-18.5 (p-cym, -PCy). $^{31}P\{^1H\}$ NMR (202 MHz, 22 °C, $CDCl_3$): 26.9 (s). $^{11}B\{^1H\}$ NMR (160 MHz, 22 °C, $CDCl_3$): -6.7 (s).

8.23. Synthesis of $[Ph_4P][(\rho\text{-cymene})RuCl_2(\kappa^1P\text{-}P^{Ph}NBPh_4)]$, (9)

$[PPh_4][P^{Ph}NBPh_4]$ (256 mg, 0.263 mmol) and $[(\rho\text{-cymene})RuCl_2]_2$ (80 mg, 0.131 mmol) were placed in a flask and dissolved in CH_2Cl_2 (10 mL). The clear red solution was stirred at ambient temperature for 3 hrs before the volatiles were removed under reduced pressure. The bright red solid was washed with diethyl ether (10 mL). Yield: 278 mg (81 %). 1H NMR (500 MHz, 22 °C, $CDCl_3$): 8.14-6.70 (overlapping m, 53H, Ph of $-PPh_2$, PPh_4 , and $-BPh_3$; C^5H-C^8H , $C^{3'}H$, and $C^{5'}H$), 6.04 (d, 2H $^3J_{HH}$ = 8 Hz, C^2H , $C^{6'}H$), 5.40 (d, 2H, $^3J_{HH}$ = 5 Hz, p-cym), 5.18 (d, 2H, $^3J_{HH}$ = 6 Hz, p-cym), 5.22 (s, 2H, $-CH_2-$), 2.58-2.52 (m, 1H, $-CH(CH_3)_2$), 1.58 (s, 3H, $-CH_3$), 0.78 (d, 6H, $^3J_{HH}$ = 7 Hz, $-CH(CH_3)_2$). $^{13}C\{^1H\}$ NMR (125 MHz, 22 °C, $CDCl_3$): 164.2 (q, $^1J_{BC}$ = 49 Hz, *ipso* C of B-Ph), 162.3 (q, $^1J_{BC}$ = 50 Hz, $C^{4'}$), 14 (Ph, $C^{1'-C^3'}$, $C^{5'}$, $C^{6'}$, C^4 and C^9), 151.3 (d, $^1J_{PC}$ = 65 Hz, C^2), 142.9-121.5 (Ph, $C^{1'-C^3'}$, $C^{5'}$, $C^{6'}$, C^4 and C^9), 117.6 (s, C^6 , C^7), 116.6 (s, C^5), 112.5 (s, C^8), 110.4-80.5 (Ar, p-cym), 50.3 (s, $-CH_2-$), 30.0 (s, $-CH(CH_3)_2$), 21.3 (s, $-CH(CH_3)_2$), 17.0 (CH_3 -p-cym). $^{31}P\{^1H\}$ NMR (202 MHz, 22 °C, $CDCl_3$): 8.55 (s). $^{11}B\{^1H\}$ NMR (160 MHz, 22 °C, $CDCl_3$): -6.8 (s).

8.24. Synthesis of [(*p*-cymene)RuCl(κ^2P,N -PN^{Bz})] [BPh₄], (10)

The ligand [PN^{Bz}] (156 mg, 0.398 mmol) was combined in a flask with [(*p*-cymene)RuCl₂]₂ (122 mg, 0.199 mmol) and NaBPh₄ (136 mg, 0.398 mmol). Acetone (20 mL) was added and the red-brown solution was heated at reflux for 26 hrs. The solution was cooled to room temperature before the volatiles were removed under reduced pressure and a dark brown residue was obtained. To the flask was added CH₂Cl₂ and the mixture was filtered through Celite. The volatiles were removed under reduced pressure yielding a brown-yellow solid. Analytically pure samples were obtained by the slow diffusion of diethyl ether into an acetone solution of the product. Yield: 306 mg (76%). Anal. Calcd. For C₆₁H₅₉BClN₂PRu•H₂O: C, 72.1; H, 6.05; N, 2.76. Found: C, 71.9; H, 5.73; N, 2.73. ¹H NMR (500 MHz, 22 °C, C₂D₆CO): 8.04-8.00 (overlapping d, 2H), 7.71-7.68 (overlapping d, 2H), 7.63-7.37, (overlapping m, 10H, -PPh₂), 7.34 (m (br), 6H, ortho-BPh), 7.13 (t, 1H, ³J_{HH} = 7 Hz, C⁴H), 7.06 (d, 2H, ³J_{HH} = 7 Hz, C⁵H, C³H), 6.90 (m (br), 8H, meta-BPh) 6.76 (t, 4H ³J_{HH} = 7 Hz, para-BPh), (d, 2H, ³J_{HH} = 7 Hz, C²H, C⁶H). 6.46 (d, 1H, ³J_{HH} = 6 Hz, *p*-cym), 6.36 (d, 1H, ³J_{HH} = 6 Hz, *p*-cym), 5.87 (d, 1H, ³J_{HH} = 6 Hz, *p*-cym), 5.63-5.56 (overlapping d, 2H, -CH₂-), 5.40 (d, 1H, ³J_{HH} = 6 Hz, *p*-cym), 2.65-2.60 (m, 1H, -CH(CH₃)₂), 1.67 (s, 3H, -CH₃), 1.21 (d, ³J_{HH} = 7 Hz, -CH(CH₃)(CH₃)), 1.12 (d, ³J_{HH} = 7 Hz, -CH(CH₃)(CH₃)). ³¹P{¹H} NMR (202 MHz, 22 °C, C₂D₆CO): -2.91 (s).

8.25. Reaction of $[\text{PPh}_4][\text{P}^{\text{iPr}}\text{NBPh}_4]$ with $[(p\text{-cymene})\text{RuCl}_2]_2$

$[\text{PPh}_4][\text{P}^{\text{iPr}}\text{NBPh}_4]$ (30 mg, 0.033 mmol) and $[(p\text{-cymene})\text{RuCl}_2]_2$ (10 mg, 0.016) were combined in an NMR tube and dissolved in CDCl_3 (0.5 mL) the solution was mixed and was monitored spectroscopically over time. NMR revealed the presence of two phosphorous-containing species, one of which was identified as complex **(7)**. Spectroscopic evidence for the formation of $[(p\text{-cymene})\text{RuCl}(\kappa^1P, N\text{-P}^{\text{iPr}}\text{NBPh}_4)]$ follows: ^1H NMR (500 MHz, 22 °C, CDCl_3): 5.39 (d, 2H, $^3J_{\text{HH}} = 6$ Hz, *p*-cym), 5.26 (d, 2H, $^3J_{\text{HH}} = 6$ Hz, *p*-cym), 5.14 (s, 2H, $-\text{CH}_2-$), 2.87-2.81 (m, 1H, $-\text{CH}(\text{CH}_3)_2$), 2.71-2.62 (m, 2H, $-\text{CH}(\text{CH}_3)_2$) 1.58 (s, 3H, $-\text{CH}_3$), 1.20 (d, 6H $^3J_{\text{HH}} = 7$ Hz, *p*-cym $-\text{CH}(\text{CH}_3)_2$), (d, 12H $^3J_{\text{HH}} = 7$ Hz, $-\text{P}-\text{CH}(\text{CH}_3)_2$). $^{31}\text{P}\{^1\text{H}\}$ NMR (202 MHz, 22 °C, CDCl_3): 29.23 (s). $^{11}\text{B}\{^1\text{H}\}$ NMR (160 MHz, 22 °C, CDCl_3): -6.6 (s).

8.26. Reaction of $[\text{PPh}_4][\text{P}^{\text{Cy}}\text{NBPh}_4]$ with $[(p\text{-cymene})\text{RuCl}_2]_2$

$[\text{PPh}_4][\text{P}^{\text{Cy}}\text{NBPh}_4]$ (32 mg, 0.033 mmol) and $[(p\text{-cymene})\text{RuCl}_2]_2$ (10 mg, 0.016) were combined in an NMR tube and dissolved in CDCl_3 (0.5 mL) the solution was mixed and was monitored spectroscopically over time. NMR revealed the presence of two phosphorous-containing species, one of which was identified as complex **(8)**. Spectroscopic evidence for the formation of $[(p\text{-cymene})\text{RuCl}(\kappa^1P, N\text{-P}^{\text{Cy}}\text{NBPh}_4)]$ follows: ^1H NMR (500 MHz, 22 °C, CDCl_3): 5.38 (d, 2H, $^3J_{\text{HH}} = 6$ Hz, *p*-cym), 5.22 (d, 2H, $^3J_{\text{HH}} = 6$ Hz, *p*-cym), 5.19 (s, 2H, $-\text{CH}_2-$),

peak crowding upfield inhibited signal assignment in this region. $^{31}\text{P}\{^1\text{H}\}$ NMR (202 MHz, 22 °C, CDCl_3): 22.4 (s).

8.27. Reaction of Complex **6** with MeCN

Complex **6** (15 mg, 0.016 mmol) was placed in a NMR tube followed by CD_3CN . The solution was monitored over time revealing a 1:1 mixture of complex **6** and a newly formed complex. Although there were many overlapping spectroscopic signals that made complete characterization difficult the following are discernible features that support the ring opened product $[(p\text{-cymene})\text{RuCl}(\text{MeCN})(\kappa^1P,N\text{-P}^{\text{Ph}}\text{NBPh}_4)]$. ^1H NMR (500 MHz, 22 °C, CD_3CN): 6.29 (d, 2H $^3J_{\text{HH}} = 8$ Hz, C^2H , C^6H), 4.91 (s, 2H, $-\text{CH}_2-$), a total of 8 doublets ($^3J_{\text{HH}} = 6$ Hz) pertaining to *p*-cymene arene signals were present. Two *p*-cymene ⁱPr methine protons were visible and a singlet at 2.23 provided evidence for coordinated MeCN. In addition, 4 doublets ($^3J_{\text{HH}} = 7$ Hz) from ⁱPr $-\text{CH}_3$ signals were present. $^{31}\text{P}\{^1\text{H}\}$ NMR (202 MHz, 22 °C, CD_3CN): 19.4 (s), $-\text{PPh}_2$.

8.28. Reaction of Complex **10** with MeCN

Complex **10** (10 mg, 0.011 mmol) was placed in an NMR tube containing a sealed capillary tube containing D_2O . MeCN was added to the tube and the solution was monitored over time revealing a 3:7 mixture of complex **10** and a

newly formed product with the following NMR data. $^{31}\text{P}\{^1\text{H}\}$ NMR (202 MHz, 22 °C, $\text{D}_2\text{O}/\text{MeCN}$): 19.9 (s), $-\text{PPh}_2$.

8.29. Synthesis of $[\text{Cp}^*\text{Ru}(\text{CO})_2(\kappa^1\text{P}-\text{P}^{\text{Ph}}\text{NBPh}_4)]$, **11**, and $[\text{Cp}^*\text{Ru}(\text{CO})(\kappa^2\text{P},\text{N}-\text{P}^{\text{Ph}}\text{NBPh}_4)]$, **12**

$\text{Cp}^*\text{RuCl}(\text{CO})_2$ (0.0500 g, 0.153 mmol) and ligand **1a** (0.120 g, 0.153 mmol) were combined, dissolved in 1,2-dichloroethane (5 mL), and refluxed for 24 hours. The next day, the cloudy yellow mixture was allowed to cool to room temperature, and then it was filtered through Celite. The volatiles were removed from the filtrate and the yellow solid was washed with diethyl ether (10 mL) before drying under reduced pressure. NMR spectroscopic analysis of the product revealed it to be a mixture of complexes **11** and **12** in an approximately 3:2 ratio. Complete NMR data of complex **11** is given below; selected NMR data for complex **12** follows: ^1H NMR (500 MHz, 22 °C, CDCl_3): 6.56 (d, 2 H, $^2J_{\text{HH}} = 7.5$ Hz, C^2H , C^6H), 5.15 (d, 1 H, $^2J_{\text{HH}} = 15$ Hz, $-\text{CH}_\text{A}\text{H}_\text{B}-$), 4.99 (d, 1 H, $^2J_{\text{HH}} = 16$ Hz, $-\text{CH}_\text{A}\text{H}_\text{B}-$), 1.72 (s, 15 H, Cp*). $^{31}\text{P}\{^1\text{H}\}$ NMR (202 MHz, 22 °C, CDCl_3): 19.4 (s, $-\text{PPh}_2$). $^{11}\text{B}\{^1\text{H}\}$ NMR (160 MHz, 22 °C, CDCl_3): -6.6 ppm (s).

8.30. Synthesis of $[\text{Cp}^*\text{Ru}(\text{CO})_2(\kappa^1\text{P}-\text{P}^{\text{Ph}}\text{NBPh}_4)]$, **11**

$\text{Cp}^*\text{RuCl}(\text{CO})_2$ (0.0500 g, 0.153 mmol) and ligand **1a** (0.120 g, 0.153 mmol) were combined, dissolved in 1,2-dichloroethane (5 mL), and refluxed for 24 hours. After cooling to room temperature, the cloudy yellow mixture was then filtered

through Celite. The volatiles were removed from the filtrate under reduced pressure yielding a yellow solid. The flask was then backfilled with CO, and then CH₂Cl₂ (5 mL) was added. The dark yellow solution was allowed to stir under CO for 24 hours. After this time, the volatiles were removed under reduced pressure yielding a pale yellow solid. The solid was washed with diethyl ether (20 mL) before drying under reduced pressure. Yield: 0.120 g (85%). Recrystallization from CH₂Cl₂/diethyl ether yielded analytically pure samples. Anal. Calcd. for C₅₉H₆₁BN₂O₂PRu: C, 72.8; H, 6.32; N, 2.88. Found: C, 72.3; H, 5.90; N, 3.21. IR (Nujol): 2044 (s), 1994 (s). ¹H NMR (500 MHz, 22 °C, CDCl₃): 7.83 (d, 1 H, ²J_{HH} = 8 Hz, C⁸H), 7.37-6.81 (overlapping m, 30 H, Ph of -PPh₂ and BPh₃, C⁵H-C⁷H and C³H, C⁵H), 6.11 (d, 2 H, ²J_{HH} = 8 Hz, C²H, C⁶H), 4.76 (s, 2 H, -CH₂-), 1.68 (s, 15 H, Cp*). ¹³C{¹H} NMR (125 MHz, 22 °C, CDCl₃): 198.1 (d, ²J_{PC} = 15 Hz, CO), 164.5 (q, ¹J_{BC} = 49 Hz, C⁴), 163.8 (q, ¹J_{BC} = 49 Hz, *ipso* C of B-Ph), 143.2 (d, ¹J_{PC} = 21 Hz, C²), 138.6-123.0 (Ph, C¹-C³, C⁵, C⁶, C⁴ and C⁹), 121.8 (s, C⁶, C⁷), 120.5 (s, C⁵), 113.1 (s, C⁸), 103.1 (s, C₅Me₅), 50.2 (s, -CH₂-), 9.75 (s, -CH₃ of Cp*). ³¹P{¹H} NMR (202 MHz, 22 °C, CDCl₃): 36.1 (s, -PPh₂). ¹¹B{¹H} NMR (160 MHz, 22 °C, CDCl₃): -6.7 ppm (s).

8.31. Synthesis of [CpRu(PPh₃)(κ²C,P-(CCHPh)-P^{Ph}NBPh₄)], (**13**)

Complex **2** (0.0500 g, 0.0471 mmol) was dissolved in CH₂Cl₂ (2 mL). Next, phenylacetylene (52 μL, 0.471 mmol) was added to the suspension via syringe, and the mixture was allowed to stir for 24 hours. The resulting clear red-orange

solution was evaporated to dryness under reduced pressure, and the red solid that remained was washed with diethyl ether (2 x 15 mL). The product was recrystallized from THF/hexanes yielding a microcrystalline red-orange solid which was washed with diethyl ether and dried under reduced pressure. Yield: 0.0410 g (75%). Anal. Calcd. for $C_{75}H_{61}BN_2P_2Ru$: C, 77.4; H, 5.28; N, 2.41. Found: C, 76.7; H, 5.54; N, 2.61. NMR spectroscopy revealed two isomers of **13** had formed in approximately a 4:1 ratio. Selected NMR spectroscopic data for each isomer follows. **Major isomer:** 1H NMR (500 MHz, 22 °C, $CDCl_3$): 5.78 (d, 2H, $^2J_{HH} = 8$ Hz, C^2H , C^6H), 4.89 (d, 1 H, $^2J_{HH} = 16$ Hz, $-CH_AH_{B^-}$), 4.71 (d, 1 H, $^2J_{HH} = 16$ Hz, $-CH_AH_{B^-}$), 4.38 (s, 5 H, Cp). $^{13}C\{^1H\}$ NMR (125 MHz, 22 °C, $CDCl_3$): 166.2 (q, $^1J_{BC} = 48$ Hz, C^4), 163.5 (q, $^1J_{BC} = 50$ Hz, *ipso* C of B-Ph), 159.6 (dd, $^2J_{PC} = 18$ Hz, $^2J_{PC} = 17$ Hz, C_α), 152.2 (d, $^1J_{PC} = 22$ Hz, C^2), 121.9 (s, C^6 , C^7), 117.7 (s, C^5), 116.1 (s, C^8), 86.2 (s, C_5H_5), 52.7 (s, $-CH_2-$). $^{31}P\{^1H\}$ NMR (202 MHz, 22 °C, $CDCl_3$): 69.0 (d, $^2J_{PP} = 35$ Hz, PPh_3), 49.1 (d, $^2J_{PP} = 35$ Hz, $-PPh_2$). **Minor isomer:** 1H NMR (500 MHz, 22 °C, $CDCl_3$): 6.00 (d, 2H, $^2J_{HH} = 8$ Hz, C^2H , C^6H), 5.15 (d, 1 H, $^2J_{HH} = 16$ Hz, $-CH_AH_{B^-}$), 4.98 (d, 1 H, $^2J_{HH} = 16$ Hz, $-CH_AH_{B^-}$), 4.62 (s, 5 H, Cp). $^{13}C\{^1H\}$ NMR (125 MHz, 22 °C, $CDCl_3$): 166.4 (q, $^1J_{BC} = 49$ Hz, C^4), 163.5 (q, $^1J_{BC} = 50$ Hz, *ipso* C of B-Ph), 155.0 (dd, $^2J_{PC} = 22$ Hz, $^2J_{PC} = 12$ Hz, C_α), 153.0 (d, $^1J_{PC} = 19$ Hz, C^2), 121.9 (s, C^6 , C^7), 118.4 (s, C^5), 114.2 (s, C^8), 87.3 (s, C_5H_5), 53.5 (s, $-CH_2-$). $^{31}P\{^1H\}$ NMR (202 MHz, 22 °C, $CDCl_3$): 69.6 (d, $^2J_{PP} = 35$ Hz, PPh_3), 50.8 (d, $^2J_{PP} = 35$ Hz, $-PPh_2$).

8.32. Synthesis of [CpRu(PPh₃)(κ²C,P-(CCHBu)-P^{Ph}NBPh₄)], (**14**)

Complex **2** (0.0600 g, 0.0565 mmol) was dissolved in CH₂Cl₂ (3 mL). Next, 1-hexyne (65 μL, 0.565 mmol) was added to the suspension via syringe, and the mixture was allowed to stir for 24 hours. The now clear orange solution was evaporated to dryness under reduced pressure, and the orange solid that remained was washed with diethyl ether (2 x 10 mL). The product was dried under reduced pressure. Yield: 0.0640 g (84%). Recrystallization from CH₂Cl₂/hexanes yielded analytically pure samples. Anal. Calcd. for C₇₃H₆₅BN₂P₂Ru•0.5CH₂Cl₂: C, 74.4; H, 5.61; N, 2.36. Found: C, 74.6; H, 5.79; N, 2.65. ¹H NMR (500 MHz, 22 °C, CDCl₃): 7.87 (d, 1 H, ²J_{HH} = 8 Hz, C⁸H), 7.53-6.80 (overlapping m, 46 H, Ph of -PPh₂, PPh₃ and BPh₃, C⁵H-C⁷H, C³H, C⁵H and C_βH), 5.89 (d, 2 H, ²J_{HH} = 8 Hz, C²H, C⁶H), 5.02 (d, 1 H, ²J_{HH} = 15 Hz, -CH_AH_B-), 4.88 (d, 1 H, ²J_{HH} = 16 Hz, -CH_AH_B-), 4.68 (s, 5 H, Cp), 2.45 (br m, 2 H, *n*-Bu), 1.67 (br m, 2 H, *n*-Bu), 1.55 (br m, 2 H, *n*-Bu), 1.10 (t, 3 H, ³J_{HH} = 7 Hz, *n*-Bu). ¹³C{¹H} NMR (125 MHz, 22 °C, CDCl₃): 166.3 (q, ¹J_{BC} = 48 Hz, C⁴), 163.4 (q, ¹J_{BC} = 49 Hz, *ipso* C of B-Ph), 154.7 (dd, ²J_{PC} = 16 Hz, ²J_{PC} = 21 Hz, C_α), 150.8 (d, ¹J_{PC} = 23 Hz, C²), 137.9-123.2 (Ph, C¹-C³, C⁵, C⁶, C⁴, C⁹ and C_β), 121.9 (s, C⁶, C⁷), 117.9 (s, C⁵), 115.5 (s, C⁸), 84.8 (s, C₅H₅), 52.8 (s, -CH₂-), 33.8 (s, *n*-Bu), 33.2 (s, *n*-Bu), 23.3 (s, *n*-Bu), 14.4 (s, *n*-Bu). ³¹P{¹H} NMR (202 MHz, 22 °C, CDCl₃): 69.0 (d, ²J_{PP} = 34 Hz, PPh₃), 52.2 (d, ²J_{PP} = 34 Hz, -PPh₂). ¹¹B{¹H} NMR (160 MHz, 22 °C, CDCl₃): -6.7 ppm (s).

8.33. Synthesis of $[\text{Cp}^*\text{Ru}(\text{PPh}_3)(\kappa^2\text{C},P\text{-}(\text{CCHPh})\text{-P}^{\text{Ph}}\text{NBPh}_4)]$, (15)

(a) **Method A.** Complex **3** (0.0500 g, 0.0442 mmol) was dissolved in CH_2Cl_2 (4 mL). Next, phenylacetylene (49 μL , 0.442 mmol) was added to the solution via syringe, and the mixture was allowed to stir for 24 hours. The resulting clear dark red solution was evaporated to dryness under reduced pressure, and the red solid that remained was washed with diethyl ether (2 x 15 mL). Yield: 0.031 g (60%). Recrystallization from CH_2Cl_2 /hexanes yielded analytically pure samples. Anal. Calcd. for $\text{C}_{80}\text{H}_{71}\text{BN}_2\text{P}_2\text{Ru}\cdot 0.5\text{CH}_2\text{Cl}_2$: C, 75.7; H, 5.68; N, 2.19. Found: C, 75.3; H, 6.33; N, 2.04. ^1H NMR (500 MHz, 22 °C, CDCl_3): 7.69-6.78 (overlapping m, 44 H, Ph of $-\text{PPh}_2$, PPh_3 and BPh_3 , C^5H , C^8H , C^3H and C^5H), 6.76 (s, 1 H, C_βH), 6.64-6.37 (m, 5H, Ph), 6.18 (br, 2 H, C^6H , C^7H), 5.83 (d, 2 H, $^2J_{\text{HH}} = 8$ Hz, C^2H , C^6H), 5.05 (d, 1 H, $^2J_{\text{HH}} = 15$ Hz, $-\text{CH}_\text{A}\text{H}_\text{B}-$), 4.74 (d, 1 H, $^2J_{\text{HH}} = 15$ Hz, $-\text{CH}_\text{A}\text{H}_\text{B}-$), 1.30 (s, 15 H, Cp^*). $^{13}\text{C}\{^1\text{H}\}$ NMR (125 MHz, 22 °C, CDCl_3): 166.0 (q, $^1J_{\text{BC}} = 48$ Hz, C^4), 163.4 (q, $^1J_{\text{BC}} = 50$ Hz, *ipso* C of B-Ph), 162.2 (dd, $^2J_{\text{PC}} = 18$ Hz, $^2J_{\text{PC}} = 22$ Hz, C_α), 155.2 (d, $^1J_{\text{PC}} = 21$ Hz, C^2), 139.4-123.1 (Ph, C^1 - C^3 , C^5 , C^6 , C^4 , C^9 and C_β), 121.9 (s, C^6 , C^7), 119.1 (s, C^5), 114.4 (s, C^8), 95.6 (s, C_5Me_5), 53.2 (s, $-\text{CH}_2-$), 9.91 (s, $-\text{CH}_3$ of Cp^*). $^{31}\text{P}\{^1\text{H}\}$ NMR (202 MHz, 22 °C, CDCl_3): 67.1 (d, $^2J_{\text{PP}} = 32$ Hz, PPh_3), 51.9 (d, $^2J_{\text{PP}} = 32$ Hz, $-\text{PPh}_2$). $^{11}\text{B}\{^1\text{H}\}$ NMR (160 MHz, 22 °C, CDCl_3): -6.7 ppm (s).

(b) **Method B.** $\text{Cp}^*\text{RuCl}(\text{CCHPh})(\text{PPh}_3)$ (0.100 g, 0.157 mmol) and AgOTf (0.040 g, 0.157 mmol) were combined, dissolved in THF (10 mL) and allowed to stir for 30 minutes. Ligand **1a** (0.124 g, 0.157 mmol) in THF was added via cannula

to the deep, dark purple solution turning it cloudy, dark orange-red. The mixture was allowed to stir for 1 hour, and then the volatiles were removed under reduced pressure. The product was extracted into CH₂Cl₂ (20 mL) and filtered through Celite. The volatiles were removed from the deep, dark red filtrate yielding a red solid. The solid was washed with diethyl ether (15 mL) before drying under reduced pressure. Yield: 0.131 g (68%). The NMR spectroscopic data of the red solid were identical to that observed for the product isolated using Method A.

8.34. Synthesis of [Cp*Ru(PPh₃)(κ²C,P-(CCHBu)-P^{Ph}NBPh₄)], (**16**)

Complex **3** (0.0700 g, 0.0618 mmol) was dissolved in CH₂Cl₂ (4 mL). Next, 1-hexyne (71 μL, 0.618 mmol) was added to the solution via syringe, and the mixture was allowed to stir for 24 hours. The resulting clear orange solution was evaporated to dryness under reduced pressure, and the orange-red solid that remained was washed with diethyl ether (2 x 15 mL). Yield: 0.0420 g (56%). Recrystallization from CH₂Cl₂/hexanes and washing with diethyl ether yielded analytically pure samples. Anal. Calcd. for C₇₈H₇₅BN₂P₂Ru•0.5CH₂Cl₂: C, 75.0; H, 6.10; N, 2.23. Found: C, 75.5; H, 5.97; N, 2.56. ¹H NMR (500 MHz, 22 °C, CDCl₃): 7.64-6.19 (overlapping m, 46 H, Ph of -PPh₂, PPh₃ and BPh₃, C⁵H-C⁸H, C³H, C⁵H), 5.82 (d, ¹J_{HH} = 8 Hz, C²H, C⁶H), 5.57 (m, 1H, C_βH), 5.05 (d, 1 H, ²J_{HH} = 15 Hz, -CH_AH_B-), 4.68 (d, 1 H, ²J_{HH} = 15 Hz, -CH_AH_B-), 2.34 (br m, 1 H, *n*-Bu), 2.04 (br m, 1 H, *n*-Bu), 1.58 (br m, 4 H, *n*-Bu), 1.27 (s, 15 H, Cp*), 0.96 (t, 3 H, ³J_{HH} = 7 Hz, *n*-Bu). ¹³C{¹H} NMR (125 MHz, 22 °C, CDCl₃): 166.2 (q, ¹J_{BC} = 48 Hz, C⁴),

163.4 (q, $^1J_{BC} = 49$ Hz, *ipso* C of B-Ph), 154.2 (d, $^1J_{PC} = 19$ Hz, C^2), 153.3 (dd, $^2J_{PC} = 22$ Hz, $^2J_{PC} = 19$ Hz, C_α), 136.6-123.5 (Ph, $C^{1'}$ - $C^{3'}$, $C^{5'}$, $C^{6'}$, C^4 and C^9), 121.9 (s, C^6 , C^7), 121.6 (s, C_β), 118.4 (s, C^5), 114.9 (s, C^8), 94.8 (s, C_5Me_5), 53.1 (s, -CH₂-), 34.9 (s, *n*-Bu), 33.9 (s, *n*-Bu), 22.7 (s, *n*-Bu), 14.3 (s, *n*-Bu), 9.84 (s, C_5Me_5). $^{31}P\{^1H\}$ NMR (202 MHz, 22 °C, $CDCl_3$): 66.5 (d, $^2J_{PP} = 33$ Hz, PPh_3), 52.5 (d, $^2J_{PP} = 33$ Hz, $-PPh_2$). $^{11}B\{^1H\}$ NMR (160 MHz, 22 °C, $CDCl_3$): -6.8 ppm (s).

8.35. General experimental procedure for the reaction of complex **6** and 1-phenylacetylene

An NMR tube was charged with complex **6** (20 mg, 0.022 mmol) and dissolved in CD_2Cl_2 (0.5 mL). 1-phenylacetylene (2.42 μ L, 0.022 mmol) was added and the contents of the tube were mixed. The contents of the NMR tube were heated at 60°C for 24 hours. After 20 minutes at 60°C the solution appeared as a dark red colour. ^{31}P NMR revealed the formation of two new phosphorus-containing compounds in a 9:1 ratio. $^{31}P\{^1H\}$ NMR (202 MHz, 22 °C, CD_2Cl_2): 55.4 ppm (major product), 53.4 ppm (minor product). Although 1H and $^{13}C\{^1H\}$ NMR spectra were of poor quality for complete characterization of the compounds generated by this reaction, analysis of the $^{13}C\{^1H\}$ NMR spectrum showed the absence of a peak pertaining to the C_α of the desired vinylidene complex.

8.36. General experimental procedure for the reaction of complex **6** and 1-hexyne

An NMR tube was charged with complex **6** (22 mg, 0.024 mmol) and dissolved in CD₂Cl₂ (0.5 mL). The alkyne, 1-hexyne (2.80 μL, 0.024 mmol) was added and the contents of the NMR tube were mixed. The contents of the NMR tube were heated at 60°C for 24 hours. After 20 minutes at 60°C the solution appeared as a dark red colour. ³¹P NMR revealed the formation of two new phosphorus-containing compounds in a 8:2 ratio. ³¹P{¹H} NMR (202 MHz, 22 °C, CD₂Cl₂): 54.2 ppm (major product), 53.9 ppm (minor product). Although ¹H and ¹³C{¹H} NMR spectra were of poor quality for complete characterization of the compounds generated by this reaction, analysis of the ¹³C{¹H} NMR spectrum showed the absence of a peak pertaining to the C_α of the desired vinylidene complex.

8.37. Synthesis of Cp*RuCl(CCHPh)(κ²P,N-P^{Cy}NBPh₄) (**18**)

Ligand **1c** (153 mg, 0.169 mmol) was placed in a flask containing [Cp*RuCl]₄ (46 mg, 0.042 mmol) and the components were dissolved in CH₂Cl₂ (10 mL). The dark blue solution was stirred at room temperature for 20 minutes and then phenylacetylene (16 μL, 0.17 mmol) was added dropwise inducing a colour change initially to dark blue-green and quickly to dark orange-red. The mixture was stirred at room temperature for 4 hours and then filtered through Celite. The volatiles were removed from the filtrate and the residue was recrystallized from THF/hexanes yielding a dark red solid. Crude yield 105 mg

(61%). An impurity limited the complete characterization of this complex, however, the following NMR data provides evidence for the formation of the title complex. ^1H NMR (500 MHz, 22 °C, CDCl_3): 6.79 (d, 2 H, $^3J_{\text{HH}} = 7$ Hz, C^3H , C^5H), 6.64 (d, 2 H, $^3J_{\text{HH}} = 8$ Hz, C^2H , C^6H), 5.38 (d, 1 H, $^2J_{\text{HH}} = 16$ Hz, $-\text{CH}_\text{A}\text{H}_\text{B}-$), 5.18 (d, 1 H, $^2J_{\text{HH}} = 16$ Hz, $-\text{CH}_\text{A}\text{H}_\text{B}-$), 4.86 (d, $J = 2$ Hz, 1 H, C_βH), 1.94 (s, $-\text{CH}_3$ of C_5Me_5). $^{13}\text{C}\{^1\text{H}\}$ NMR (125 MHz, 22 °C, CDCl_3): 345.4 (d, $^2J_{\text{PC}} = 13$ Hz, C_α), 166.7 (q, $^1J_{\text{BC}} = 48$ Hz, C^4), 163.4 (q, $^1J_{\text{BC}} = 49$ Hz, *ipso* C of B-Ph), 157.5 (d, $^1J_{\text{PC}} = 27$ Hz, C^2), 142.0 (d, $^1J_{\text{PC}} = 14$ Hz, P-CH of Cy) 137.2-123.5 (Ph, C^1 - C^3 , C^5 , C^6 , C^4 and C^9), 121.9 (s, C^6 , C^7), 116.8 (s, C_β), 116.1 (s, C^5), 113.4 (s, C^8), 102.2 (s, C_5Me_5), 50.4 (s, $-\text{CH}_2-$), 35.4-20.8 (C_6H_{11}), 12.0 (s, $-\text{CH}_3$ of C_5Me_5). $^{31}\text{P}\{^1\text{H}\}$ NMR (202 MHz, 22 °C, CDCl_3): 29.9 (s, $-\text{PCy}_2$). $^{11}\text{B}\{^1\text{H}\}$ NMR (160 MHz, 22 °C, CDCl_3): -6.6 (s).

8.38. Synthesis of $\text{Cp}^*\text{RuCl}(\text{CCH}^t\text{Bu})(\kappa^2\text{P},\text{N}-\text{P}^{\text{Cy}}\text{NBPh}_4)$ (**19**)

Ligand **1c** (311 mg, 0.312 mmol) and $[\text{Cp}^*\text{RuCl}]_4$ (90 mg, 0.083 mmol) were placed in a flask and dissolved in CH_2Cl_2 (20 mL). The dark blue solution was stirred at room temperature for 20 minutes and then *tert*-butylacetylene (37 μL , 0.34 mmol) was added dropwise. After the addition of the alkyne, the solution turned to dark green-blue for a brief period before turning bright red-pink. The mixture was stirred at room temperature for 4 hours before being filtered through Celite. The volatiles were removed from the bright red filtrate yielding a solid of similar colour. The solid was recrystallized using THF/hexanes. Yield: 171 mg (55%). An impurity limited the complete characterization of this complex,

however, the following NMR data provides evidence for the formation of the title complex. ^1H NMR (500 MHz, 22 °C, CD_2Cl_2): 6.64 (d, 2 H, $^3J_{\text{HH}} = 7$ Hz, C^2H , C^6H), 5.42 (d, 1 H, $^2J_{\text{HH}} = 16$ Hz, $-\text{CH}_\text{A}\text{H}_\text{B}-$), 5.35 (d, 1 H, $^2J_{\text{HH}} = 16$ Hz, $-\text{CH}_\text{A}\text{H}_\text{B}-$), 3.76 (s, 1 H, C_βH), 1.92 (s, $-\text{CH}_3$ of C_5Me_5). $^{13}\text{C}\{^1\text{H}\}$ NMR (125 MHz, 22 °C, CD_2Cl_2): 340.0 (d, $^2J_{\text{PC}} = 14$ Hz, C_α), 165.6 (q, $^1J_{\text{BC}} = 49$ Hz, C^4), 163.4 (q, $^1J_{\text{BC}} = 49$ Hz, *ipso* C of B-Ph), 158.0 (d, $^1J_{\text{PC}} = 25$ Hz, C^2), 141.6 (d, $^1J_{\text{PC}} = 14$ Hz, P-CH of Cy), 136.7-123.0 (Ph, C^1 - C^3 , C^5 , C^6 , C^4 and C^9), 121.9 (s, C^6 , C^7), 121.9 (s, C_β), 121.8 (s, C^6 , C^7), 116.6 (s, C^5), 112.8 (s, C^8), 100.8 (s, C_5Me_5), 49.9 (s, $-\text{CH}_2-$), 35.4-25.0 (C_6H_{11} , $-\text{tBu}$), 11.6 (s, $-\text{CH}_3$ of C_5Me_5). $^{31}\text{P}\{^1\text{H}\}$ NMR (202 MHz, 22 °C, CD_2Cl_2): 30.7 (s, $-\text{PCy}_2$). $^{11}\text{B}\{^1\text{H}\}$ NMR (160 MHz, 22 °C, CD_2Cl_2): -6.7 (s).

8.39. General experimental procedure for the attempted protonation of **18** and **19** using HBF_4

Generally, an NMR tube was charged with **18** or **19** (26 mg and 25 mg respectively, 0.026 mmol). The complex was dissolved in CD_2Cl_2 (0.5 mL) and the NMR tube was cooled to -80°C before a 54 wt% solution of HBF_4 in Et_2O was added (4.3 μL). The tube was inverted immediately after the addition of the acid inducing a colour change of the solution to orange-red. The contents of the NMR tube were kept at low temperature prior to being transferred to a pre-cooled NMR probe (-60°C). Decomposition of the borate moiety was supported by ^{11}B NMR revealing the disappearance of the sharp signals pertaining to the parent vinylidene complexes accompanied by the appearance of broad signals downfield.

8.40. X-ray Crystallography

Complex 2:

A clear, yellow rod-like specimen of $2 \cdot 2\text{CH}_2\text{Cl}_2 \cdot (\text{CH}_3\text{CH}_2)_2\text{O}$, with approximate dimensions 0.06 mm x 0.13 mm x 0.19 mm, was used for the X-ray crystallographic analysis. The X-ray intensity data were measured on a Bruker Apex2 diffractometer using MoK α radiation. Data were collected on a Bruker Apex2 SMART CCD system with MoK α radiation at -100°C . Consecutive 0.5 degree omega scans were used to ensure complete coverage, and the total exposure time was 2.96 hours. The frames were integrated with the Bruker SAINT software package (Apex2 2013.10.1) using a narrow-frame algorithm. The integration of the data using an orthorhombic unit cell yielded a total of 59803 reflections to a maximum θ angle of 28.33° (0.75 Å resolution), of which 16002 were independent (average redundancy 3.737, completeness = 99.6%, $R(\text{int}) = 5.98\%$, $R\sigma = 8.90\%$) and 12036 (75.22%) were greater than $2\sigma(F^2)$. The final cell constants of $a = 16.9751(8)$ Å, $b = 18.6007(8)$ Å, $c = 20.4062(9)$ Å, and volume = $6443.2(5)$ Å³, are based upon the refinement of the XYZ-centroids of 7046 reflections above $20 \sigma(I)$ with $4.553^\circ < 2\theta < 39.05^\circ$. Data were corrected for absorption effects using the numerical method (SADABS). The ratio of minimum to maximum apparent transmission was 0.914. The calculated minimum and maximum transmission coefficients (based on crystal size) are 0.9093 and 0.9864. The structure was solved and refined using the Bruker SHELXTL 2013 Software Package, using the space group $P2_12_12_1$, with $Z = 4$ for the formula unit

$C_{73}H_{69}BCl_4N_2OP_2Ru$. The final anisotropic full-matrix least-squares refinement on F^2 with 743 variables converged at $R_1 = 5.81\%$ for the observed data, and $wR_2 = 15.64\%$ for all data. The goodness-of-fit was 1.037. The largest peak in the final difference electron density synthesis was $1.084 e^-/\text{\AA}^3$ and the largest hole was $-0.803 e^-/\text{\AA}^3$, with an RMS deviation of $0.100 e^-/\text{\AA}^3$. On the basis of the final model, the calculated density was 1.346 g/cm^3 and $F(000)$, 2704 e^- . The main molecule showed no disorder, but three disordered solvent molecules were refined: two molecules of CH_2Cl_2 (0.61(1) and 0.510(6)) and one molecule of diethyl ether (0.763(7)).

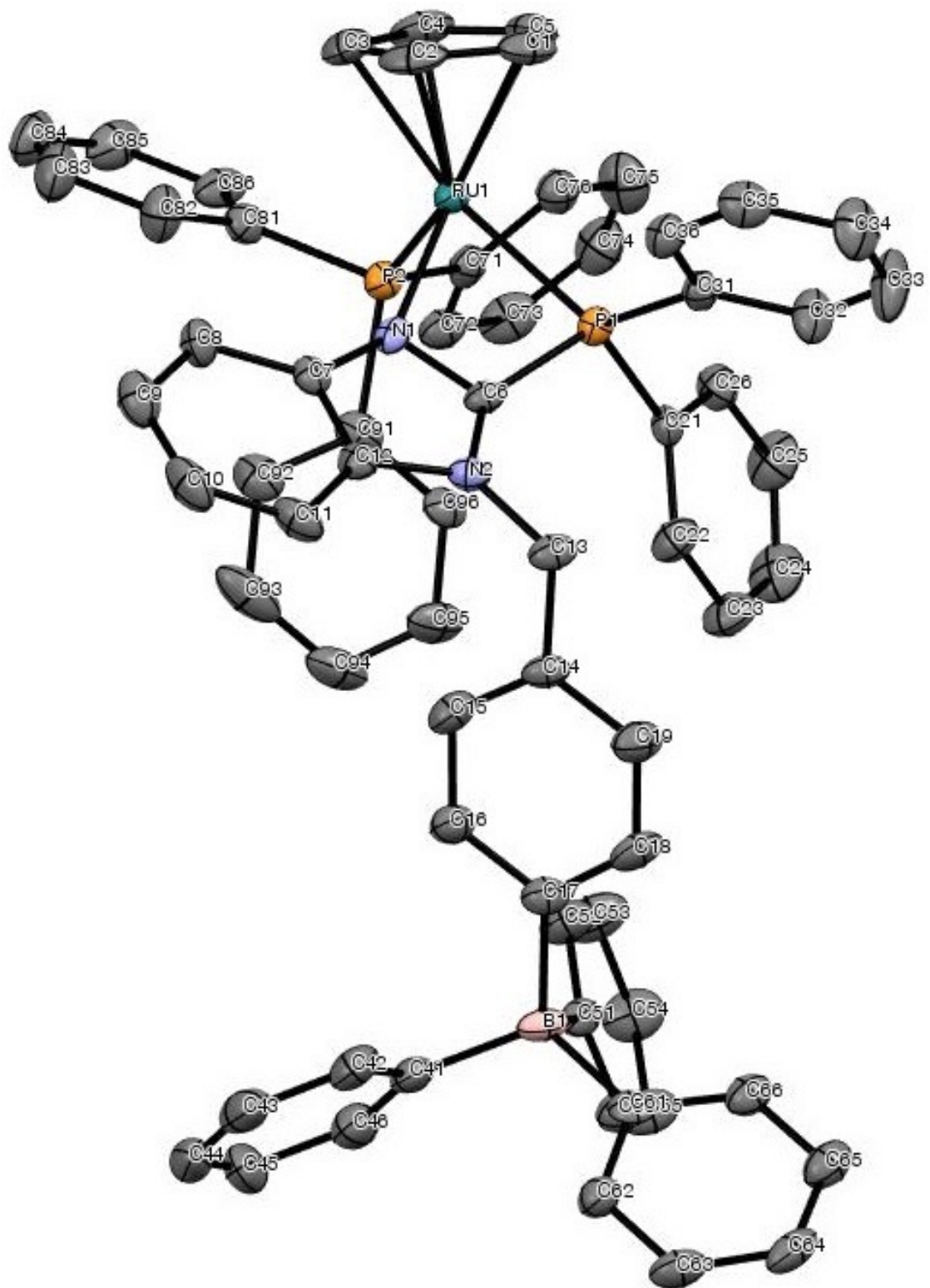


Figure 39. Fully labeled crystal structure of complex 2. H atoms are omitted for clarity.

Table 4. Bond Lengths for complex **2** (bond lengths with H omitted).

Atom 1	Atom 2	Length (Å)
Ru1	P2	2.3159(15)
Ru1	P1	2.3420(15)
Ru1	N1	2.163(5)
Ru1	C5	2.193(6)
Ru1	C4	2.1688(7)
Ru1	C3	2.177(6)
Ru1	C2	2.217(6)
Ru1	C1	2.233(7)
P2	C91	1.833(7)
P2	C81	1.838(6)
P2	C71	1.830(6)
P1	C6	1.823(6)
P1	C31	1.827(6)
P1	C21	1.800(6)
N2	C6	1.353(7)
N2	C13	1.468(7)
N2	C12	1.390(8)
N1	C7	1.379(7)
N1	C6	1.333(7)
C95	C96	1.378(9)
C94	C95	1.384(11)
C93	C94	1.416(12)
C92	C93	1.394(10)
C91	C96	1.384(9)
C91	C92	1.401(9)
C9	C10	1.392(11)
C85	C86	1.394(10)
C84	C85	1.365(11)
C83	C84	1.382(11)
C82	C83	1.378(10)
C81	C86	1.404(9)
C81	C82	1.385(9)
C8	C9	1.403(10)
C75	C76	1.383(9)

Atom 1	Atom 2	Length (Å)
C74	C75	1.372(11)
C73	C74	1.372(11)
C72	C73	1.387(9)
C71	C76	1.391(9)
C71	C72	1.405(9)
C7	C8	1.403(8)
C7	C12	1.385(8)
C65	C66	1.393(9)
C64	C65	1.372(10)
C63	C64	1.372(10)
C62	C63	1.422(9)
C61	C66	1.395(9)
C61	C62	1.399(9)
C55	C56	1.373(9)
C54	C55	1.371(10)
C53	C54	1.389(10)
C52	C53	1.380(10)
C51	C56	1.386(9)
C51	C52	1.389(9)
C45	C46	1.402(11)
C44	C45	1.366(12)
C43	C44	1.383(12)
C42	C43	1.404(10)
C41	C46	1.380(10)
C41	C42	1.398(9)
C4	C5	1.392(10)
C35	C36	1.383(9)
C34	C35	1.362(10)
C33	C34	1.376(10)
C32	C33	1.393(9)
C31	C36	1.408(8)
C31	C32	1.371(9)
C3	C4	1.416(11)
C25	C26	1.399(9)
C24	C25	1.365(11)
C23	C24	1.387(11)

Atom 1	Atom 2	Length (Å)
C22	C23	1.389(9)
C21	C26	1.386(8)
C21	C22	1.388(9)
C2	C3	1.425(11)
C18	C19	1.383(9)
C17	C18	1.393(9)
C16	C17	1.389(9)
C15	C16	1.400(9)
C14	C19	1.374(9)
C14	C15	1.387(9)
C13	C14	1.519(8)
C11	C12	1.404(8)
C10	C11	1.366(10)
C1	C5	1.421(10)
C1	C2	1.396(11)
B1	C61	1.641(9)
B1	C51	1.657(9)
B1	C41	1.654(10)
B1	C17	1.654(9)

Table 5. Bond Angles for complex **2** (bond angles involving H omitted).

Atom 1	Atom 2	Atom 3	Angle (°)
Ru1	C91	P2	116.4(2)
Ru1	C81	P2	111.7(2)
Ru1	C71	P2	117.5(2)
Ru1	C7	N1	147.3(4)
Ru1	C6	P1	83.64(18)
Ru1	C6	N1	104.2(4)
Ru1	C5	C4	72.3(4)
Ru1	C5	C1	69.8(4)
Ru1	C4	C5	70.5(4)
Ru1	C4	C3	70.7(4)
Ru1	C31	P1	118.8(2)
Ru1	C3	C4	71.3(4)

Atom 1	Atom 2	Atom 3	Angle (°)
Ru1	C3	C2	69.6(4)
Ru1	C21	P1	131.0(2)
Ru1	C2	C3	72.6(4)
Ru1	C2	C1	71.1(4)
Ru1	C1	C5	72.8(3)
Ru1	C1	C2	72.3(4)
P2	N1	Ru1	90.90(13)
P2	C96	C91	120.1(5)
P2	C92	C91	121.4(5)
P2	C86	C81	122.5(5)
P2	C82	C81	119.2(5)
P2	C76	C71	120.6(5)
P2	C72	C71	121.7(5)
P2	C5	Ru1	113.9(2)
P2	C4	Ru1	90.9(2)
P2	C3	Ru1	104.0(2)
P2	C2	Ru1	141.2(2)
P1	P2	Ru1	97.90(6)
P1	N2	C6	141.9(4)
P1	N1	Ru1	67.65(12)
P1	N1	C6	104.4(4)
P1	C5	Ru1	107.90(19)
P1	C4	Ru1	142.9(2)
P1	C36	C31	118.9(4)
P1	C3	Ru1	158.1(2)
P1	C26	C21	118.8(5)
P1	C22	C21	122.8(5)
P1	C2	Ru1	120.5(2)
N2	N1	C6	112.3(5)
N2	C7	C12	106.7(5)
C94	C96	C95	120.6(7)
C94	C92	C93	120.8(7)
C93	C95	C94	118.0(7)
C92	C96	C91	118.1(6)
C91	C95	C96	122.3(7)
C91	C93	C92	120.1(7)

Atom 1	Atom 2	Atom 3	Angle (°)
C91	C71	P2	102.3(3)
C9	C11	C10	123.1(7)
C86	C84	C85	119.9(7)
C86	C82	C81	118.2(6)
C84	C82	C83	121.2(7)
C83	C85	C84	119.7(7)
C81	C91	P2	103.5(3)
C81	C85	C86	120.7(7)
C81	C83	C82	120.3(7)
C81	C71	P2	103.7(3)
C8	N1	C7	131.2(5)
C8	C10	C9	120.7(6)
C76	C74	C75	120.5(7)
C75	C73	C74	119.5(7)
C72	C76	C71	117.8(6)
C72	C74	C73	120.9(7)
C71	C75	C76	121.0(7)
C71	C73	C72	120.2(7)
C7	C9	C8	117.2(6)
C7	C6	N1	105.9(5)
C66	C64	C65	120.1(6)
C65	C63	C64	119.9(6)
C63	C61	C62	122.2(6)
C62	C66	C61	115.3(6)
C62	C64	C63	119.4(6)
C61	C65	C66	123.1(6)
C6	C21	P1	110.3(3)
C56	C54	C55	119.3(7)
C54	C52	C53	118.2(7)
C53	C55	C54	120.0(7)
C52	C56	C51	114.3(6)
C51	C61	B1	108.3(5)
C51	C55	C56	123.9(6)
C51	C53	C52	124.2(7)
C51	C41	B1	108.5(5)
C51	C17	B1	108.4(5)

Atom 1	Atom 2	Atom 3	Angle (°)
C5	N1	Ru1	155.2(2)
C5	C4	Ru1	37.2(3)
C5	C3	Ru1	63.0(3)
C5	C2	C1	107.7(6)
C46	C44	C45	120.3(8)
C45	C41	C46	122.1(8)
C43	C45	C44	120.0(7)
C43	C41	C42	122.9(7)
C42	C46	C41	116.0(7)
C42	C44	C43	118.6(7)
C41	C61	B1	111.6(5)
C4	N1	Ru1	148.5(2)
C36	C32	C31	119.8(6)
C36	C34	C35	120.7(6)
C33	C35	C34	119.9(6)
C33	C31	C32	119.4(6)
C32	C34	C33	120.8(7)
C31	C6	P1	103.6(3)
C31	C35	C36	119.5(6)
C31	C21	P1	103.6(3)
C3	N1	Ru1	111.6(2)
C3	C5	C4	108.8(7)
C3	C4	Ru1	38.0(3)
C3	C1	C2	108.6(7)
C26	C24	C25	118.8(7)
C25	C21	C26	121.4(6)
C23	C25	C24	121.4(7)
C23	C21	C22	120.9(6)
C22	C26	C21	118.4(6)
C22	C24	C23	119.1(7)
C2	C3	Ru1	37.8(3)
C2	N1	Ru1	98.1(2)
C2	C5	Ru1	62.1(3)
C2	C4	Ru1	62.6(3)
C2	C4	C3	106.7(7)
C18	C16	C17	114.0(6)

Atom 1	Atom 2	Atom 3	Angle (°)
C18	C14	C19	121.4(7)
C17	C41	B1	109.1(5)
C17	C19	C18	122.9(6)
C16	C14	C15	118.9(6)
C15	C19	C14	118.2(6)
C15	C17	C16	124.4(7)
C14	N2	C13	114.0(5)
C13	C6	N2	127.7(5)
C13	C19	C14	118.8(6)
C13	C15	C14	123.0(5)
C13	C12	N2	126.1(5)
C12	N1	C7	108.9(5)
C12	C6	N2	106.2(5)
C12	C10	C11	115.6(7)
C11	N2	C12	130.0(6)
C11	C7	C12	123.3(6)
C1	N1	Ru1	117.8(2)
C1	C5	Ru1	37.4(3)
C1	C4	Ru1	62.3(3)
C1	C4	C5	108.2(6)
C1	C3	Ru1	62.6(3)
C1	C2	Ru1	36.6(3)
B1	C66	C61	121.3(5)
B1	C56	C51	121.3(6)
B1	C52	C51	124.3(6)
B1	C46	C41	125.3(6)
B1	C42	C41	118.7(6)
B1	C18	C17	124.1(5)
B1	C16	C17	121.9(6)
P2	C1	Ru1	150.92(18)
P1	C32	C31	121.4(5)
P1	C1	Ru1	97.71(19)
C8	C12	C7	119.9(5)
C17	C61	B1	110.8(5)
B1	C62	C61	123.4(6)

Complex 4:

One rod-shaped X-ray quality-crystal of **4** approximate size 0.13 x 0.16 x 0.20 mm was selected; it did not differ in habit from the bulk of the crystalline sample. Data were collected at -100 °C with a Bruker Apex2 system using MoK α radiation ($\lambda = 0.71073 \text{ \AA}$) using a series of 0.5 degree omega scans for coverage to approximately 0.70 \AA . Initial unit cell parameters were determined from 100 consecutive 0.5 degree frames, and data were collected for the resultant monoclinic cell in four shells. Data were processed using SAINT, and scaled using the numerical method (SADABS), and then solved using the SHELX program suite in the monoclinic space group $P2_1/n$. All non-hydrogen atoms were refined anisotropically, and hydrogen atoms were refined isotropically as riding on their parent atoms. The final anisotropic full-matrix least squares refinement on F^2 with 635 variables converged at $R1 = 8.09\%$ for the observed data, and the largest residual electron density peak was $1.853 \text{ e}/\text{\AA}^3$, associated with Ru1.

Software:

- 1) SAINT and SADABS: APEX2 v.2014.11-0 software suite, Bruker AXS Inc., Madison, WI.
- 2) SHELX: (a) "A Short History of SHELX" Sheldrick, G.M. *Acta. Cryst.* A64, 112-122. (b) SHELXTL as part of the APEX2 v.2013.10 software suite.
- 3) PLATON SQUEEZE: A.L. Spek (2009) *Acta Cryst.* D65, 148-155. "Platon: A multipurpose crystallographic tool."

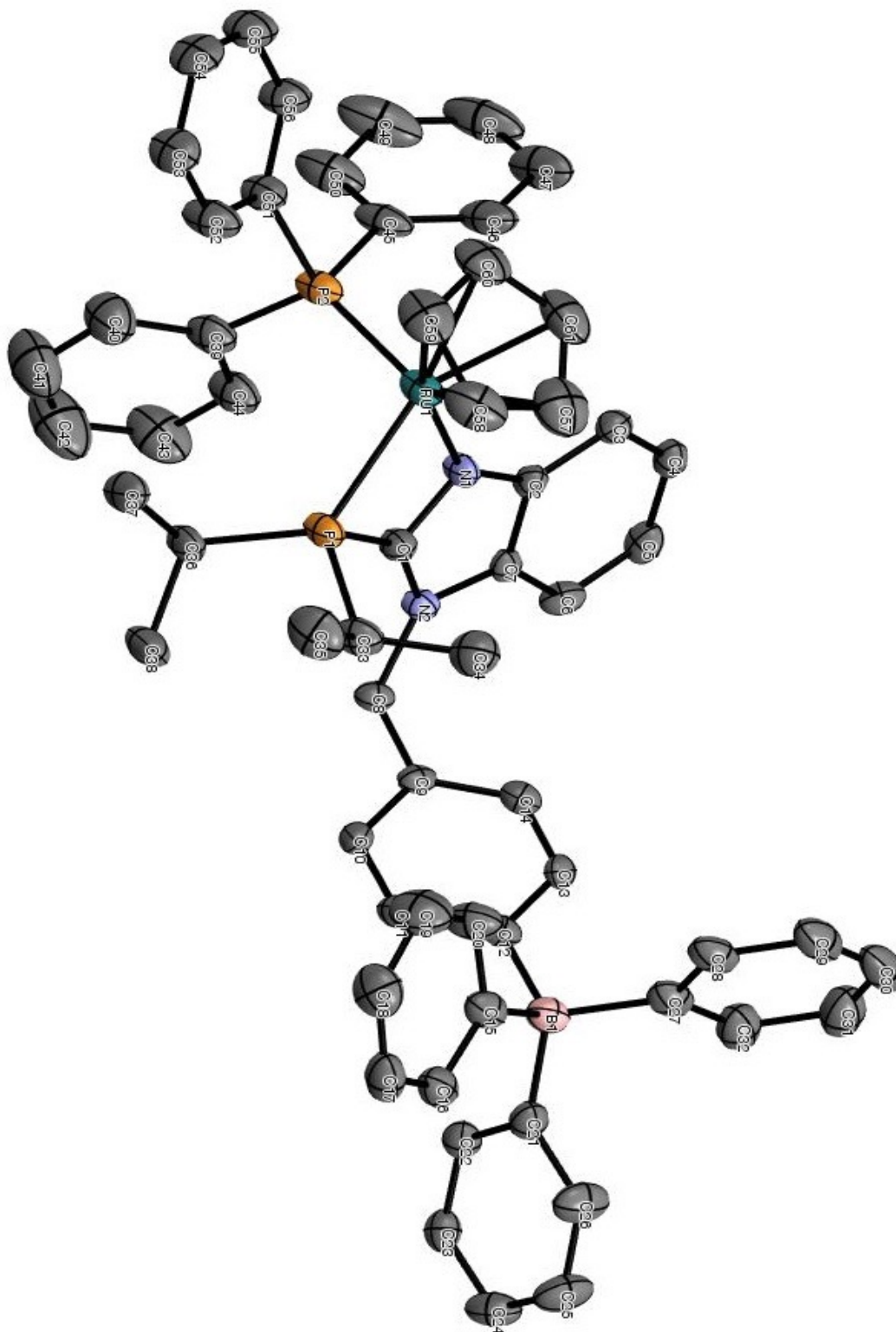


Figure 40. Fully labeled crystal structure of complex 4. H atoms are omitted for clarity.

Table 6. Bond Lengths for complex **4** (bond lengths with H omitted).

Atom 1	Atom 2	Length (Å)
Ru1	P1	2.3824(15)
Ru1	P2	2.3227(19)
Ru1	N1	2.136(4)
Ru1	C57	2.231(8)
Ru1	C58	2.216(7)
Ru1	C59	2.198(6)
Ru1	C60	2.202(6)
Ru1	C61	2.214(7)
P1	C1	1.840(6)
P1	C33	1.849(6)
P1	C36	1.860(6)
P2	C39	1.844(7)
P2	C45	1.850(6)
P2	C51	1.839(6)
N1	C1	1.341(7)
N1	C2	1.384(7)
N2	C1	1.361(7)
N2	C7	1.404(7)
N2	C8	1.475(6)
B1	C12	1.668(8)
B1	C15	1.637(9)
B1	C21	1.646(9)
B1	C27	1.651(9)
C2	C3	1.391(7)
C2	C7	1.400(7)
C3	C4	1.393(8)
C4	C5	1.402(8)
C5	C6	1.382(8)
C6	C7	1.397(7)
C8	C9	1.509(7)
C9	C10	1.387(8)
C9	C14	1.393(8)
C10	C11	1.386(8)
C11	C12	1.388(8)

Atom 1	Atom 2	Length (Å)
C12	C13	1.402(8)
C13	C14	1.391(8)
C15	C16	1.404(8)
C15	C20	1.419(9)
C16	C17	1.393(9)
C17	C18	1.363(10)
C18	C19	1.377(10)
C19	C20	1.3756(10)
C21	C22	1.388(8)
C21	C26	1.429(8)
C22	C23	1.386(8)
C23	C24	1.388(9)
C24	C25	1.389(10)
C25	C26	1.375(9)
C27	C28	1.392(9)
C27	C32	1.404(10)
C28	C29	1.402(9)
C29	C30	1.379(12)
C30	C31	1.368(12)
C31	C32	1.393(10)
C33	C34	1.544(9)
C33	C35	1.548(9)
C36	C37	1.522(8)
C36	C38	1.538(8)
C39	C40	1.401(10)
C39	C44	1.392(9)
C40	C41	1.378(12)
C41	C42	1.419(13)
C42	C43	1.364(13)
C43	C44	1.367(10)
C45	C46	1.382(11)
C45	C50	1.391(11)
C46	C47	1.400(10)
C47	C48	1.419(14)
C48	C49	1.370(14)
C49	C50	1.395(10)

Atom 1	Atom 2	Length (Å)
C51	C52	1.385(9)
C51	C56	1.391(9)
C52	C53	1.391(9)
C53	C54	1.397(10)
C54	C55	1.366(10)
C55	C56	1.397(9)
C57	C58	1.406(11)
C57	C61	1.427(12)
C58	C59	1.415(11)
C59	C60	1.418(10)
C60	C61	1.410(11)

Table 7. Bond Angles for complex **4** (bond angles involving H omitted).

Atom 1	Atom 2	Atom 3	Angle (°)
Ru(1)	P(2)	P(1)	98.15(6)
Ru(1)	N(1)	P(2)	91.79(14)
Ru(1)	N(1)	P(1)	67.15(12)
Ru(1)	N(1)	C(61)	103.8(2)
Ru(1)	N(1)	C(60)	135.9(2)
Ru(1)	N(1)	C(59)	162.9(3)
Ru(1)	N(1)	C(58)	128.2(3)
Ru(1)	N(1)	C(57)	100.4(3)
Ru(1)	C(61)	P(2)	111.4(2)
Ru(1)	C(61)	P(1)	149.6(2)
Ru(1)	C(61)	C(58)	62.2(3)
Ru(1)	C(61)	C(57)	37.5(3)
Ru(1)	C(60)	P(2)	88.8(2)
Ru(1)	C(60)	P(1)	155.9(2)
Ru(1)	C(60)	C(61)	37.3(3)
Ru(1)	C(60)	C(58)	62.2(3)
Ru(1)	C(60)	C(57)	62.2(3)
Ru(1)	C(59)	P(2)	102.9(2)
Ru(1)	C(59)	P(1)	118.4(2)
Ru(1)	C(59)	C(61)	62.8(3)

Atom 1	Atom 2	Atom 3	Angle (°)
Ru(1)	C(59)	C(60)	37.6(3)
Ru(1)	C(59)	C(58)	37.4(3)
Ru(1)	C(59)	C(57)	62.4(3)
Ru(1)	C(58)	P(2)	139.9(2)
Ru(1)	C(58)	P(1)	99.5(2)
Ru(1)	C(58)	C(57)	36.9(3)
Ru(1)	C(57)	P(2)	148.4(2)
Ru(1)	C(57)	P(1)	113.4(2)
P(2)	C(45)	Ru(1)	115.6(3)
P(2)	C(39)	Ru(1)	121.3(2)
P(2)	C(39)	C(45)	99.1(3)
P(1)	C(36)	Ru(1)	128.8(2)
P(1)	C(33)	Ru(1)	119.3(2)
P(1)	C(33)	C(36)	105.0(3)
P(1)	C(1)	Ru(1)	83.07(17)
P(1)	C(1)	C(36)	111.5(3)
P(1)	C(1)	C(33)	103.3(3)
N(2)	C(7)	C(8)	124.2(4)
N(2)	C(1)	C(8)	129.1(4)
N(2)	C(1)	C(7)	106.5(4)
N(1)	C(2)	Ru(1)	145.4(4)
N(1)	C(1)	Ru(1)	106.7(3)
N(1)	C(1)	C(2)	107.6(4)
C(9)	C(14)	C(8)	121.0(5)
C(9)	C(10)	C(8)	121.9(5)
C(9)	C(10)	C(14)	117.1(5)
C(8)	N(2)	C(9)	112.9(4)
C(7)	C(6)	N(2)	131.0(5)
C(7)	C(6)	C(2)	122.1(5)
C(7)	C(2)	N(2)	107.0(4)
C(61)	C(60)	Ru(1)	70.9(4)
C(61)	C(60)	C(57)	107.6(7)
C(61)	C(57)	Ru(1)	71.9(4)
C(60)	C(61)	Ru(1)	71.8(4)
C(60)	C(61)	C(59)	108.6(7)
C(60)	C(59)	Ru(1)	71.0(4)

Atom 1	Atom 2	Atom 3	Angle (°)
C(6)	C(5)	C(7)	116.3(5)
C(59)	C(60)	Ru(1)	71.3(4)
C(59)	C(58)	Ru(1)	72.0(4)
C(59)	C(58)	C(60)	107.2(7)
C(58)	C(59)	Ru(1)	70.6(4)
C(58)	C(57)	Ru(1)	72.1(4)
C(58)	C(57)	C(59)	108.9(7)
C(57)	C(61)	Ru(1)	70.6(5)
C(57)	C(58)	Ru(1)	71.0(5)
C(57)	C(58)	C(61)	107.7(8)
C(56)	C(51)	C(55)	119.0(6)
C(55)	C(54)	C(56)	121.5(6)
C(54)	C(55)	C(53)	120.2(6)
C(52)	C(51)	C(53)	121.9(6)
C(51)	C(56)	P(2)	121.7(5)
C(50)	C(45)	C(49)	121.2(9)
C(5)	C(6)	C(4)	122.3(5)
C(49)	C(48)	C(50)	119.3(9)
C(48)	C(49)	C(47)	121.2(7)
C(47)	C(46)	C(48)	117.9(8)
C(46)	C(45)	C(47)	121.4(8)
C(45)	C(50)	P(2)	121.7(6)
C(45)	C(46)	P(2)	119.2(6)
C(45)	C(46)	C(50)	119.0(7)
C(44)	C(43)	C(39)	120.7(7)
C(43)	C(42)	C(44)	121.0(8)
C(42)	C(43)	C(41)	119.4(9)
C(41)	C(40)	C(42)	119.7(8)
C(40)	C(41)	C(39)	119.8(7)
C(4)	C(3)	C(5)	121.1(5)
C(39)	C(44)	P(2)	116.9(5)
C(39)	C(44)	C(40)	119.2(7)
C(39)	C(40)	P(2)	123.9(5)
C(36)	C(38)	P(1)	115.7(5)
C(36)	C(37)	P(1)	109.9(4)
C(36)	C(37)	C(38)	110.1(5)

Atom 1	Atom 2	Atom 3	Angle (°)
C(33)	C(35)	P(1)	112.1(5)
C(33)	C(34)	P(1)	112.4(4)
C(33)	C(34)	C(35)	110.2(6)
C(32)	C(31)	C(27)	122.3(7)
C(31)	C(30)	C(32)	120.7(8)
C(30)	C(31)	C(29)	119.2(7)
C(3)	C(2)	C(4)	117.3(5)
C(29)	C(30)	C(28)	119.7(7)
C(28)	C(27)	C(29)	122.8(7)
C(27)	C(32)	B(1)	120.5(6)
C(27)	C(28)	C(32)	115.2(6)
C(27)	C(28)	B(1)	124.2(6)
C(26)	C(25)	C(21)	122.6(6)
C(25)	C(26)	C(24)	121.3(6)
C(24)	C(23)	C(25)	117.7(6)
C(23)	C(22)	C(24)	120.3(5)
C(22)	C(23)	C(21)	124.2(5)
C(21)	C(26)	B(1)	120.3(5)
C(21)	C(22)	C(26)	113.8(5)
C(21)	C(22)	B(1)	125.8(5)
C(20)	C(19)	C(15)	123.3(6)
C(2)	N(1)	C(7)	107.7(4)
C(2)	N(1)	C(3)	131.3(5)
C(2)	C(3)	C(7)	121.0(5)
C(19)	C(20)	C(18)	120.7(7)
C(18)	C(17)	C(19)	118.3(7)
C(17)	C(18)	C(16)	121.3(6)
C(16)	C(17)	C(15)	122.6(6)
C(15)	C(20)	B(1)	120.9(5)
C(15)	C(16)	C(20)	113.6(6)
C(15)	C(16)	B(1)	125.5(5)
C(14)	C(13)	C(9)	120.7(5)
C(13)	C(14)	C(12)	123.1(5)
C(12)	C(13)	B(1)	123.3(5)
C(12)	C(11)	C(13)	114.6(5)
C(12)	C(11)	B(1)	122.1(5)

Atom 1	Atom 2	Atom 3	Angle (°)
C(11)	C(10)	C(12)	123.3(5)
C(10)	C(11)	C(9)	121.2(5)
C(1)	N(2)	P(1)	145.2(4)
C(1)	N(1)	P(1)	102.9(4)
C(1)	N(1)	N(2)	111.2(5)
B(1)	C(15)	C(27)	112.2(5)
B(1)	C(27)	C(12)	110.0(5)
B(1)	C(21)	C(27)	109.0(5)
B(1)	C(21)	C(12)	109.1(5)
B(1)	C(15)	C(21)	109.3(5)
B(1)	C(15)	C(12)	107.1(5)

References

- [1] J. J. Soldevila-Barreda, I. Romero-Canelón, A. Habtemariam, P. J. Sadler, *Nat. Commun.* **2015**, *6*, 6582-6591.
- [2] J. M. Walker, A. McEwan, R. Pycko, M. L. Tassotto, C. Gottardo, J. Th'ng, R. Wang, G. J. Spivak, *Eur. J. Inorg. Chem.* **2009**, 4629–4633.
- [3] P. R. Florindo, D. M. Pereira, P. M. Borralho, C. M. P. Rodrigues, M. F. M. Piedade, A. C. Fernandes, *J. Med. Chem.* **2015**, *58*, 4339–4347.
- [4] B. Biersack, M. Zoldakova, K. Effenberger, R. Schobert, *Eur. J. Med. Chem.* **2010**, *45*, 1972–1975.
- [5] M. H. Garcia, T. S. Morais, P. Florindo, M. F. M. Piedade, V. Moreno, C. Ciudad, V. Noe, *J. Inorg. Biochem.* **2009**, *103*, 354–361.
- [6] C. S. Allardyce, P. J. Dyson, D. J. Ellis, P. A. Salter, R. Scopelliti, *J. Organomet. Chem.* **2003**, *668*, 35–42.
- [7] C. G. Hartinger, P. J. Dyson, *Chem. Soc. Rev.* **2009**, *38*, 391-401.
- [8] E. L.-M. Wong, R. W.-Y. Sun, N. P. Y. Chung, C.-L. S. Lin, N. Zhu, C.-M. Che, *J. Am. Chem. Soc.* **2006**, *128*, 4938–4939.
- [9] L. Duan, F. Bozoglian, S. Mandal, B. Stewart, T. Privalov, A. Llobet, L. Sun, *Nat. Chem.* **2012**, *4*, 418–423.
- [10] W. E. Piers, *Organometallics* **2011**, *30*, 13–16.
- [11] Y. Xu, A. Fischer, L. Duan, L. Tong, E. Gabrielsson, B. Åkermark, L. Sun, *Angew. Chem. Int. Ed.* **2010**, *49*, 8934–8937.

- [12] L. Duan, Y. Xu, M. Gorlov, L. Tong, S. Andersson, L. Sun, *Chem. Eur. J.* **2010**, *16*, 4659–4668.
- [13] M. Orlandi, R. Argazzi, A. Sartorel, M. Carraro, G. Scorrano, M. Bonchio, F. Scandola, *Chem. Commun.* **2010**, *46*, 3152–3154.
- [14] D. G. H. Hetterscheid, J. I. van der Vlugt, B. de Bruin, J. N. H. Reek, *Angew. Chem. Int. Ed.* **2009**, *48*, 8178–8181.
- [15] L. Duan, A. Fischer, Y. Xu, L. Sun, *J. Am. Chem. Soc.* **2009**, *131*, 10397–10399.
- [16] R. H. Grubbs, *Angew. Chem. Int. Ed.* **2006**, *45*, 3760–3765.
- [17] R. Noyori, *Angew. Chem. Int. Ed.* **2002**, *41*, 2008–2022.
- [18] J. Halpern, *Pure Appl. Chem.* **2001**, *73*, 209–220.
- [19] B. M. Trost, M. U. Frederiksen, M. T. Rudd, *Angew. Chem. Int. Ed.* **2005**, *44*, 6630–6666.
- [20] T. Naota, H. Takaya, S.-I. Murahashi, *Chem. Rev.* **1998**, *98*, 2599–2660.
- [21] K. Van Gorp, *Catal. Today* **1999**, *52*, 349–361.
- [22] C. A. Busacca, D. R. Fandrick, J. J. Song, C. H. Senanayake, *Adv. Synth. Catal.* **2011**, *353*, 1825–1864.
- [23] P. Dupau, *Top. Organomet. Chem.* **2012**, *42*, 47–64.
- [24] A. Fürstner, *Chem. Commun.* **2011**, *47*, 6505–7.
- [25] A. Fürstner, *Isr. J. Chem.* **2011**, *51*, 329–345.
- [26] D. G. Gillingham, A. H. Hoveyda, *Angew. Chem. Int. Ed.* **2007**, *46*, 3860–3864.

- [27] A. Z. Fadhel, P. Pollet, C. L. Liotta, C. A. Eckert, *Molecules* **2010**, *15*, 8400–8424.
- [28] P. T. Anastas, L. B. Bartlett, M. M. Kirchhoff, T. C. Williamson, *Catal. Today* **2000**, *55*, 11–22.
- [29] P. T. Anastas, M. M. Kirchhoff, T. C. Williamson, *Appl. Catal., A* **2001**, *221*, 3–13.
- [30] R. A. Sheldon, *Chem. Commun.* **2008**, 3352–3365.
- [31] V. Walsh, J. Goodman, *Soc. Sci. Med.* **1999**, 1215–1225.
- [32] G. Bodeker, C. van Klooster, E. Weisbord, *J. Altern. Complement. Med.* **2014**, *20*, 810–822.
- [33] K. C. Nicolaou, E.J. Sorensen, N. Winssinger, *J. Chem. Ed.* **1998**, *75*, 1225–1258.
- [34] H. Martinez, N. Ren, M. E. Matta, M. A. Hillmyer, *Polym. Chem.* **2014**, *5*, 3507–3532.
- [35] C. S. Higman, J. A. M. Lummiss, D. E. Fogg, *Angew. Chem. Int. Ed.* **2016**, *55*, 3552–3565.
- [36] R. H. Grubbs, S. Chang, *Tetrahedron* **1998**, *54*, 4413–4450.
- [37] A. M. Lozano-Vila, S. Monsaert, A. Bajek, F. Verpoort, *Chem. Rev.* **2010**, *110*, 4865–4909.
- [38] X. Wu, M. Tamm, *Beilstein J. Org. Chem.* **2011**, *7*, 82–93.
- [39] A. Fürstner, *Angew. Chem. Int. Ed.* **2014**, *53*, 8587–8598.

- [40] B. Haberlag, M. Freytag, C. G. Daniliuc, P. G. Jones, M. Tamm, *Angew. Chem. Int. Ed.* **2012**, *51*, 13019–13022.
- [41] A. Ahlers, T. de Haro, B. Gabor, A. Fürstner, *Angew. Chem Int. Ed.* **2015**, *128*, 1428–1433.
- [42] K. Jyothish, W. Zhang, *Angew. Chem. Int. Ed.* **2011**, *50*, 8478–8480.
- [43] P. Persich, J. Llaveria, R. Lhermet, T. de Haro, R. Stade, A. Kondoh, A. Fürstner, *Chem. Eur. J.* **2013**, *19*, 13047–13058.
- [44] K. J. Ralston, H. C. Ramstadius, R. C. Brewster, H. S. Niblock, A. N. Hulme, *Angew. Chem. Int. Ed.* **2015**, *127*, 7192–7196.
- [45] A. Fürstner, *Science* **2011**, *341*, 1357–1364.
- [46] M. B. Herbert, R. H. Grubbs, *Angew. Chem. Int. Ed.* **2015**, *54*, 5108–5024.
- [47] P. M. Cromm, S. Schaubach, J. Spiegel, A. Fürstner, T. N. Grossmann, H. Waldmann, *Nat. Commun.* **2016**, *7*, 11300–11307.
- [48] J. W. Herndon, *Coord. Chem. Rev.* **2006**, *250*, 1889–1964.
- [49] J. W. Herndon, *Coord. Chem. Rev.* **2009**, *253*, 86–179.
- [50] J. W. Herndon, *Coord. Chem. Rev.* **2012**, *256*, 1281–1376.
- [51] J. W. Herndon, *Coord. Chem. Rev.* **2016**, *317*, 1–121.
- [52] S. R. Caskey, M. H. Stewart, Y. J. Ahn, M. J. A. Johnson, J. L. C. Rowsell, J. W. Kampf, *Organometallics* **2007**, *26*, 1912–1923.
- [53] L. R. Moore, E. C. Western, R. Craciun, J. M. Spruell, D. A. Dixon, K. P. O'Halloran, K. H. Shaughnessy, *Organometallics* **2008**, *27*, 576–593.

- [54] C. M. Thomas, J. C. Peters, *Inorg. Chem.* **2004**, *43*, 8–10.
- [55] J. C. Thomas, J. C. Peters, *Inorg. Chem.* **2003**, *42*, 5055–5073.
- [56] J. P. Tassone, R. C. Mawhinney, G. J. Spivak, *J. Organomet. Chem.* **2015**, *776*, 153–156.
- [57] (a) S. Qiao, D. A. Hoic, G. C. Fu, *J. Am. Chem. Soc.* **1996**, *118*, 6329–6330. (b) D. A. Hoic, W. M. Davis, G. C. Fu, *J. Am. Chem. Soc.* **1996**, 8176–8177.
- [58] (a) J. Li, L. Liu, Y. Fu, Q. Guo, *Tetrahedron* **2006**, *62*, 4453–4462. (b) R. S. Edmundson, *Dictionary of Organophosphorus Compounds* **1988**, Chapman and Hall LTD., 820.
- [59] J. C. Peters, J. D. Feldman, T. D. Tilley, *J. Am. Chem. Soc.* **1999**, *121*, 9871–9872.
- [60] A. Phanopoulos, P. W. Miller, N. J. Long, *Coord. Chem. Rev.* **2015**, *299*, 39–60.
- [61] J. D. Feldman, J. C. Peters, T. D. Tilley, *Organometallics* **2002**, *21*, 4065–4070.
- [62] M. C. Lipke, T. D. Tilley, *Angew. Chem. Int. Ed.* **2012**, *51*, 11115–11121.
- [63] M. C. Lipke, T. D. Tilley, *J. Am. Chem. Soc.* **2013**, *135*, 10298–10301.
- [64] S. D. Brown, T. A. Betley, J. C. Peters, *J. Am. Chem. Soc.* **2003**, *125*, 322–323.
- [65] S. D. Brown, J. C. Peters, *J. Am. Chem. Soc.* **2004**, *126*, 4538–4539.
- [66] A. M. Geer, C. Tejel, J. A. López, M. A. Ciriano, *Angew. Chem. Int. Ed.*

- 2014**, 53, 5614–5618.
- [67] C. C. Lu, C. T. Saouma, M. W. Day, J. C. Peters, *J. Am. Chem. Soc.* **2007**, 129, 4–5.
- [68] J. M. Walker, A. Cox, R. Wang, G. J. Spivak, *Organometallics* **2010**, 29, 6121–6124.
- [69] S. Jiménez, J. A. López, M. A. Ciriano, C. Tejel, A. Martínez, R. A. Sánchez-Delgado, *Organometallics* **2009**, 28, 3193–3202.
- [70] J. C. Thomas, J. C. Peters, *J. Am. Chem. Soc.* **2001**, 123, 5100–5101.
- [71] J. C. Thomas, T. A. Betley, J. C. Peters, *J. Am. Chem. Soc.* **2002**, 124, 1146–1147.
- [72] J. C. Thomas, J. C. Peters, *Polyhedron* **2004**, 23, 2901–2913.
- [73] N. P. Mankad, J. C. Peters, *Chem. Commun.* **2008**, 1061–1063.
- [74] T. A. Betley, J. C. Peters, *Inorg. Chem.* **2003**, 42, 5074–5084.
- [75] C. M. Thomas, J. C. Peters, *Inorg. Chem.* **2004**, 43, 8–10.
- [76] M. T. Beach, J. M. Walker, T. G. Larocque, J. L. Deagle, R. Wang, G. J. Spivak, *J. Organomet. Chem.* **2008**, 693, 2921–2928.
- [77] J. P. Tassone, R. C. Mawhinney, G. J. Spivak, *J. Organomet. Chem.* **2015**, 776, 153–156.
- [78] A. Macchioni, *Chem. Rev.* **2005**, 105, 2039–2074.
- [79] M. Stradiotto, K. D. Hesp, R. J. Lundgren, *Angew. Chem. Int. Ed.* **2009**, 49, 494–512.
- [80] C. C. Lu, J. C. Peters, *J. Am. Chem. Soc.* **2002**, 124, 5272–5273.

- [81] K. S. W. Beck, *Chem. Rev.* **1988**, *88*, 1405–1421.
- [82] A. Franzke, A. Pfaltz, *Chem. Eur. J.* **2011**, *17*, 4131–4144.
- [83] R. Chauvin, *Eur. J. Inorg. Chem.* **2000**, 577–591.
- [84] F. Wu, R. F. Jordan, *Organometallics* **2006**, *25*, 5631–5637.
- [85] P. J. Fischer, L. Avena, T. D. Bohrmann, M. C. Neary, G. K. Putka, K. P. Sullivan, *Organometallics* **2014**, *33*, 1300–1309.
- [86] J.-Q. Zhou, H. Alper, *Organometallics* **1994**, *13*, 1586–1591.
- [87] J.-Q. Zhou, H. Alper, *J. Chem. Soc., Chem. Commun.* **1991**, 233–234.
- [88] T. A. Betley, J. C. Peters, *Angew. Chem. Int. Ed.* **2003**, *42*, 2385–2389.
- [89] R. J. Lundgren, M. A. Rankin, R. McDonald, G. Schatte, M. Stradiotto, *Angew. Chem. Int. Ed.* **2007**, *46*, 4732–4735.
- [90] T. A. Betley, J. C. Peters, *Angew. Chem. Int. Ed.* **2003**, *42*, 2385–2389.
- [91] W.-H. Zhang, S. W. Chien, T. S. A. Hor, *Coord. Chem. Rev.* **2011**, *255*, 1991–2024.
- [92] H. A. McManus, P. J. Guiry, *Chem. Rev.* **2004**, *104*, 4151–4202.
- [93] P. Braunstein, *Chem. Rev.* **2006**, *106*, 134–159.
- [94] S.-J. Chen, Y.-Q. Li, Y.-Y. Wang, X.-L. Zhao, Y. Liu, *J. Mol. Catal. A: Chem.* **2015**, *396*, 68–76.
- [95] R. Giri, S. Thapa, *Synlett* **2015**, *26*, 709–715.
- [96] W.-C. Lee, J. M. Sears, R. A. Enow, K. Eads, D. A. Krogstad, B. J. Frost, *Inorg. Chem.* **2013**, *52*, 1737–1746.
- [97] H. Grützmacher, *Angew. Chem. Int. Ed.* **2008**, *47*, 1814–1818.

- [98] P. Braunstein, *J. Organomet. Chem.* **2004**, 689, 3953–3967.
- [99] P. Braunstein, F. Naud, *Angew. Chem. Int. Ed.* **2001**, 40, 680–699.
- [100] R. Lindner, B. van den Bosch, M. Lutz, J. N. H. Reek, J. I. van der Vlugt, *Organometallics* **2011**, 30, 499–510.
- [101] M. Bassetti, *Eur. J. Inorg. Chem.* **2006**, 2006, 4473–4482.
- [102] G. Espino, F. A. Jalón, B. R. Manzano, M. Pérez-Manrique, K. Mereiter, D. Quiñonero, *Supramolecular Chem.* **2012**, 24, 787–798.
- [103] A. Caballero, F. A. Jalón, B. R. Manzano, G. Espino, M. Pérez-Manrique, A. Mucientes, F. J. Pobleto, M. Maestro, *Organometallics* **2004**, 23, 5694–5706.
- [104] M. Bassetti, *Eur. J. Inorg. Chem.* **2006**, 2006, 4473–4482.
- [105] D. B. Grotjahn, *Chem. Eur. J.* **2005**, 11, 7146–7153.
- [106] T. Li, I. Bergner, F. N. Haque, M. Zimmer-De Iuliis, D. Song, R. H. Morris, *Organometallics* **2007**, 26, 5940–5949.
- [107] D. B. Grotjahn, E. J. Kragulj, C. D. Zeinalipour-Yazdi, V. Miranda-Soto, D. A. Lev, A. L. Cooksy, *J. Am. Chem. Soc.* **2008**, 130, 10860–10861.
- [108] D. B. Grotjahn, *Pure Appl. Chem.* **2010**, 82, 635–647.
- [109] D. B. Grotjahn, J. E. Kraus, H. Amouri, M.-N. Rager, A. L. Cooksy, A. J. Arita, S. A. Cortes-Llamas, A. A. Mallari, A. G. DiPasquale, C. E. Moore, L. M. Liable-Sands, J. D. Golen, L. N. Zakharov, A. L. Rheingold, *J. Am. Chem. Soc.* **2010**, 132, 7919–7934.
- [110] J. Tao, F. Sun, T. Fang, *J. Organomet. Chem.* **2012**, 698, 1–6.

- [111] S. Harkal, F. Rataboul, A. Zapf, C. Fuhrmann, T. Riermeier, A. Monsees, M. Beller, *Adv. Synth. Catal.* **2004**, *346*, 1742–1748.
- [112] B. Milde, D. Schaarschmidt, T. Ruffer, H. Lang, *Dalton Trans.* **2012**, *41*, 5377–5390.
- [113] B. Milde, R. Packheiser, S. Hildebrandt, D. Schaarschmidt, T. Ruffer, H. Lang, *Organometallics* **2012**, *31*, 3661–3671.
- [114] T. Schulz, C. Torborg, S. Enthaler, B. Schaffner, A. Dumrath, A. Spannenberg, H. Neumann, A. Börner, M. Beller, *Chem. Eur. J.* **2009**, *15*, 4528–4533.
- [115] K. Junge, B. Wendt, F. A. Westerhaus, A. Spannenberg, H. Jiao, M. Beller, *Chem. Eur. J.* **2012**, *18*, 9011–9018.
- [116] V. Díez, G. Espino, F. A. Jalón, B. R. Manzano, M. Pérez-Manrique, *J. Organomet. Chem.* **2007**, *692*, 1482–1495.
- [117] N. J. Beach, A. E. Williamson, G. J. Spivak, *J. Organomet. Chem.* **2005**, *690*, 4640–4647.
- [118] N. J. Beach, H. A. Jenkins, G. J. Spivak, *Organometallics* **2003**, *22*, 5179–5181.
- [119] N. J. Beach, J. M. Walker, H. A. Jenkins, G. J. Spivak, *J. Organomet. Chem.* **2006**, *691*, 4147–4152.
- [120] H. Slebocka-Tilk, J. L. Cocho, Z. Frankman, R. S. Brown, *J. Am. Chem. Soc.* **1984**, *106*, 2421–2431.
- [121] R. S. Brown, M. Zamkanej, J. L. Cocho, *J. Am. Chem. Soc.* **1984**, *106*,

- 5222–5228.
- [122] M. A. Jalil, T. Yamada, S. Fujinami, T. Honjo, H. Nishikawa, *Polyhedron* **2001**, *20*, 627–633.
- [123] R. Langer, A. Gese, D. Gesevičius, M. Jost, B. R. Langer, F. Schneck, A. Venker, W. Xu, *Eur. J. Inorg. Chem.* **2015**, *2015*, 696–705.
- [124] P. C. Kunz, I. Thiel, A. L. Noffke, G. J. Reiß, F. Mohr, B. Spingler, *J. Organomet. Chem.* **2012**, *697*, 33–40.
- [125] A. G. Sergeev, T. Schulz, C. Torborg, A. Spannenberg, H. Neumann, M. Beller, *Angew. Chem. Int. Ed.* **2009**, *48*, 7595–7599.
- [126] T. Schulz, C. Torborg, B. Schäffner, J. Huang, A. Zapf, R. Kadyrov, A. Börner, M. Beller, *Angew. Chem. Int. Ed.* **2009**, *48*, 918–921.
- [127] Y. Wan, C. Wallinder, B. Plouffe, H. Beaudry, A. K. Mahalingam, X. Wu, B. Johansson, M. Holm, M. Botoros, A. Karlén, A. Pettersson, F. Nyberg, L. Fandriks, N. Gallo-Payet, A. Hallberg, M. Alterman, *J. Med. Chem.* **2004**, *47*, 5995–6008.
- [128] J. Ruiz, A. F. Mesa, *Chem. Eur. J.* **2012**, *18*, 4485–4488.
- [129] D. J. Irvine, C. Glidewell, D. J. Cole-Hamilton, J. C. Barnes, A. Howie, *J. Chem. Soc., Dalton Trans.* **1991**, 1765–1772.
- [130] A. Krasovskiy, P. Knochel, *Angew. Chem. Int. Ed.* **2004**, *43*, 3333–3336.
- [131] A. Wacker, H. Pritzkow, W. Siebert, *Eur. J. Inorg. Chem.* **1999**, *1999*, 789–793.
- [132] D. P. Curran, A. Solovyev, M. Makhlof Brahmi, L. Fensterbank, M.

- Malacria, E. Lacôte, *Angew. Chem. Int. Ed.* **2011**, *50*, 10294–10317.
- [133] A. Wacker, H. Pritzkow, W. Siebert, *Eur. J. Inorg. Chem.* **1999**, 789–793.
- [134] H. Nöth, H. Vahrenkamp, *Chem. Ber.* **1966**, *99*, 1049–1067.
- [135] W. Clegg, K. Izod, W. McFarlane, P. O'Shaughnessy, *Organometallics* **1999**, *18*, 3950–3952.
- [136] A. G. Avent, D. Bonafoux, C. Eaborn, M. S. Hill, P. B. Hitchcock, J. D. Smith, *J. Chem. Soc., Dalton Trans.* **2000**, 2183–2190.
- [137] E. A. MacLachlan, M. D. Fryzuk, *Organometallics* **2005**, *24*, 1112–1118.
- [138] P. Chattopadhyay, R. Rai, P. S. Pandey, *Synth. Commun.* **2006**, *36*, 1857–1861.
- [139] Y.-B. Bai, A.-L. Zhang, J.-J. Tang, J.-M. Gao, *J. Agric. Food Chem.* **2013**, *61*, 2789–2795.
- [140] K. Moedritzer, L. Maier, L. C. D. Groenweghe, *J. Chem. Eng. Data* **1962**, *7*, 307–310.
- [141] L. R. Milgrom, P. J. F. Dempsey, G. Yahioğlu, *Tetrahedron* **1996**, *52*, 9877–9890.
- [142] D. J. Adams, J. A. Bennett, D. Duncan, E. G. Hope, J. Hopewell, A. M. Stuart, A. J. West, *Polyhedron* **2007**, *26*, 1505–1513.
- [143] D. J. M. Snelders, G. van Koten, R. J. M. Klein Gebbink, *Chem. Eur. J.* **2010**, *17*, 42–57.
- [144] U. Beckmann, D. Süslüyan, P. C. Kunz, *Phosphorus, Sulfur, and Silicon Relat. Elem.* **2011**, *186*, 2061–2070.

- [145] J. A. S. Howell, N. Fey, J. D. Lovatt, P. C. Yates, P. McArdle, D. Cunningham, E. Sadeh, H. E. Gottlieb, Z. Goldschmidt, M. B. Hursthouse, M. E. Light, *J. Chem. Soc., Dalton Trans.* **1999**, 3015–3028.
- [146] A. Muller, S. Otto, A. Roodt, *Dalton Trans.* **2008**, 650–657.
- [147] A. Tohmé, H. Sahnoune, T. Roisnel, V. Dorcet, J.-F. Halet, F. Paul, *Organometallics* **2014**, 33, 3385–3398.
- [148] M. N. Chevykalova, L. F. Manzhukova, N. V. Artemova, Y. N. Luzikov, I. E. Nifantev, E. E. Nifantev, *Russ. Chem. Bull., Int. Ed.* **2003**, 52, 78–84.
- [149] S. A. Serron, L. Luo, C. Li, M. E. Cucullu, E. D. Stevens, S. P. Nolan, *Organometallics* **2001**, 14, 5290–5297.
- [150] A. D. Hunter, T. R. Williams, B. M. Zarzyczny, H. W. Bottesch II, S. A. Dolan, K. A. McDowell, D. N. Thomas, C. H. Mahler, *Organometallics* **2016**, 35, 2701–2706.
- [151] J. Shen, E. D. Stevens, S. P. Nolan, *Organometallics* **1998**, 17, 3000–3005.
- [152] C. Li, S. Serron, S. P. Nolan, *Organometallics* **1997**, 15, 4020–4029.
- [153] S. A. Serron, L. Luo, E. D. Stevens, S. P. Nolan, *Organometallics* **1996**, 15, 5209–5215.
- [154] S. A. Serron, S. P. Nolan, *Organometallics* **1995**, 14, 4611–4616.
- [155] F. L. Joslin, J. T. Mague, D. M. Roundhill, *Polyhedron* **1991**, 10, 1713–1715.
- [156] F. L. Joslin, M. P. Johnson, J. T. Mague, D. M. Roundhill,

Organometallics **1991**, *10*, 2781–2794.

- [157] I. de los Ríos, M. J. Tenorio, J. Padilla, M. C. Puerta, P. Valerga, *J. Chem. Soc., Dalton Trans.* **1996**, 377–381.
- [158] P. Kumar, A. K. Singh, S. Sharma, D. S. Pandey, *J. Organomet. Chem.* **2009**, *694*, 3643–3652.
- [159] G. Espino, F. A. Jalón, M. Maestro, B. R. Manzano, M. Pérez-Manrique, A. C. Bacigalupe, *Eur. J. Inorg. Chem.* **2004**, 2542–2552.
- [160] L. D. Quin, *A Guide to Organophosphorus Chemistry*, John Wiley and Sons, New York, **2000**.
- [161] S. Özkar, C. Kayran, A. Tekkaya, *Turk. J. Chem.* **1996**, *20*, 74–79.
- [162] P. E. Garrou, *Chem. Rev.* **1980**, *81*, 229–266.
- [163] E. Lindner, R. Fawzi, H. A. Mayer, K. Eichele, W. Hiller, *Organometallics* **1992**, *11*, 1033–1043.
- [164] A. Caballero, F. A. Jalón, B. R. Manzano, G. Espino, M. Pérez-Manrique, A. Mucientes, F. J. Pobleto, M. Maestro, *Organometallics* **2004**, *23*, 5694–5706.
- [165] J. Tauchman, B. Therrien, G. Süss-Fink, P. Štěpnička, *Organometallics* **2012**, *31*, 3985–3994.
- [166] Y. Zhao, Z. He, S. Li, J. Tang, G. Gao, J. Lan, J. You, *Chem. Commun.* **2016**, *52*, 4613–4616.
- [167] M. Di Vaira, S. Seniori Costantini, F. Mani, M. Peruzzini, P. Stoppioni, *J.*

Organomet. Chem. **2004**, 689, 1757–1762.

- [168] F. Boeck, T. Kribber, L. Xiao, L. Hintermann, *J. Am. Chem. Soc.* **2011**, 133, 8138–8141.
- [169] K. Mauthner, C. Slugovc, K. Mereiter, R. Schmid, K. Kirchner, *Organometallics* **1997**, 16, 1956–1961.
- [170] D. B. Grotjahn, V. Miranda-Soto, E. J. Kragulj, D. A. Lev, G. Erdogan, X. Zeng, A. L. Cooksy, *J. Am. Chem. Soc.* **2008**, 130, 20–21.
- [171] D. B. Grotjahn, *Dalton Trans.* **2008**, 6497–12.
- [172] R. D. Adams, A. Davison, J. P. Selegue, *J. Am. Chem. Soc.* **1979**, 101, 7232–7238.
- [173] Y.-S. Yen, Y.-C. Lin, Y.-H. Liu, Y. Wang, *Organometallics* **2007**, 26, 1250–1255.
- [174] M. I. Bruce, B. C. Hall, N. N. Zaitseva, B. W. Skelton, A. H. White, *J. Chem. Soc., Dalton Trans.* **1998**, 1793–1804.
- [175] M. Jiménez-Tenorio, M. C. Puerta, P. Valerga, M. A. Ortuño, G. Ujaque, A. Lledós, *Inorg. Chem.* **2013**, 52, 8919–8932.
- [176] M. Jiménez-Tenorio, M. C. Puerta, P. Valerga, M. A. Ortuño, G. Ujaque, A. Lledós, *Organometallics* **2014**, 33, 2549–2560.
- [177] P. J. Fagan, M. D. Ward, J. C. Calabrese, *J. Am. Chem. Soc.* **1989**, 111, 1698–1719.
- [178] E. V. Mutseneck, C. Reus, F. Schödel, M. Bolte, H.-W. Lerner, M.

Wagner, *Organometallics* **2010**, *29*, 966–975.

- [179] A. C. Hillier, W. J. Sommer, B. S. Yong, J. L. Petersen, L. Cavallo, S. P. Nolan, *Organometallics* **2003**, *22*, 4322–4326.
- [180] H. Aneetha, M. Jiménez-Tenorio, M. C. Puerta, P. Valerga, V. N. Sapunov, R. Schmid, K. Kirchner, K. Mereiter, *Organometallics* **2002**, *21*, 5334–5346.
- [181] L. Luo, S. P. Nolan, *Organometallics* **1994**, *13*, 4781–4786.
- [182] L. Jafarpour, S. P. Nolan, *J. Organomet. Chem.* **2001**, *617*, 17–27.
- [183] A. B. Pangborn, M. A. Giardello, R. H. Grubbs, R. K. Rosen, F. J. Timmers, *Organometallics* **1996**, *15*, 1518–1520.
- [184] O. V. Starikova, G. V. Dolgushin, L. I. Larina, P. E. Ushakov, T. N. Komarova, V. A. Lopyrev, *Russ. J. Org. Chem.* **2004**, *39*, 1467–1470.
- [185] F. L. Joslin, J. T. Mague, D. M. Roundhill, *Organometallics* **1991**, *10*, 521–524.
- [186] M. S. Chinn, D. M. Heinekey, *J. Am. Chem. Soc.* **1990**, *112*, 5166–5175.
- [187] A. Gazit, K. Yee, A. Uecker, F.-D. Böhmer, T. Sjöblom, A. Östman, J. Waltenberger, G. Golomb, S. Banai, M. C. Heinrich, A. Levitzki, *Bioorg. Med. Chem.* **2003**, *11*, 2007–2018.

Curriculum Vitae

PERSONAL DATA

Jesse Walker
MSc. (Lakehead University)
230 Beckwick Rd.
Thunder Bay, Ontario
P7N 1G7
(807) 472-3095
jmwalker@lakeheadu.ca

ACADEMIC AND RESEARCH QUALIFICATIONS

PhD Candidate (Lakehead University, Thunder Bay, Ontario)
Estimated Graduation 2016
Supervisor: Dr. Greg Spivak
Thesis: Ruthenium Half-Sandwich Zwitterions: Coordination Behavior of New Hemilabile Phosphinobenzimidazole Anions.

Master of Science (Lakehead University, Thunder Bay, Ontario)
Graduate of 2009
Supervisor: Dr. Greg Spivak
Thesis: Ruthenium-Tris(pyrazolyl)methane Complexes as Potential Candidates for Cancer Chemotherapy Agents.

Honours Bachelor of Science (Lakehead University, Thunder Bay, Ontario)
Graduate of 2007 (First Class Standing)
Supervisor: Dr. Greg Spivak
Major: Chemistry (Health Professional Stream)
Thesis: The Synthesis Ruthenium Carbynes via Dehydrohalogenation of Ruthenium Carbene Precursors.

PROFESSIONAL EMPLOYMENT EXPERIENCE

Cyclotron Associate (Thunder Bay Regional Research Institute)
Working under the supervision of Dr. Michael Campbell
August 2015- Present

Projects/Duties include the following:

- Performing various duties to complete application for Licence to Produce, Possess and Process isotopes (radiation surveys, installation and testing of equipment).
- Testing and operation of systems to produce ^{18}F FDG, Na^{18}F , and ^{11}C CO_2 .
- Method development and validation, operation, and maintenance of analytical equipment including: multichannel analyzer, radio-TLC plate reader, well counter, dose calibrator, GC-FID, HPLC (UV, ECD, and radio detectors), osmometer, melting point apparatus, pH meter, endotoxin assay reader.
- Standard operating procedure development for radiopharmaceutical production/quality control and general operation of the facility.
- General facility maintenance and monitoring.
- Chemical research.
- Training new employees.

Training and skills acquired:

- Nuclear Energy Worker Training.
- Cyclotron and radiopharmaceutical safety training.
- First aid.
- Transportation of dangerous goods training.
- General operation of TR-24 cyclotron.
- Laura Radiopharmaceutical analysis software.
- Genie 2000 MCA software.
- Scan-Ram radio-TLC detector training.
- Agilent GC-FID training.
- Waters ECD training.
- Flow-Ram radio-HPLC detector training.
- GE Fastlab radiochemical synthesizer operation.
- GE Tracerlab FX N, and GE Tracerlab FX C radiochemical synthesizer operation and programming.
- Sofie Biosciences Elixys radiochemical synthesizer operation and programming.
- Operation of TEMA dose calibrator.

Research Assistant (Lakehead University, Thunder Bay, Ontario)
Working under the supervision of Dr. John Th'ng
October 2009-September 2010

Projects include the following:

- Screening various compounds for anticancer properties.

- Cell cycle specific phosphorylation of mutated histone H1 in human cells.

Skills acquired include:

- Tissue culture techniques.
- Performing MTT cell proliferation assays.
- Protein/DNA extraction and purification methods.
- Gel electrophoresis.
- Western blotting.
- Cloning.

Research Assistant (Lakehead University, Thunder Bay, Ontario)

Working under the supervision of Dr. Greg Spivak

2005-2011 – Full time during summer months and part time throughout the academic years.

Projects include the following:

- Ligand synthesis.
- Design, synthesis, characterization, and evaluation of various ruthenium-based coordination compounds for catalytic and anti-cancer applications.

Skills acquired:

- Use of standard methods to synthesize, purify and characterize chemical compounds.
- Synthesis and manipulation of air-sensitive compounds under inert atmospheric conditions using standard Schlenk techniques.
- Use of nuclear magnetic resonance spectroscopy to characterize chemical compounds- both data acquisition and interpretation.
- Use of gas chromatography to evaluate the catalytic efficiency of coordination compounds.
- Experience working with:
 - Optical microscopy.
 - Scanning electron microscopy.
 - Infrared spectroscopy.
 - Ultraviolet-visible spectroscopy.
 - Chromatography.
 - X-ray diffraction.
 - Computational chemistry.

HONOURS

**Natural Sciences and Engineering Research Council of Canada
Postgraduate Scholarship (NSERC PGS-D).**
2012-2015

Powell Equipment Ltd. LU 30th Anniversary Graduate Bursary.
2012

Ontario Graduate Scholarship Science and Technology (OGSST).
2007-2009

Lakehead University Faculty Research Scholarship
2008, 2009, 2011

Lakehead Graduate Bursary
2008-2009, 2011-2015.

Lakehead University In-Course Scholarship
2006-2007

TEACHING EXPERIENCE

CLASSROOM TEACHING POSITIONS:

Mathematics Instructor (Confederation College, Thunder Bay, Ontario)	
Literacy and Basic Skills Program	Spring 2010-Summer 2011.
Academic & Career Entrance Program	Spring 2010-Summer 2011.

TEACHING ASSISTANT POSITIONS:

Graduate Assistant (Lakehead University, Thunder Bay, Ontario)

Analytical Chemistry II (Chem 3131)	Winter 2013.
Introductory Chemistry (Chem 1110)	Fall 2013.
Organic Chemistry I (Chem 2211)	Fall 2013/2014.
Organic Chemistry II (Chem 2231)	Winter 2013/2014/2015.
Organic Chemistry III (Chem 3231)	Fall 2011/2012.
Northern Environmental Chemistry (Chem 2610)	Winter 2012.

Inorganic Chemistry I (Chem 2351)	Winter 2012/2013/2014/ 2015.
Inorganic Chemistry II (Chem 3371)	Fall 2011/2012/2014.
Modern Chemistry I (Chem 1110)	2007/08 and 2008/09 academic years.
Modern Chemistry II (Chem 1130)	2007/08 and 2008/09 academic years.

Teaching Assistant (Lakehead University, Thunder Bay, Ontario)

Organic and Biochemistry for Health Sciences (Chem 1210)	2006/07 academic year.
---	------------------------

TUTORING:

Tutor (Confederation College, Thunder Bay, Ontario) College Access Program	Winter semester 2011.
--	-----------------------

Tutor (Lakehead University, Thunder Bay, Ontario) Native Nursing Program	2006/07 academic year.
--	------------------------

Tutor (Lakehead University, Thunder Bay, Ontario) Foundations of Chemistry	2006/07 academic year.
--	------------------------

MENTORING:

Laboratory Mentor (Lakehead University, Thunder Bay, Ontario)

Stefanie Perrier	2015/16 academic year.
Monika Jorgenson	2014/15 academic year.
Joseph Tassone	2011/12 academic year.
Ashley Esarik	2010/11 academic year.
Alex Cox	2009/10 academic year.
Justin Deagle	2007/08 academic year.
Michael Beach	2006/07 academic year.
Timothy Larocque	2005/06 academic year.

COMMITTEES

VP Finance (Lakehead University, Thunder Bay, Ontario) Lakehead Chemistry Club	2005/06 and 2006/07
--	---------------------

CONTRIBUTIONS TO RESEARCH AND DEVELOPMENT

Conferences Presentations (Presenter in bold; **P** = poster; **L** = lecture; **I** = invited lecture; **A** = attendee):

- “*Anionic Tetraphenylborate-Functionalized Phosphinobenzimidazole [P,N]-Chelates: Tuning Hemilability in Ruthenium Half-Sandwich Zwitterions*”, **J. M. Walker**, J. P. Tassone, H. A. Jenkins and G. J. Spivak, 97th Annual Canadian Society for Chemistry Conference (Vancouver, British Columbia, Canada) June 2014 (**P**).
- “*The Synthesis of an Anionic, Tetraphenylborate-Functionalized, [P,N]-Hybrid Phosphinobenzimidazole Ligand and its Hemilabile Behaviour in Ruthenium Zwitterion Chemistry*”, **J. M. Walker**, J. P. Tassone, H. A. Jenkins and G. J. Spivak, 24rd Annual Lakehead University Graduate Student Conference (Thunder Bay, Ontario, Canada), March 2014 (**P**).
- “*Anionic, Hemilabile P,N Hybrid Ligands in Ruthenium Chemistry and Catalysis: Pushing the Limits of Ligand Multifunctionality*”, J. M. Walker, J. P. Tassone and **G. J. Spivak**, 96th Annual Canadian Society for Chemistry Conference (Quebec City, Quebec, Canada) May 2013 (**P**).
- “*Ruthenium Piano-Stool Complexes Containing a New Anionic P-N Donor Ligand*”, **J. M. Walker**, J. P. Tassone and G. J. Spivak, 23rd Annual Lakehead University Graduate Student Conference (Thunder Bay, Ontario, Canada), February 2013 (**P**).
- “*Structural and Catalytic Properties of Ruthenium Piano-Stool Complexes Bearing an Anionic Tripodal Phosphine*”, J. M. Walker, A. M. Cox, R. Wang and **Gregory J. Spivak**. 93rd Canadian Society for Chemistry Conference and Exhibition (Toronto, Ontario, Canada), May 2010 (**P**).
- “*Ruthenium-Tris(pyrazolyl)methane Complexes as Potential Candidates for Cancer Chemotherapy Agents*”, **J. M Walker**, R. Pycko, A. McEwan, M. L. Tassotto, C. Gottardo, J. Th’ng. G. J. Spivak. 2nd Georgian Bay International Conference on Bioinorganic Chemistry (Parry Sound, Ontario, Canada), May 2009 (**P**).

- “*Ruthenium-Tris(pyrazolyl)methane Complexes as Candidates for Anticancer drugs*”, **J. M. Walker**, R. Pycko, A. McEwan, M.L. Tassotto, C. Gottardo, J. Th’ng, G. J. Spivak, 19th Graduate Student Conference (Thunder Bay, Ontario, Canada), February 2009 (**P**).
- “*Hemilabile Tridentate Iminophosphine Ligands: Applications to Ruthenium-Vinylidene and -Carbyne Chemistry*” N. J. Beach, H. A. Jenkins, J. M. Walker and **Gregory J. Spivak**. 89th Canadian Society for Chemistry Conference and Exhibition (Halifax, Nova Scotia, Canada), May 2006 (**P**).
- Electrochemical Society of Canada Fall Symposium (Thunder Bay, Ontario, Canada). September 2006 (**A**).

Peer-Reviewed Journal Publications

- “*The synthesis of an anionic, tetraphenylborate-functionalized, [P,N]-hybrid phosphinobenzimidazole ligand and its hemilabile behaviour in ruthenium zwitterion chemistry*”, **J. M. Walker**, J. P. Tassone, H. A. Jenkins, G. J. Spivak, *J. Organomet. Chem.*, **2014**, 761, 56-63.
- “*Ruthenium piano-stool complexes containing mono- or bidentate pyrrolidinylalkylphosphines and their reactions with small molecules*”, M.T. Beach, **J.M. Walker**, R. Wang, and G.J. Spivak, *J. Organomet. Chem.*, **2011**, 696, 3198-3205.
- “*Synthesis and Reactivity of $[(\eta^3\text{-PhB}(\text{CH}_2\text{PPh}_2)_3)\text{Ru}(\text{NCMe})_3]\text{PF}_6$ and Its Potential as a Transfer Hydrogenation Catalyst*”, **J. M. Walker**, A. M. Cox, R. Wang, G. J. Spivak. *Organometallics*, **2010**, 29, 6121-6124.
- “*Ruthenium-Tris(pyrazolyl)methane Complexes Capable of Inhibiting Cancer Cell Growth*”, **J. M. Walker**, R. Pycko, A. McEwan, M. L. Tassotto, C. Gottardo, J. Th’ng, R. Wang, G. J. Spivak. *Eur. J. Inorg. Chem.*, **2009**, 4629–4633.
- “*The (phosphino)tetraphenylborate ligand in ruthenium-arene chemistry*”, M.T Beach, **J. M. Walker**, T.G. Laroque, J.L. Deagle, R. Wang, G.J. Spivak, *J. Organomet. Chem.*, **2008**, 693, 2921-2928.

- “*Ruthenium vinylidene and carbyne complexes containing a multifunctional tridentate ligand with a PNN donor set*”, N. J. Beach, **J. M. Walker**, H. J. Jenkins, G. J. Spivak, *J. Organomet. Chem.*, **2006**, 691, 4147-4152.

Membership

Membership, Chemical Institute of Canada.